Copyright

by

Brian Davis Cowan

2010

The Thesis Committee for Brian Davis Cowan
Certifies that this is the approved version of the following thesis:

Temporal and Spatial Variability of Cave-air Carbon Dioxide in Central Texas, USA

APPROVED BY
SUPERVISING COMMITTEE:

Supervisor:

Jay L Banner

John M Sharp Jr

Daniel O Breecker

MaryLynn Musgrove

Temporal and Spatial Variability of Cave-air Carbon Dioxide in Central Texas, USA

by

Brian Davis Cowan, B.S.

Thesis

Presented to the Faculty of the Graduate School of

The University of Texas at Austin

in Partial Fulfillment

of the Requirements

for the Degree of

Master of Science in Geological Sciences

The University of Texas at Austin

May 2010

Abstract

Temporal and Spatial Variability of Cave-air Carbon Dioxide in Central Texas, USA

Brian Davis Cowan, M.S. Geo. Sci.

The University of Texas at Austin, 2010

Supervisor: Jay L. Banner

There is the potential for bias in the speleothem paleoclimate record due to fluctuations in speleothem growth. A previous study in three central Texas tourist caves has shown that speleothem calcite growth rates vary seasonally in response to density-driven fluctuations in cave-air CO_2. Three undeveloped caves and three tourist caves in central Texas were monitored to determine 1) if seasonal CO_2 fluctuations are unique to the tourist caves that have been impacted by anthropogenic activity, 2) the extent to which cave-air CO_2 concentrations are controlled by natural variations in cave geometry, host rocks, cave volume and overlying soils and 3) how variable cave-air CO_2 concentrations are on shorter timescales such as diurnal timescales or in response to storm events. Nearly 150 lateral transects into six caves (three tourist caves and three undeveloped caves) over three years show that CO_2 concentrations vary seasonally in five of the caves with peak concentrations in the warmer months and lower concentrations in the cooler months. These seasonal CO_2 fluctuations occurred independent of cave volume, geometry, the amount of visitation, and overlying soil thickness.

Nearly 30,000 measurements taken using logging CO_2 meters over two years reveal that all caves monitored experienced large diurnal cave-air CO_2 fluctuations that can be accounted for by diurnally fluctuating barometric pressure. Typical diurnal CO_2 fluctuations in the undeveloped caves were 10,000-15,000 ppm and in the tourist caves 500-1,500 ppm. Air speed measurements taken at two caves confirm that large volumes of air flow into and out of the caves in response to diurnal barometric pressure fluctuations. At one cave 0.95 cave volumes exited the cave during one "exhalation" lasting 7.75 hours and at the other over 15 cave volumes during one "exhalation" lasting 8.83 hours.

Previous cave ventilation studies have treated caves as independent systems that do not exchange gases with the surrounding epikarst; however, we present a conceptual model of airflow through epikarst in which significant subsurface airflow occurs not only in caves, but also through the fractures and dissolution cavities that are typically connected to the caves. This is the only mechanism that can account for the large volume of air flowing into and out of the caves on a diurnal basis and the magnitude and timing of cave air CO_2 fluctuations in response to changes in barometric pressure. These results suggest that some speleothem records might be biased due to cave ventilation. This is a serious and poorly recognized source of error in many speleothem paleoclimate records. Diurnal and seasonal cave ventilation may also lead to increased temporal resolution in the speleothem record if diurnal or seasonal layers of calcite are deposited.

Table of Contents

List of Tables viii

List of Figure ix

CHAPTER 1. GENERAL INTRODUCTION, BACKGROUND AND PHYSICAL SETTING 1

1.1. Organization 1

1.2. Background 1

1.2.1. Speleothem formation 1

1.2.2. Suitability of speleothems as paleoenvironmental proxies 2

1.3. Potential Speleothem Proxy Bias 3

1.3.1. Speleothem growth rate 4

1.3.2. Trace element composition 5

1.3.3. Stable isotopes 6

1.4. Significance of Research 6

1.5. Study Area 8

1.5.1. General Setting 8

1.5.2. Undeveloped caves 8

1.5.3 Tourist caves 9

1.6 Controls on Cave-air CO_2 Variability 10

1.6.1. Cave ventilation 10

1.6.2. Cave CO_2 sources 12

CHAPTER 2. SEASONAL AND SPATIAL VARIABILITY OF CAVE-AIR CO_2 IN CENTRAL TEXAS 15

2.1. Abstract 15

2.2. Introduction 16

2.3. Methods 17

2.4. Results 20

2.5. Discussion 20

2.5.1. Regional controls on cave-air CO_2 20

2.5.2. Site-specific controls on cave-air CO_2 22

2.5.3. Implications for speleothem paleoclimate studies 25
2.6. Conclusions 26

CHAPTER 3. DIURNAL AND STORM-SCALE CAVE-AIR CO2 FLUCTUATIONS AND AIRFLOW THROUGH KARST 29

3.1. Abstract 29
3.2. Introduction 30
3.3. Methods and Study Area 32
3.4. Results 38
3.5. Discussion 40
3.5.1. Diurnal barometric ventilation 41
3.5.2. Cave-specific controls on ventilation 43
3.5.3. Subterranean airflow in karst settings 44
3.5.4. Conceptual model of cave ventilation 46
3.6. Implications 47

APPENDIX A. METHODS AND SITE DESCRIPTIONS 74

APPENDIX B. DATA ANALYSIS 92

REFERENCES 105

VITA 113

List of Tables

Table 1: Characteristics of monitored caves and overlying soils 50

Table 2: Volume of air ventilated from WP and MR 51

Table 3: Correlation between cave-air CO_2 concentrations, atmospheric temperature and pressure.....52

Table 4: Correlation between cave-air CO_2 concentrations, atmospheric temperature and pressure at WP.....53

Table B1: Cave air CO_2 concentrations measured along transects of the undeveloped caves 95

Table B2: Cave air CO_2 concentrations measured along transects of the tourist caves 99

Table B3: Airspeed measurements taken at WP 102

Table B4: Airspeed measurements taken at MR 103

Table B5: Soil depths and measurement locations.....104

List of Figures

Figure 1: Map of cave locations 54

Figure 2: Hydrostratigraphic section of the study area 55

Figure 3: Map of seasonal monitoring stations 56

Figure 4: Cave-air CO_2 concentrations and outside temperature 57

Figure 5: Representative warm and cool season transects in IS and WP.....58

Figure 6: Mean CO_2 concentrations vs. distance from cave entrance 59

Figure 7: Map of logging stations 60

Figure 8: Representative diurnal cave-air CO_2 fluctuations.....61

Figure 9: Seasonal cave air CO_2 fluctuations at logging stations.....62

Figure 10: Representative CO_2 fluctuations during storm events 63

Figure 11: Representative warm and cool season CO_2 concentrations at ISST and ISLM 64

Figure 12: Cave air CO_2 concentrations at WP2, WP5 and WP7 and surface temperature and barometric pressure fluctuations 65

Figure 13: Cave-air CO_2 concentrations and cave air density-outside air density at ISST, ISLM, MR3 and WP7 67

Figure 14: Correlation between cave-air CO_2 concentrations, air density and barometric pressure 71

Figure 15: CO_2 concentrations and airspeeds measured at the entrances of WP and MR 72

Figure16: Conceptual model of subterranean airflow and CO_2 flux in the study area 73

Figure A1: Picture of Vaisala logging CO2 meter and protective housing 90

Figure A2: Locations of CO2 logging stations 91

CHAPTER 1: GENERAL INTRODUCTION, BACKGROUND AND PHYSICAL SETTING

1.1 ORGANIZATION

This thesis is organized into three chapters. The first chapter presents general background information about the study area and the importance of understanding the mechanisms that control cave-air CO_2 fluctuations. The second chapter investigates the controls on seasonal cave-air CO_2 fluctuations in the central Texas region. Chapter three discusses the controls on shorter-term cave-air CO_2 fluctuations (i.e. diurnal and storm-scale). The appendix that follows presents a compilation of the data collected for this study and detailed descriptions of the study sites and methods.

1.2. BACKGROUND

1.2.1. Speleothem formation

Speleothems are typically formed by the accumulation of calcite that is precipitated from water that is supersaturated with respect to this mineral. The process of speleothem formation ultimately begins in the soil zone where recharging meteoric water comes into contact with the soil atmosphere, which has an elevated CO_2 concentration due to heterotrophic and autotrophic respiration. When water comes into contact with the soil air that has a higher partial pressure of CO_2 (pCO_2), some of the CO_2 dissolves into the water, making it more acidic. As the slightly acidic water flows through the epikarst it may dissolve the limestone until becoming saturated with respect to calcite or coming in contact with a lower pCO_2 environment (i.e. a cavity or cave). When the solution enters a lower pCO_2 environment, CO_2 may degas from the solution causing it to become supersaturated with respect to calcite, which causes calcite deposition to occur. Over time, successive layers of calcite are formed one atop the other leading to the formation

of a speleothem such as a stalactite, stalagmite or flowstone. Speleothems are well suited for paleoenvironmental reconstructions because the composition of infiltrating water, and thus the composition of the speleothem calcite, is affected by climatic conditions.

1.2.2 Suitability of speleothems as paleoenvironmental proxies

In recent decades speleothems have been considered important archives of terrestrial climate information. Speleothems are suited for reconstructing paleoenvironmental change because they are: 1) comprised of sequential growth layers that can be dated via radiometric and other non-analytical methods; 2) their composition and growth rate is influenced by climatic conditions; 3) they can be deposited nearly continuously for thousands to hundreds of thousands of years; and 4) they are found in a wide range of climates.

One of the longest known speleothem records comes from China and covers 224,000 years (Wang et al., 2008). Long records such as this are quite useful for studying climate shifts influenced by mechanisms that operate on longer timescales (i.e. orbital climate forcing). Other speleothem records offer information about seasonal climate variability (i.e. Fleitmann et al., 2004; Polyak and Asmerom, 2001), and even individual storm events (Frappier, et al., 2007). These types of climate reconstructions might prove useful for resource management planning purposes as they may yield high-resolution information about the natural variability of weather patterns within a region on a decadal to centennial timescale (i.e. rainfall and temperature extremes).

Speleothem proxies are interpreted to record environmental parameters such as temperature, rainfall source and the amount and type of vegetation. Unfortunately these parameters may not be directly transferred to speleothems. In-cave processes can influence the incorporation of these proxies into speleothem calcite or may alter drip

water composition prior to calcite deposition. The majority of speleothem studies focus on paleoclimate reconstruction and not on calibrating speleothems to well-understood modern cave systems. Such calibration of the speleothem record is imperative for the understanding and interpretation of speleothem records. Concerns include the effect of fluctuating cave-air CO_2 concentration on calcite precipitation and the geochemical evolution of water within caves (i.e. Tooth and Fairchild, 2003; Spötl et al., 2005).

1.3. Potential For Sepleothem Proxy Bias

The role of CO_2 degassing in speleothem formation was not fully appreciated until Holland et al. (1964) confirmed that CO_2 degassing is one of the primary process responsible for speleothem growth. Until recently, relatively few studies have focused on the variation of CO_2 concentration in cave air (Fairchild et al., 2007).

The calcite precipitation-dissolution equation is given below (Eq. 1):

Eq. 1: $Ca^{2+} + 2HCO^{3-} \Leftrightarrow CaCO_3 + H_2O + CO_2$

As Eq. 1 suggests, CO_2 degassing or evaporation is necessary for calcite deposition to occur. As the pCO_2 of cave air increases, drip water degassing can be inhibited and calcite deposition may slow or cease (Fairchild et al., 2006; Banner et al., 2007). This might introduce bias into the speleothem record because drip water composition during times of non-growth might not be recorded in speleothem calcite or the composition of the drip water might be altered before speleothem calcite is deposited. If these processes are taking place, it is possible that the bias that is introduced might be systematic and could be corrected for. Below is a discussion on how fluctuating cave-air CO_2 might introduce bias into the speleothem record.

1.3.1. Speleothem growth rate

Speleothem growth rate is often used as a proxy for rainfall. It is typically assumed that growth layer thickness and hiatuses in growth are controlled by drip rate, which is controlled by changes in rainfall (Baker et al., 1993; Genty and Quinif, 1996; Qin et al., 1999; Musgrove et al., 2001; Polyak and Asmerom, 2001). It is likely that this assumption is valid in many instances, however, there is evidence that high cave-air CO_2 concentrations can inhibit speleothem growth rates (Banner et al., 2007; Baldini et al., 2008) thus the possibility that growth rate might be affected by cave-air CO_2 should not be dismissed without close examination. Although it is difficult to tell if the growth rate of a speleothem was slowed by inhibited drip water degassing, the crystal fabric of speleothem growth layers may offer clues as to the mechanism (or mechanisms) that control growth rate.

Crystal defects affect speleothem fabrics and are thought to be caused by several factors including the availability of foreign ions in drip water and rapid growth (Frisia et al., 2000). For example, columnar fabrics may form under constant drip rates and slower degassing, whereas dendritic fabrics may form under rapid degassing or variable discharge (Frisia et al., 2000). A close examination of the crystal fabric of growth layers might reveal clues that suggest alternating periods of rapid and slow growth (i.e. alternating columnar and dendritic layers), which could indicate alternating periods of stronger degassing due to low cave-air CO_2 concentrations and periods of weak degassing due to higher cave-air CO_2 concentrations. Changes in mineralogy from calcite to aragonite indicate periods of drying and might suggest that drip rate changes are indeed responsible for changes in calcite growth rates, not cave-air CO_2 fluctuations (Railsback et al., 1994). A pattern of alternating columnar and dendritic fabric was observed in speleothem lamina in a well-constrained cave system in Gibraltar (Mattey et al., 2009).

That study showed that alternating speleothem fabrics were correlated with seasonal cave-air CO_2 fluctuations.

1.3.2. Trace element composition

Cave-air CO_2 fluctuations may also affect the trace element composition of speleothems, which has been used as a proxy for rainfall. In caves where drip water trace element composition varies seasonally, periods of non-deposition due to high cave-air CO_2 concentrations might cause speleothem calcite composition to be biased to times when cave-air CO_2 is lower and speleothem growth is faster. Prior calcite precipitation (PCP) may also cause the trace element composition of speleothems to be biased. PCP refers to the precipitation of calcite up gradient from the point where a speleothem is being deposited and has been shown to affect the concentration of trace elements in speleothem forming drip water (i.e. Mattey et al., 2009; Wong, 2008). For example, if calcite is deposited as drip water flows along the outside of a stalactite or in the vadose zone above a cave, the concentration of Mg and Sr in the water may increase due to preferential exclusion of Sr and Mg from the calcite crystal lattice. This increase in Mg and Sr in the water can lead to an increase in the Mg and Sr concentration of speleothem calcite precipitated from the enriched water. Because CO_2 degassing is the primary driver of calcite growth, we expect the effect of PCP to increase when air CO_2 is lower and drip water degassing is stronger. In caves with seasonally fluctuating cave-air CO_2 concentrations, PCP could lead to a negative correlation between cave-air CO_2 and the concentration of Mg and Sr in speleothem calcite, thus a pattern of seasonally varying Mg and Sr would be detected in speleothem growth layers and might be incorrectly interpreted as reflecting rainfall.

1.3.3. Stable isotopes

Stable isotope ratios ($\delta^{13}C$ and $\delta^{18}O$) are typically used as proxies for vegetation and rainfall respectively. Studies have shown that $\delta^{13}C$ and $\delta^{18}O$ values not only respond to environmental changes, but to in-cave processes as well. Drip water may undergo significant kinetic isotope effects due to rapid CO_2 degassing or rayleigh distillation that causes departures from equilibrium isotope fractionation between HCO_3^- and $CaCO_3$ (Mickler et al., 2004). Because the rate of drip water degassing is largely controlled by the difference between the pCO_2 of the drip water and cave air, the magnitude of departure from equilibrium isotope fractionation (if any) may change as cave-air CO_2 concentrations fluctuate. In fact, a study of a modern stalagmite by Mattey et al. (2009) showed that annual growth lamina preserved seasonal $\delta^{13}C$ and $\delta^{18}O$ cycles that were attributed to cave ventilation. If this effect is not accounted for, changes in the $\delta^{13}C$ and $\delta^{18}O$ composition of speleothems might be incorrectly interpreted as reflecting climatic changes and not in-cave processes.

1.4. SIGNIFICANCE OF RESEARCH

Recently, there has been renewed interest in better understanding how cave ventilation and cave-air CO_2 concentrations vary temporally and spatially and how these variations might affect in-cave processes related to speleothem deposition (i.e. Spotl et al., 2005). In fact, Fairchild et al. (2007) highlights the need for more studies of cave ventilation in order to make better interpretations of speleothem paleoenvironmental proxies. This thesis addresses that need by building on previous research conducted in three central Texas tourist caves that found calcite growth rates to be correlated with cave-air CO_2 concentration (Banner et al., 2007). The authors attributed the seasonal fluctuations of cave-air CO_2 concentrations to changes in cave ventilation caused by seasonal surface temperature fluctuations.

In three of the caves studied by Banner et al. (2007), calcite deposition peaked in the cooler months, when cave-air CO_2 concentrations were low. In the warmer months, elevated cave-air CO_2 concentrations inhibited drip water degassing, resulting in a significant decrease or cessation of calcite deposition. These results further support the hypothesis that in-cave processes tied to cave-air CO_2 concentration might introduce bias into the speleothem record. More interestingly, the caves are located approximately 130 km apart, suggesting that the potential for a regionally extensive seasonal bias in the speleothem record exists. Often when proxies are regionally reproducible among spatially disparate records more confidence is placed in the paleoenvironmental interpretations, as it is assumed that climate is responsible for the reproducibility; however, the reproducibility might also be attributed to fluctuations of cave-air CO_2 (Banner et al., 2007). It is important to determine if seasonal cave-air CO_2 fluctuations in the central Texas caves are unique to the tourist caves, which have been modified from their natural state and subjected to large numbers of visitors, or if they are a naturally occurring phenomenon. It is also important to better understand the mechanisms that control cave-air CO_2 fluctuations on seasonal and even shorter timescales.

CO_2 fluctuations in the tourist caves may result from 1) modifications to their natural connectivity with the surface atmosphere during their development for tourism, 2) significant human visitation and 3) non-anthropogenic influences. Variations in non-anthropogenic factors such as cave volume, stratigraphic unit, cave geometry and soil thickness may also influence the extent and timing of ventilation. We compare the timing and magnitude of CO_2 fluctuations in three undeveloped caves, with those measured in two of the tourist caves studied by Banner et al. (2007). The undeveloped caves were chosen for comparison with the tourist caves because they are 1) centrally located between the tourist caves, 2) formed in similar stratigraphic units, 3) overlain by similar

soil and vegetation, 4) receive similar rainfall amounts, 5) experience similar surface temperature fluctuations, and 6) receive relatively little visitation outside of our monitoring trips.

1.5. STUDY AREA

1.5.1. General setting

The study area is located near Austin, Texas (Fig. 1), and is composed of karstified Lower Cretaceous marine carbonates overlain by a thin calcareous clay soil that supports oak and juniper savannah. Soils across the study area are thin and commonly contain limestone fragments sourced from the underlying bedrock (Cooke et al., 2007). The undeveloped caves are overlain by the Speck series soils that are classified as stony clay loams, Inner Space Cavern (IS) is overlain by Eckrant series soils that are classified as silty clays and stony clays. Natural Bridge North Cave (NBN) and Natural Bridge South Cave (NBS) are overlain by exposed bedrock and Comfort and Eckrant series soils that are classified as extremely stony clays and gravely clay loams (USDA, 1974; USDA, 1983; USDA, 1984). All study caves, with the exception of NBN and NBS, are located within the Edwards Group, a Lower Cretaceous marine limestone unit with interbedded dolomitic layers. NBN and NBS are located within the upper member of the Glen Rose Limestone and the Walnut Member of the Edwards Group. Within the study area, the Edwards Group can be subdivided into several hydrostratigraphic units with different structural and hydrologic characteristics (Fig. 2) (Maclay and Small, 1976; Small et al., 1996).

1.5.2. Undeveloped caves

The undeveloped caves, Whirlpool Cave, Maple Run Cave and District Park Cave (Figure 3; hereafter referred to as WP, MR and DP respectively), are located in the

Edwards Group within the Barton Springs Segment of the Edwards Aquifer (Figure 2). The following is adapted from Hauwert (2009). Caves and solution cavities in the Barton Springs Segment develop preferentially along more soluble bedding planes and their orientation is controlled by fractures and faults. Horizontal passages generally develop in high permeability units and vertical passages typically develop in low permeability units and are often associated with fractures. These geologic controls are expressed in the geometry of the undeveloped caves.

WP is approximately 22,000 m^3 in size and is located in the Grainstone and Kirschberg members of the Edwards Limestone. After entering WP the passage quickly descends approximately 10 m though the less-permeable Grainstone member. The cave passage then enters the Kirschberg member and become relatively wide and horizontal. MR is approximately 600 m^3 in size and is located in the Leached and Collapsed, Regional Dense and Grainstone members of the Edwards Limestone. Much of MR is located in a large collapsed rubble pile, thus cave passage tends to be tortuous and vertical in nature. The collapsed geometry of MR is characterized by many small passages that are inaccessible to humans, but undoubtedly allow for significant air movement through the subsurface in the vicinity of the cave. DP, the smallest cave at only 100 m^3, is located in the Kirschberg member. Like WP, its passages are somewhat horizontal and wide.

1.5.3. Tourist caves

Natural Bridge Caverns is divided into two caves, Natural Bridge North (NBN) and Natural Bridge South (NBS) (Figure 3), located within the interbedded limestone and dolomitic units of the upper Glen Rose and lower Walnut formation, which are also Lower Cretaceous in age (Figure 2). NBN and NBS are approximately 250,000 m^3 and

150,000 m^3 in size, are more vertical as they descend through the Walnut Formation and become horizontal in the Glen Rose formation. The two caves are adjacent to each other, not well connected, and have separate entrances. The entrances of NBN and NBS are sealed by double glass doors that are only opened when tour groups enter and exit. Inner Space Cavern (IS) is approximately 75,000 m^3 in size and is located in the Cyclic and Marine members of the Edwards Group. The passages of IS are horizontal and no natural entrance to the cave presently exists (Figure 3). During development of IS for tourism, an entrance tunnel approximately 4 m in diameter was excavated, and remains unsealed. There are several sediment-filled sinks within the cave that suggest the cave was open to the atmosphere in the past (Slaughter, 1966). To increase visitor comfort, man-made ventilation shafts equipped with fans were installed in IS, NBN and NBS. Ventilation fans are manually operated and in use sporadically during operating hours (10:00-18:00 CST) during the warmer months (March-September).

1.6. CONTROLS ON CAVE-AIR CO_2 VARIABILITY

1.6.1. Cave ventilation

Cave ventilation is an important control on cave-air CO_2 concentrations, both seasonally and on shorter timescales and is dependent on multiple factors including fluctuations of the outside air temperature and barometric pressure, cave geometry and prevailing winds (e.g. Villar, 1985; Fernandez et al., 1986; Hoyos, et al., 1998; Buecher, 1999; Bourges et al., 2001; Spotl et al., 2005; Baldini et al., 2006; Denis et al., 2005; Bourges et al., 2006; Baldini et al., 2008; Kowalczk and Froelich, 2010). At mid latitudes, density differences between cave and atmospheric air caused by seasonal temperature variability exert a first order control on the seasonal ventilation of caves (James and Banner, 2008). In many caves, seasonal air temperature varies by only a few

degrees (Moore & Sullivan, 1997), thus cave ventilation is primarily controlled by surface air temperature and barometric pressure variability (Fairchild et al., 2006). During warmer months, cave air temperatures remain below atmospheric temperature, causing the cooler, denser cave air to stagnate and CO_2 to build up. The cave can be thought of as a semi-closed system during this time as ventilation is less efficient. As long as CO_2 sources are present (i.e. degassing of drip water or advection through fractures), the concentration of CO_2 in the cave air will continue to rise until CO_2 inputs reach equilibrium with CO_2 ventilation. When cave air temperatures are warmer than outside temperatures, the cave air becomes unstable with respect to the outside air and ventilation becomes more efficient as the denser outside air flows into the cave, mixing with and displacing the CO_2-rich cave air causing CO_2 levels within the cave to decrease. This process only applies to caves whose primary volume is lower in elevation than its entrance.

The intensity of cave ventilation is governed by cave geometry (i.e. vertical vs. horizontal, large passages vs. numerous constrictions), density differences between the cave air and outside air, distance from the cave entrance, connectivity with the surface via pores and fracture networks (primarily governed by the stratigraphic occurrence of the cave) and cave volume (Batiot-Guilhe et al., 2007). In general, stronger ventilation occurs at sites near the entrance and at sites that are not separated from the entrance by constrictions (Bourges et al., 2006). Where ventilation is limited by constrictions or distance from the entrance, CO_2 levels may remain relatively constant or continue to increase as a function of the rate of CO_2 inputs.

Diurnal ventilation is caused by barometric tides that have a periodicity of 12 and 24 hours, with the 24-hour fluctuations being the strongest (Melchior, 1993; Wallace and Hobbs, 2006). As barometric pressure increases, the pressure differential between the

atmosphere and cave forces outside air with a lower CO_2 concentration (~390 ppm) into the cave, and dilutes the high-CO_2 cave air causing a decrease in the CO_2 concentration. When barometric pressure decreases, the pressure differential is reversed and air flows out of the cave, drawing higher CO_2 air from deeper within the cave toward the entrance and causes the CO_2 concentration of the cave to increase. Evidence of such cave breathing and diurnal CO_2 fluctuations has been observed in Florida (Kowalczk and Froelich, 2010), Spain (Duenas et al., 2005; Fernandez-Cortes et al., 2009) and France (Bourges et al., 2006; Perrier and Richon, 2010).

1.6.2. Cave CO_2 sources

Known sources of cave-air CO_2 include decomposition of soil organic matter, root respiration, in-cave decomposition of organic matter, diffusion from deep sources, animal respiration, and degassing from CO_2-rich groundwater (Troester and White, 1984; Ek and Gewalt, 1985; Hanson et al., 2000; Baldini et al., 2006; Bourges; et al., 2001, Batiot-Guilhe, et al., 2007; Crossey et al., 2006). Soil respiration is likely the dominant source of soil CO_2 in the study area. The rate of respiration is affected by changes in soil temperature and soil moisture and the highest CO_2 production often occurs when soils are moist and in warm months (Amundson and Smith, 1988; Daly et al., 2008; Lloyd and Taylor, 1994; Raich and Schlesinger, 1992). The rate of CO_2 input into a cave is dependent on several factors that may vary on multiple timescales.

Degassing of CO_2-rich vadose water is a significant source of CO_2 in most caves. The concentration of CO_2 in vadose water is primarily controlled by the concentration of CO_2 in the soil air. As the water flows through the soil zone, it becomes enriched in CO_2 until the partial pressure of CO_2 (pCO_2) of the water is equal to the pCO_2 of the soil, or the water flows out of the soil zone. When CO_2-charged water comes into contact with a

lower pCO_2 environment (i.e. a cave), CO_2 degassing occurs and the air within that environment becomes slightly more CO_2 rich. Advection and/or diffusion of vadose zone air through fractures, cracks and dissolution cavities is also a significant means of transporting CO_2 to the cave atmosphere (Baldini et al., 2006; Batiot-Guilhe et al., 2007; Perrier and Richon, 2010)

CO_2 generated from decaying organic material within caves is a significant CO_2 source for caves that collect detritus or bat guano. The significance of this contribution of CO_2 is likely to vary, depending on the ability of a given cave to capture storm-washed debris or the presence of a significant bat population. Overland flows of water into a cave, sinkholes or soil piping features are required for a significant amount of organic debris to enter the caves that we monitored. Only DP receives significant amounts of organic debris via overland storm flow.

Animal respiration is another significant source of CO_2 in a cave environment, particularly in tourist caves. The concentration of CO_2 in a human breath is approximately 40,000 ppm (Miotke, 1974). A recent study of the impacts of respired CO_2 in a cave in the Czech Republic demonstrated that human respiration is a significant source of CO_2 that is proportional to the number of people in a cave and the duration of visits (Faimon et al., 2006). Likewise Linan et al. (2008) noted that cave CO_2 concentrations in Nerja Cave, Spain were correlated with visitation during certain times of the year. However, some data suggests that these elevated levels of CO_2 dissipate on hourly time scales (Faimon et al. 2006, Hoyos et al. 1998).

Three of the caves monitored (NBS, NBN, and IS) are tourist caves and receive <100 to >1,000 visitors per day, while the undeveloped caves receive few visitors. Visitation varies greatly but generally the greatest number of visits to the caves occurs in mid-March and the summer months (May-August). Other animals inhabiting caves will

affect CO_2 concentrations in similar ways, depending on population size. A few bats are commonly found in NBN, NBS, IS and MR, however not in numbers significant enough to be counted (Jim Kennedy, personal communication, April 8, 2009) or to significantly raise the concentration of CO_2 in the caves. Large mammals are unlikely to enter any of the undeveloped caves, as they are gated to exclude large mammals but allow for unimpeded airflow.

Degassing of CO_2 from phreatic water is another potential source within caves, especially where cave passages intersect the water table. Degassing occurs when high-pCO_2 phreatic water comes in contact with lower-pCO_2 air and will continue until the water reaches equilibrium with the air or it is removed from the low pCO_2 environment (i.e. flowing into a sump). Contribution of CO_2 from degassing of phreatic water will likely vary seasonally and in response to recharge events. Degassing of phreatic water might be a significant source of CO_2 in IS and NBN and NBS as they are known to flood when aquifer levels rise after particularly heavy rainfalls. Flooding of IS, NBN and NBS does not occur on a regular basis (i.e. seasonally) but only after prolonged periods of unusually wet conditions. A small stream flows through NBN periodically. Degassing of phreatic water is not likely a significant source of CO_2 in WP, MR and DP as they are located approximately 50 m above the phreatic zone and are not known to flood.

CHAPTER 2: SEASONAL AND SPATIAL VARIABILITY OF CAVE-AIR CO_2 IN CENTRAL TEXAS

2.1 ABSTRACT

The growth rate and composition of cave calcite deposits (speleothems) is often used as a proxy for past environmental change. There is, however, the potential for bias in the speleothem record due to seasonal fluctuations in calcite growth. The growth rate of speleothem calcite in Texas caves has been proposed to vary seasonally in response to density-driven fluctuations in cave-air CO_2, with lower growth rates in the warmer months when cave-air CO_2 is highest. The CO_2 concentrations in three undeveloped caves and three tourist caves 130 km apart were monitored to determine 1) if seasonal CO_2 fluctuations are unique to tourist caves, which have been modified from their natural state, and 2) the extent to which cave-air CO_2 is controlled by natural variations in cave geometry, stratigraphy, cave volume, and soils.

Nearly 150 lateral transects into six caves over three years show that CO_2 concentrations vary seasonally in five of the caves monitored, with peak concentrations in the warmer months and lower concentrations in the cooler months. The caves occur in six stratigraphic units in lower Cretaceous marine platform carbonate rocks of the Edwards Plateau and vary widely in volume (100 to 250,000 m^3) and geometry. Seasonal CO_2 fluctuations are found to be regional in extent and not due to human activity. Seasonal fluctuations are independent of cave geometry, volume, depth, soil thickness, and the hosting stratigraphic unit. Results indicate that seasonal variations in calcite deposition may introduce bias in the speleothem record, on at least a regional scale, and should be considered when reconstructing paleoclimate using speleothem proxies.

2.2 INTRODUCTION

It is important to understand the mechanisms that control speleothem growth and calcite composition. It has long been known that the concentration of CO_2 in cave air can affect the growth rate of speleothems (Holland et al., 1964) but until recently, the extent to which cave-air CO_2 fluctuations might introduce bias into the speleothem record was not fully appreciated. Recent studies in the United States (Banner et al., 2007), Austria (Spotl et al., 2005) and Ireland (Baldini et al., 2008) have demonstrated that there is potential for bias in the paleoclimate record due to changes in speleothem deposition rate and drip water chemistry cased by cave-air CO_2 fluctuations.

A recent study of calcite growth rates in four central Texas tourist caves reveals that in three of the caves, calcite growth rate varies seasonally and is inversely correlated with cave-air CO_2 concentrations (Banner et al., 2007). In the caves that experienced growth rate variations, calcite deposition peaked in the cooler months, when cave-air CO_2 concentrations were low, while in the warmer months, elevated cave-air CO_2 concentrations inhibited drip water degassing, resulting in a significant decrease or cessation of calcite deposition. The tourist caves are located approximately 130 km apart, suggesting that the potential for a regionally extensive seasonal bias in the speleothem record exists. Such regionally extensive biases in speleothem proxies (i.e. seasonal growth rate variability, isotopic shifts) might be incorrectly interpreted as a direct result of climate conditions, not as a result of speleothem deposition being affected by cave meteorology. Therefore, it is important to determine if seasonal cave-air CO_2 fluctuations in the central Texas caves are unique to the tourist caves, which are modified from their natural state and receive a large number of visitors, or if they are naturally occurring.

Seasonal CO_2 fluctuations in the tourist caves may result from 1) modifications to their natural connectivity with the surface atmosphere during their development for tourism, 2) the significant human visitation and/or 3) non-anthropogenic influences. Variations in non-anthropogenic factors such as cave volume, stratigraphic unit, cave geometry and soil thickness may also influence the extent and timing of ventilation. The hypothesis that seasonal CO_2 fluctuations in central Texas caves are regional in extent and not unique to tourist caves was tested.

The timing and magnitude of CO_2 fluctuations in the undeveloped caves, District Park, Whirlpool, and Maple Run (hereafter referred to as DP, WP and MR respectively) were compared with those measured in the tourist caves studied by Banner et al. (2007), Natural Bridge North Cavern, Natural Bridge South Cavern and Inner Space Cavern (hereafter referred to as NBN, NBS, and IS respectively). The undeveloped caves were chosen for comparison with the tourist caves because they are 1) centrally located between the tourist caves, 2) are formed in similar stratigraphic units as the tourist caves, 3) are overlain by similar soil and vegetation, 4) receive similar rainfall amounts, 5) experience similar surface temperature fluctuations, and 6) receive little visitation outside of the monitoring trips (Figure 1; Table 1).

2.3. METHODS

CO_2 concentrations were measured along transects from the entrance of each cave inward (Figure 3) using a portable Telaire 7001 CO_2 meter. Monitoring stations are described in Appendix A. From August 2006 to August 2007 a Telaire CO_2 meter was calibrated to an average atmospheric value of 380 ppm. Local atmospheric CO_2 concentrations likely differ from 380 ppm due to anthropogenic and natural variations, however these variations are likely within the instrument's range of uncertainty (50 ppm

or 5% of the total CO_2 concentration). Beginning in June 2007, a zero-point calibration was performed using argon gas. Atmospheric CO_2 concentrations were measured before and after each field transect to check for post-calibration drift. When a drift of greater than 100 ppm was detected, all data from that transect were considered unreliable and are not reported here.

Although all caves were monitored with varying frequency, ranging from weekly to monthly, each cave was visited multiple times during each season in order to assess seasonal variability. Cave-air CO_2 concentrations in IS, NBN and NBS were monitored on a 4-6 week basis from 2001 to May 2010. MR, WP and DP were each visited 2-4 times monthly between July 2006 and October 2007. No transects were taken in these caves from November 2007 to July 2008. In August 2008, monitoring resumed in these three caves and continued through July 2009.

Significant increases in CO_2 concentration due to operator respiration have been reported (Baldini et al., 2006). Due to the ruggedness of the undeveloped caves, it was impractical to wear CO_2 scrubbing respirators or other devices that remove exhaled CO_2 from where measurements were being taken. To account for operator bias, several experiments to estimate operator-caused bias were performed. Upon arriving at a measurement site, the initial CO_2 concentration was recorded. The operators then waited for a period of five minutes to determine if there was a rise in CO_2 concentration as a result of respiration. This experiment was repeated at several sites within each undeveloped cave. No increase in CO_2 concentration greater than the instrument error (±50 ppm) was measured and occasionally, small decreases (20-30 ppm) within instrument error were observed. Measurements reported here were typically recorded within two to three minutes of arrival at each site and no measurements were taken after

spending five minutes at a site. Based on this protocol, operator bias is considered to be insignificant compared to the magnitude of seasonal cave-air CO_2 fluctuations observed.

Total cave volume is reported for each cave (Table 1). All volumes are estimated from survey maps and physical measurements, and are presented herein to compare relative cave volumes. To facilitate comparison between caves and between visits to each cave, a cave-weighted mean CO_2 concentration was calculated for each transect:

$$\text{Eq. 2-1 weighted mean} = [(C_{s1} \bullet V_{s1}) + (C_{s2} \bullet V_{s2}) + \ldots..] / V_t$$

Where C_{s1} is the CO_2 concentration measured at site 1, V_{s1} is the volume of passage at site 1 and V_t is the volume of the whole transect. Because cave-air CO_2 concentrations are both temporally and spatially variable, the weighted means are reported as an estimation of the magnitude and timing of seasonal variability.

Soil thicknesses were measured above each cave by hammering a 1.7-meter stake with a radius of 1 cm into the soil until refusal (Table 1). Measurements were taken every ten meters along a sixty meter transect, and a minimum of three transects were measured at each cave. Average soil thickness ranging from 31 cm above Whirlpool Cave to 42 cm above Maple Run Cave (Table 1). Impervious cover was visually estimated by superimposing cave maps on satellite images of the land surface above the caves. Part of IS is overlain by engineered fill for Interstate Highway 35 that is several meters thick and approximately 35% of the cave is overlain by impervious cover. Cave NBN is overlain by approximately 20% impervious cover and Cave NBS is overlain by approximately 10% impervious cover. DP, WP and MR are not overlain by impervious cover.

2.4. RESULTS

The weighted mean of the cave-air CO_2 concentration is presented in Figure 4. Values used to calculate weighted mean are given in Appendix B. Daily average surface temperature measured at a National Climate Data Center weather station (COOP ID: 410428) located in Austin, Texas (Figure 4) are presented. The timing of seasonal CO_2 fluctuations was consistent between all caves, however the magnitude of CO_2 fluctuations varied considerably, especially between the undeveloped and tourist caves.

The concentration of CO_2 in the tourist and undeveloped caves show strong seasonal variability. CO_2 concentrations were lowest during the cooler season (November through April) and elevated throughout the warm season (May through October) and concentrations generally increased with increasing distance from the cave entrances (Figure 5). With the exception of MR, the average CO_2 concentration at each station was well correlated ($r^2 > 0.25$) with distance from the entrance (Table 1). At MR there is not a strong correlation between average CO_2 concentration at each station and distance from the entrance ($r^2 = 0.05$) however, there is a stronger correlation between average CO_2 concentration at each station and depth ($r^2 = 0.29$).

2.5. DISCUSSION

2.5.1. Regional controls of cave-air CO_2

Cave-air CO_2 concentrations varied significantly in all caves monitored. High CO_2 concentrations were measured during the warmer months and lower concentrations were measured during the cooler months (Figure 4). Likely, seasonal ventilation is driven by density differences between outside and cave air caused by seasonal atmospheric temperature fluctuations. If anthropogenic effects are responsible for the seasonal

fluctuations of cave-air CO_2, then significant CO_2 fluctuations would only occur in tourist caves; however, large seasonal fluctuations of cave-air CO_2 were observed in all caves.

Although seasonal fluctuations of cave-air CO_2 were observed in the undeveloped caves and tourist caves, visitation cannot be dismissed as a significant source of CO_2 to the tourist caves without closer examination. Visitation to all three tourist caves reaches a maximum during the summer, when cave-air CO_2 levels are most elevated. There are, however, two key observations that suggest visitor respiration is not the primary control on seasonal CO_2 fluctuations: 1) visitation rates peak in March and July each year, but CO_2 concentrations remain elevated throughout the summer and not in March and 2) the highest CO_2 concentrations occur in Cave NBS, the least visited tourist cave (Banner et al., 2007). These lines of evidence suggest that the seasonal CO_2 fluctuations observed in the tourist caves are indeed a natural phenomenon and not due to visitation.

It is also important to note that the tourist caves (IS, NBN and NBS) use ventilation fans to remove some of the CO_2-rich air from the caves during the summer months. No detailed record of fan usage exists, but preliminary data from logging CO_2 meters installed in both caves exhibit high summertime cave-air CO_2 concentrations with no intermittent excursions to near atmospheric values. Although diurnal CO_2 fluctuations >500 ppm were routinely detected, the maximum CO_2 concentrations were measured during the afternoon hours, when fans were typically turned on. The lowest CO_2 concentrations were typically measured during the overnight hours, when the ventilation fans were typically not in use. This suggests that CO_2 inputs are sufficient to maintain elevated concentrations throughout the warmer months, even though ventilation fans undoubtedly remove CO_2-rich air from the caves. Similar diurnal patterns were observed in all undeveloped caves for which logging meters were deployed.

There was significant variability in the magnitude of seasonal cave-air CO_2 fluctuations (Figure 4), but seasonal weather patterns cannot explain the inter-cave variability. All of the caves are located within 120 km of each other and experience similar seasonal weather patterns. Additionally, the three undeveloped caves are located within 5 km of each other and experience nearly identical seasonal and storm-scale weather patterns; yet the magnitude and exact timing of CO_2 fluctuations within these caves are not identical, suggesting that some site-specific parameters play a role in cave ventilation.

2.5.2. Site-specific controls of cave-air CO_2

2.5.2.1. Soils, vegetation and groundcover

Soil thickness does not appear to be an important control on cave-air CO_2 variability in the study area. If soil thickness were an important control on cave-air CO_2 concentrations, we expect to see variations in the average CO_2 concentrations at monitoring stations that are overlain by thicker soils relative to other stations in the same cave. At IS, sites ISHW and ISST are overlain by engineered fill that is several meters thick and sites ISDC and ISLM are overlain by much thinner soils (approximately 41 cm; Table 1). If soil thickness were an important control on cave-air CO_2 variability at IS, there would likely be a weaker correlation between CO_2 concentration and distance from the cave entrance due to the highly variable soil thickness above the cave. Instead, there is a strong correlation ($r^2 = 0.87$) between average CO_2 concentration and distance from the entrance (Figure 6).

The large difference in peak CO_2 concentrations at each cave suggests that soil thickness is not a major control on cave-air CO_2 concentrations in the study area. Soil type, thickness and vegetative cover is relatively uniform across the study sites, with the

exception of IS (Table 1); yet peak CO_2 concentrations vary by as much as 10,000 ppm between caves. This finding is best illustrated by comparing NBN and NBS. Soil thicknesses are similar above both caves (33 cm at NBS and 34 cm at NBN), and the caves are located adjacent to one another. Nevertheless, peak CO_2 values at NBN did not exceed 10,000 ppm at any site, while peak CO_2 values at NBS consistently exceeded 20,000 ppm during the summer months of 2006 and were consistently higher than the CO_2 concentration in NBN the following two summers (Figure 4). It is important to note that NBS and NBN are overlain by different amounts of impervious cover (approximately 10% of NBS and 20% of NBN), which could account for some of the intra-cave variability in peak CO_2 but likely not the magnitude observed.

2.5.2.2. Cave volume

The data suggest that cave volume is an important control on the magnitude of seasonal cave-air CO_2 fluctuations. With the notable exception of NBS, peak CO_2 concentrations in the tourist caves were significantly lower than the undeveloped caves (Figure 4). As a cave's volume increases its surface area to volume ratio decreases, thus larger caves will require a greater flux of CO_2 per unit of surface area to achieve the same magnitude increase in CO_2 concentration as a smaller cave. The soils in the study area are all similar in composition and thickness, so it is likely that the amount of CO_2 production per unit area above each cave is similar. Thus, the tourist caves might have a greater net flux of CO_2 into them compared to the undeveloped caves. However, the volume of the tourist caves relative to their footprint (the total area of surface directly overlying the cave passages) is much greater (Table 1), therefore the flux of CO_2 into the tourist caves per unit volume may actually be less than the flux of CO_2 per unit volume in the undeveloped caves. Cave-air CO_2 concentrations in the smaller caves rarely dropped below 4,000 ppm, the threshold above which Banner et al. (2007) noticed a significant

decrease in calcite growth. This suggests that smaller caves may have higher cave-air CO_2 concentrations on average leading to less speleothem growth than larger caves located in the same region.

2.5.2.3. Stratigraphy and cave geometry

In the study area, cave geometry is influenced by stratigraphy (Russell, 2007; Hauwert, 2009). For example, much of MR is within units that are more conducive to cave formation via leach and collapse (Rose, 1972) and mean CO_2 concentration is better correlated with depth of the monitoring stations than distance from the entrance (Table 1). The better correlation with depth might be attributed to the ease with which air can circulate through the rock units in which the cave is formed. Much of the cave is formed in a collapsed rubble pile with interconnected void space (Figure 2). Airflow within the subsurface near MR is likely not limited to the known cave passages, but also through the void spaces within the rubble pile that makes up much of the cave.

Initial results from high frequency monitoring at IS, MR and WP verify that strong seasonal CO_2 fluctuations do occur in all caves monitored with the exception of MR, which did not experience seasonal cave-air CO_2 fluctuations but did experience large diurnal CO_2 fluctuations (Cowan et al., 2009). The lack of seasonal fluctuations in MR can be attributed to diurnal ventilation of the cave caused by diurnal barometric pressure fluctuations and the porous geologic units that MR is located in. Air speed measurements taken at the cave reveal that a volume of air nearly 15 times greater than the volume of known passage is ventilated from MR during a 9-hour period. These daily ventilation patterns in MR appear to be due to the global "atmospheric tide" (Melcior, 1983; Wallace and Hobbs, 2006) that has been shown to affect cave meteorology (i.e. Sondag et al., 2003; Bourges et al., 2006). The apparent seasonality of cave-air CO_2 transects taken in

MR can be attributed to the timing of cave ventilation caused by seasonal shifts in the atmospheric tide and the timing of the visits, which typically occurred between 12:00 and 15:00 CST. Initial results from logging CO_2 meters confirm that CO_2 concentrations in IS and WP do fluctuate seasonally and diurnally. Logging CO_2 meters were only deployed in NBN for two months and recorded diurnal CO_2 fluctuations as well.

In contrast to MR, several other caves studied (WP, IS and NBN) are formed in stratigraphic units known for lateral cave development (Hauwert, 2009) and CO_2 concentrations in these caves is well correlated with distance from the entrance (Figure 6). It is important to note that the undeveloped caves form in different stratigraphic units than the tourist caves (Figure 2) and it is likely that the stratigraphic characteristics of the hosting and overlying units affect the ventilation and CO_2 inputs of the caves. Therefore, it is possible that the smaller seasonal cave-air CO_2 fluctuations in the tourist caves could be attributed to the stratigraphic units that the caves are located in, not their larger volumes. While the data suggests that stratigraphic controls in cave geometry (i.e. vertical or horizontally trending passages) does influence the spatial variability of CO_2 within the caves, more monitoring of a larger number of caves in a wide range of stratigraphic units is needed to fully understand the relative importance of this control on cave-air CO_2.

2.5.2.4. Distance from cave entrance

With the exception of MR, the cave-air CO_2 concentration was correlated with distance from the cave entrance (Figure 6). This is likely related to ventilation efficiency. As cooler outside air flows into a cave it will come into contact with the cave walls, which remain at a relatively stable temperature year round. As the denser outside air is continually warmed by the cave walls its density will decrease and ventilation will

become less efficient with distance from the entrance. This suggests that speleothems located nearer to cave entrances will experience lower CO_2 concentrations overall and thus may grow faster than speleothems located further from a cave entrance.

2.5.3. Implications for speleothem paleoclimate studies

Strong seasonal CO_2 fluctuations were detected in all caves monitored, suggesting that seasonal cave ventilation is a regional phenomenon. Elevated CO_2 concentrations were detected in all caves during the warmer months, and lower concentrations during cooler months. This observation implies that even in regions where proxies are regionally reproducible among spatially disparate records, seasonal fluctuations of cave-air CO_2 may cause a seasonal bias in calcite growth as higher calcite growth rates have been demonstrated to occur in cooler months (Banner et al., 2007). Higher concentrations of CO_2 in cave air can inhibit calcite deposition and, where drip water composition varies seasonally, might cause speleothems to be more reflective of drip water composition during times when calcite growth is faster due to lower cave-air CO_2 concentrations.

Hiatuses in speleothem growth are often assumed to indicate a decrease in drip rate, however, the possibility of non-growth during times when drip water is present should be considered. Banner et al. (2007) found that speleothem growth in three central Texas caves were well correlated with cave-air CO_2 concentrations and not drip water availability. Other studies corroborate this finding through direct measurement of water chemistry or calculations based on cave air measurements (Baldini et al., 2008 and Spotl et al., 2005). Such regionally extensive biases in speleothem proxies (i.e. seasonal growth rate variability, isotopic shifts) might be incorrectly interpreted as a direct result of climate conditions, rather than as a result of speleothem deposition being affected by cave meteorology. Seasonal changes in speleothem growth also indicate that there is

significant potential for improving temporal resolution in speleothem paleoclimate records.

2.6. CONCLUSIONS

Nearly 150 lateral transects into six caves over three years show that CO_2 concentrations vary seasonally in all of the caves monitored with peaks in CO_2 concentration in the warmer months and lower concentrations in the cooler months. These seasonal CO_2 fluctuations are attributed to seasonally variable cave ventilation that is controlled by atmospheric temperature fluctuations. Cave-air CO_2 concentrations are lowest in the cooler months due to stronger ventilation. In the cooler months when the outside air is cooler and denser than the cave-air, CO_2-depleted outside air sinks into the cave and mixes with the CO_2 rich cave air causing a decrease in the cave-air CO_2 concentration. In the warmer months, when the outside air is less dense, cave ventilation becomes much weaker and CO_2 concentrations increase.

Seasonal CO_2 fluctuations in the study area do not appear to be caused by anthropogenic influences including cave visitation. If anthropogenic influences were controlling seasonal CO_2 fluctuations in the study area, it would be unlikely that seasonal CO_2 fluctuations would occur in the undeveloped caves, as they have not been modified greatly and receive a relatively large number of visitors. Instead, the largest CO_2 fluctuations were observed in the undeveloped caves. As well, the timing of peak CO_2 concentrations in the tourist caves does not coincide with visitation, which peaks in March and July each year. Instead, CO_2 concentrations remain elevated throughout the summer and through September. Additionally, the highest CO_2 concentrations occur in Cave NBS, the least visited tourist cave.

Seasonal fluctuations were independent of cave volume, geometry, depth, soil thickness and hosting stratigraphic unit. Significant seasonal CO_2 fluctuations were measured in all caves; however, the magnitude of CO_2 fluctuations does appear to be influenced by cave volume and geometry. In general, the peak CO_2 concentrations in the smaller caves were much greater than peak concentrations in the larger caves. Additionally, the caves are located in seven distinct stratigraphic units. Portions of IS are overlain by engineered fill that is several meters thick, yet significant CO_2 fluctuations were measured in all the caves.

It is important to note that the presence of seasonal CO_2 fluctuations does not necessarily indicate that seasonal variations in calcite deposition rates are occurring. The rate of calcite deposition is dependent on the interplay of multiple factors including: temperature, CO_2 concentration, relative humidity, the concentration of calcium in the drip water and drip rate. The CO_2 concentration in some caves was seldom below 4,000 ppm, the concentration at which Banner et al. (2007) saw a decrease in calcite precipitation.

To understand modern and ancient variability of speleothem deposition it is essential that the mechanisms controlling cave ventilation be understood in greater detail. Future research should focus on seasonal and short-term variability (i.e. diurnal or storm scale) in cave ventilation, and the influence of ventilation on disequilibrium calcite precipitation or periods of cessation of calcite deposition. It is clear that continuous monitoring with logging CO_2 meters will help address the complexities of cave ventilation.

CHAPTER 3: DIURNAL AND STORM-SCALE CAVE-AIR CO_2 FLUCTUATIONS AND AIRFLOW THROUGH EPIKARST

3.1. ABSTRACT

The growth rate and composition of cave calcite deposits (speleothems) is often used as a proxy for past environmental change. There is, however, the potential for bias in the speleothem record due to fluctuations in calcite growth that are caused by fluctuations of cave-air CO_2 concentrations. A previous study in central Texas tourist caves attributed seasonal fluctuations of calcite growth rates to density-driven fluctuations in cave-air CO_2 caused by cave ventilation, highlighting the importance of understanding how cave-air CO_2 concentrations fluctuate on seasonal and shorter timescales. For this study, two tourist caves and two undeveloped caves were monitored at three hour intervals from October 2007 to December 2009 to determine 1) if cave-air CO_2 concentrations vary significantly seasonally and on shorter timescales, 2) what mechanism or mechanisms control cave-air CO_2 concentrations and 3) the extent that cave-air CO_2 is controlled by natural variations in cave geometry, stratigraphy, cave volume and soils.

Nearly 30,000 measurements taken over two years reveal that CO_2 concentrations vary on seasonal and diurnal timescales and in response to weather disturbances. Diurnal CO_2 fluctuations were nearly synchronous with diurnal barometric pressure fluctuations, with typical diurnal fluctuations in the undeveloped caves of approximately 10,000-15,000 ppm and typical diurnal fluctuations in the tourist caves of 500-1,500 ppm. The timing and magnitude of these fluctuations was greatly altered when weather disturbances passed through the area.

Caves in the study area are known to "breathe" diurnally due to barometric pumping. When barometric pressure decreased, air was sucked out of the caves and

when barometric pressure increased air was forced into the caves. One undeveloped cave ventilated at a rate of one cave volume every 34 minutes or over 10 times the cave volume ventilated daily, and the other at a rate of one cave volume every 504 minutes or nearly one cave volume ventilated daily. We present a conceptual model of airflow through epikarst in which significant subsurface airflow occurs not only in caves, but also through the fractures and dissolution cavities that are typical of a karst terrain. The findings suggest that significant diurnal and storm-scale CO_2 fluctuations occur in cave atmospheres potentially affecting the timing and amount of calcite deposition and consequently biasing the speleothem paleoclimate record.

3.2. INTRODUCTION

Because the use of speleothems as paleoclimate proxies is increasing, it is important to understand the mechanisms that control speleothem growth rate and composition. Although there are many such potential mechanisms, here we focus on the concentration of CO_2 in cave air. It has been long known that the concentration of CO_2 in cave air can affect the growth rate of speleothems (Holland et al., 1964) but it only recently became clear the extent to which cave-air CO_2 fluctuations might introduce bias into the speleothem record. Recent studies in the United States (Banner et al., 2007), Austria (Spotl et al., 2005) and Ireland (Baldini et al., 2008) have demonstrated that there is potential for bias in the speleothem record due to changes in speleothem deposition rate and drip water chemistry caused by cave-air CO_2 fluctuations.

The concentration of CO_2 in cave atmospheres is a function of the rate of CO_2 input into the cave, the rate of CO_2 diffusion from the cave atmosphere and the rate of air exchange between the cave and atmosphere (hereafter referred to as ventilation). Ventilation is the primary control on shorter-term (i.e. diurnal and storm event) cave-air CO_2 fluctuations and is caused by barometric pressure fluctuations and density

differences between cave and outside air (e.g. Villar, 1985; Fernandez et al., 1986; Hoyos, et al., 1998; Buecher, 1999; Bourges et al., 2001; Spotl et al., 2005; Baldini et al., 2006; Denis et al., 2005; Bourges et al., 2006; Baldini et al., 2008; Kowalczk and Froelich, 2010). Ventilation directly affects the concentration of CO_2 in cave air, which is known to influence parameters (i.e. saturation, pH, alkalinity) that effect calcite precipitation and may alter the elemental and isotopic composition of drip water and precipitated calcite (Hendi, 1971; Mickler et al., 2004, 2006). As well, higher concentrations of CO_2 in cave air can inhibit calcite deposition (Banner et al., 2007).

The calcite precipitation-dissolution equation is given below (Eq. 3-1):

Eq. 3-1: $Ca^{2+} + 2HCO^{3-} \Leftrightarrow CaCO_3 + H_2O + CO_2$

As Eq. 3-1 suggests, CO_2 degassing from drip water or the evaporation of water is necessary for calcite deposition to occur. As the CO_2 concentration of cave air increases, dripwater degassing can be inhibited and calcite deposition may slow or cease (Fairchild et al., 2006; Banner et al., 2007). This would introduce bias into a speleothem record, as drip water composition during times of non-growth is not recorded in speleothems. Alternatively, seasonal speleothem deposition might leave behind discernable annual banding, which might allow for seasonal resolution in many speleothem records. Other factors such as Ca concentration, relative humidity and temperature can affect calcite deposition, but in the study area the concentration of CO_2 in cave air is likely the dominant process (Banner et al., 2007). Because cave-air CO_2 concentration influences speleothem deposition, it is important that there is a thorough understanding of how CO_2 concentrations vary temporally and spatially, in the context of a single cave and

regionally. This knowledge will help elucidate the mechanisms that control cave ventilation, the concentration of CO_2 in cave air, and ultimately, speleothem growth.

The research questions addressed in the study area are: "What controls short-term (i.e. diurnal) cave ventilation?" and "Do the primary controls on ventilation vary temporally with season, weather conditions and/or other external forcing?" This study tests the hypothesis that short-term fluctuations of cave-air CO_2 are caused by variations in cave ventilation primarily controlled by fluctuations in atmospheric temperature and pressure. To test this hypothesis, logging CO_2 meters were deployed in four caves located on the Edwards Plateau in central Texas. These caves are ideally suited for this approach as they are located up to 120 km apart and vary widely in size and geometry. To determine the mechanisms that control cave CO_2 fluctuations in the study area, CO_2 concentrations were compared with local meteorological conditions.

3.3. METHODS AND STUDY AREA

Cave-air CO_2 concentrations were measured at several stations within Inner Space Cavern, Natural Bridge North Cavern, Maple Run Cave and Whirlpool Cave (Figure 1 and Figure 7; referred to hereafter as IS, NBN, MR, and WP respectively) with Vaisala GM70 hand-held carbon dioxide meters. The CO_2 concentration is measured via infrared absorption technology as air diffuses into the probe chamber. Accuracy is within ±20 ppm CO_2 or 2% of the reading, whichever is larger, and long term stability is <±5%/2 years according to the manufacturers specifications. All meters were factory calibrated at least every two years and most were factory calibrated at least once every year. Meters were replaced with a fully charged unit every 3-5 weeks, data was retrieved, and accuracy and maintenance checks performed. Occasionally values >100 ppm below atmospheric (385 ppm) or well above the typical range for the cave environment (>32,000 ppm) were recorded, typically these values occurred as single point outliers such that the rate of CO_2

increase or decrease could not be explained by natural processes; these values are considered erroneous and are not considered herein.

Readings below 385 ppm are considered erroneous as this value represents the average atmospheric CO_2 concentration for the duration of the study as measured by the National Oceanic and Atmospheric Administration (NOAA) at a network of globally distributed monitoring sites (www.ncdc.gov). It is likely that photosynthetic and anthropogenic factors slightly alter the local atmospheric CO_2 concentration; however, a study of the temporal and spatial variability of CO_2 concentrations in Essen, Germany (comparable in size to Austin, Texas) reveals that local atmospheric variability is small (typically 50 ppm) and typically within the error of the meters (Henninger, 2008).

Erroneous readings were likely due to a variety of reasons including electronics failure, tampering, and most often, condensation on the probe tip due to the high humidity cave environment, which interferes with infrared absorption readings that the meters use to calculate CO_2 concentrations. A small number of erroneous data points are typical of Vaisala meters deployed in caves (approximately 5-10 during a typical length deployment during this study); however, if a significant number (>10) of erroneous values were recorded during the deployment of a meter, all data from that deployment are considered unreliable and are not reported here. After removal from the humid cave environment and an appropriate drying period, meters were tested for accuracy using nitrogen gas and a flow-through chamber. Meters giving erroneous readings were sent for factory repair and recalibration. See Appendix A for a detailed description of these procedures.

To ensure that changes in CO_2 concentration were accurately captured with three hour logging intervals, cave-air CO_2 concentrations were initially logged at 30-minute intervals. Thirty minute logging intervals continued from November 2007 through

January 2008. In February 2008 the logging interval was increased to one hour and this interval was maintained through October 2008. In November 2008, all logging intervals were increased to three hours. When comparing the structure of CO_2 concentration curves, no significant difference was detected between the different logging intervals. For this reason the three-hour logging interval was continued for the remainder of the study. See Appendix A for a complete list of stations and a more detailed description of the meters, data collection and maintenance.

This study primarily focuses on five monitoring sites, two located within IS (ISST and ISLM), MR3 and WP7 (Figure 7). Two additional sites in WP (WP3 and WP5) and one site in NBN (NBCT) were monitored for a short time and are discussed in more detail below. The two sites within IS, ISST and ISLM, are located 260 m and 460 m from the cave entrance respectively and monitoring began at both sites in November 2007. The ISST station is located approximately 5 meters from the tourist trail and is behind a large flowstone formation that is approximately 5 meters in diameter. The ISLM station is located approximately 10 meters from the tourist trail. Neither station recorded distinguishable increases in CO_2 when tour groups were present, suggesting that they were not greatly influenced by the respiration of cave visitors. The site located within NBN (NBCT) is approximately 200 m from the cave entrance and was installed in March 2008 but only maintained through May 2008. Glass doors seal the entrances to NBN. The site located within MR (MR3) was installed in November 2007, is approximately 22 m from the entrance and the passage leading from the entrance to MR3 is very narrow and tortuous. There are three monitoring stations in WP (WP3, WP5 and WP7), however only one site (WP7) was monitored long term. WP3 and WP5 were monitored from 8/18/2009 to 9/20/2009 and are located approximately 20 m and 60 m from the cave entrance respectively. This short deployment was meant to determine how

the timing and magnitude of CO_2 fluctuations changed with distance from the entrance. Station WP7 is approximately 100 m from the entrance and was established in October 2008. Due to meter malfunctions, theft and vandalism, only limited data is available for this station. To determine the CO_2 concentration within the epikarst surrounding the caves, CO_2 measurements were also taken at the openings of various fractures and dissolution cavities within each cave.

All weather data was obtained from the following National Climate Data Center (NCDC) weather stations that report hourly data: 1) New Braunfels Municipal Airport station (COOP ID: 416275), 15 km from NBN and NBS, 2) Georgetown Lake station (COOP ID: 413507), 8 km from IS and 3) Camp Mabry weather station (COOPID: 410428), 14 km from MR and WP. The weather data may all be accessed at http://www.ncdc.noaa.gov). Relative humidity readings were not reported for the stations selected however dew point and temperature were reported for all stations. Relative humidity (RH) was calculated as follows:

$$\text{Eq. 3-2: } RH = V_p / SV_p$$

$$\text{Eq. 3-3: } SV_p = SV_{p0} \exp(lv/Rv*(1/T_0 - 1/T_D))$$

$$\text{Eq. 3-4: } V_p = SV_{p0} \exp(lv/Rv*(1/T_0 - 1/T))$$

Where RH is relative humidity, V_p is the vapor pressure of water in the air, SV_p is the saturation vapor pressure of water in the air, SV_{p0} is the reference saturation vapor pressure at 0°C, lv is the latent heat of vaporization of water (2.5×10^6 J/kg), Rv is the gas constant for water vapor (461.5 JK/kg), T_0 is the reference temperature (273.15 K), T_D is the measured dew point temperature (in K) and T is the measured air temperature (in K).

The difference between the cave moist-air density and atmospheric moist-air density was calculated (after James and Banner, 2008) and compared to CO_2 fluctuations for several time intervals and correlation analysis was performed. Moist-air density was calculated as follows:

Eq. 3-5: $\rho=[P*(1+XM)]/[R*(T+273.15)*(1+1.16078*XM)$

Eq. 3-6: $XM = 0.622*VP/(P-VP)$

Eq. 3-7: $VP = RH*SVP/100$

Eq. 3-8: $SVP = 0.61121*e^{[17.67*T/(T+243.5)}$

Where ρ is the moist air density, P is the barometric pressure (kPa), XM is a mixing ratio, R is the gas constant for dry air (2.870×10^2 J/(kg*K)), T is temperature (C), VP is vapor pressure, SVP is saturation vapor pressure and RH is relative humidity. When the outside air density is greater than the cave air density ($\rho_{cave} < \rho_{outside}$) density driven ventilation is expected to occur, and when the cave air is denser than the outside air ($\rho_{cave} > \rho_{outside}$) it is not. No logging temperature or barometric pressure probes were deployed in the cave. Thus, for density calculations we assume the cave barometric pressure is the same as the outside pressure and the average cave air temperature measured during each time interval examined was used for density calculations. The use of average cave air temperatures is considered appropriate for air density calculations as cave air temperatures typically vary by only a few degrees annually and the time intervals chosen were between one and two months in duration.

The volume of air ventilated from WP and MR on 12/29/2009 and 2/25/2010 respectively was calculated from measured air speeds at the cave entrances. Several

measurements were taken using a Kestrel 4300 hand-held anemometer. The operational range of the anemometer is 0.8-60 m/s with a resolution of 0.1 m/s. Most caves in the region are known to have periods of sustained outward and inward flow, or "breathe," on a daily basis. Airflow measurements were taken at the cave entrances beginning when a sustained outgoing air current was detected and continued approximately every two hours until a reversal in airflow direction was measured. The areas of the cave entrances were measured and the volume of air exiting the caves was calculated (Table 2). A Vaisala logging CO_2 meter was placed at each entrance and the CO_2 concentration of the air exiting the cave was measured for the duration of air speed measurement. Air speeds at the entrance of IS were below the range of the anemometer on all occasions that measurements were attempted and airspeeds at NBN were not recorded as the entrances are sealed by glass doors.

The effective volume of epikarst ventilated by the entrances of MR and WP was calculated using as follows:

Eq. 3-9: $P_1V = n_1RT - [P_2V = n_2RT]$

Eq. 3-10: $(P_1-P_2)V = (n_1-n_2)RT$

Eq. 3-11: $\Delta P(V) = \Delta nRT$

Eq. 3-12: $V = (\Delta n/\Delta P)RT$

Where P_1 is the barometric pressure outside the cave at the beginning of cave exhalation, P_2 is the barometric pressure outside the cave at the end of cave exhalation, ΔP is the change in barometric pressure outside the cave from the beginning of cave exhalation, n_1 and n_2 cannot be directly measured, but Δn, the molar volume of gas exhaled from the cave, was estimated from the measured volume of gas ventilated from the cave during exhalation assuming that the gas behaves as an ideal gas at STP (22.41 L/mole of gas), R is the ideal gas constant (8.314 m^3-Pa/mol-k), T is the ideal

temperature (273.15 K), and V is volume of voids within the epikarst ventilated at the cave entrance.

A novel airflow tracer test was conducted in two caves near MR and WP. Barker Ranch Cave and Blowing Fern cave were selected for this test because they are located approximately 200 meters apart, are known to have significant airflow and are both in some of the same geologic units as WP and MR. The elevation of Barker Ranch Cave is approximately 5 m lower than Blowing Fern. A large quantity of incense was burned in Barker Ranch Cave and the arrival of the incense fragrance at Blowing Fern Cave was timed. If detected at Blowing Fern Cave, the fragrance of incense would indicate airflow through the fracture and dissolution cavity network within the epikarst separating Barker Ranch and Blowing Fern Cave.

3.4. RESULTS

All caves experienced diurnal CO_2 fluctuations (Figure 8), and with the exception of MR, experienced seasonal CO_2 fluctuations (Figure 9). The timing of diurnal CO_2 fluctuations within all caves was nearly identical. Maximum concentrations were typically reached between 14:00 and 18:00 CST each day and minimum concentrations were typically reached between 00:00 and 06:00 CST each day. Typical diurnal fluctuations in the undeveloped caves (MR and WP) were approximately 10,000-15,000 ppm whereas typical diurnal fluctuations in the tourist caves (IS and NBN) were 500-1,500 ppm. Correlation analysis reveals that neither outside temperature nor pressure exerted a dominant control on cave-air CO_2 concentrations at all times (Table 3). All correlation values reported are considered statistically significant ($p < 0.03$).

Lateral CO_2 transects measured from entrances into cave interiors show that cave-air CO_2 concentrations were most elevated at monitoring stations furthest from the cave entrances. For example, CO_2 concentrations at ISLM were typically greater than at ISST,

which is approximately 200 meters closer to the cave entrance. This trend was more evident in warmer months when CO_2 levels were elevated (Figure 11). From 8/18/2009 to 9/20/2009, when three logging meters were deployed in WP, CO_2 concentrations were elevated at stations furthest from the cave entrance relative to those measured at stations closer to the cave entrance (Figure 12). As distance from the entrance increased, cave-air CO_2 became less correlated with outside temperature and better correlated with barometric pressure (Table 4). Rarely, CO_2 concentrations at stations further from the cave entrances were less than or equal to concentrations at stations closer to the entrances, suggesting that cave ventilation had become sufficiently strong to ventilate deeper stations at the same rate as stations near the entrances. These deep ventilation events were typically associated with cooler surface temperatures and/or significant changes in barometric pressure (i.e. Figure 10).

Figures 13A through 13D compare cave-air CO_2 concentrations with atmospheric and cave air density for caves IS, MR and WP. If density-driven ventilation were controlling diurnal CO_2 fluctuations, we expect cave CO_2 to be lowest when the outside air is more dense than the cave air causing outside air to flow into the cave and mixing with and displacing the higher CO_2 cave air. In general, diurnal CO_2 fluctuations are not well correlated with diurnal fluctuations in air density; however, when a three-day running mean of density and CO_2 was taken, CO_2 was typically better correlated with density, especially during the cool season (Figure 14). During the warmer season, when outside temperatures were always well above cave air temperatures, cave-air CO_2 was often better correlated with barometric pressure than air density (Figure 14).

Cave ventilation measurements were taken at the entrances of WP and MR on 12/29/2009 and 2/26/2010 respectively. Measurements taken at WP revealed that the cave ventilated at a rate of one full cave volume every 504 minutes. At MR the cave

ventilated at a rate of one full cave volume approximately every 33 minutes. It is important to note that the caves each have only one entrance, there were no airflow reversals during the measurement period and only airspeed measurements taken during sustained outward airflow were used for these calculations. During the airspeed measurements, logging CO_2 meters were deployed inside WP and MR near the entrances. The CO_2 concentration of the air exiting both caves steadily rose once sustained outward airflow began and continued to rise until sustained outward airflow ceased (Figure 15). When cave airflow reversals occurred (air began flowing into the cave) the concentration of CO_2 at the cave entrances dropped to atmospheric values within 5 minutes.

3.5. DISCUSSION

In a karst setting such as the Edwards Plateau, the subsurface is highly permeable to fluids and caves often act as conduits for rapid fluid flow from the surface to the subsurface. The data presented here suggests that caves also act as conduits for the rapid flow of air (a fluid) between the subsurface and surface. Significant diurnal CO_2 fluctuations were detected in all caves studied (Figure 8). Typically CO_2 was lowest during the overnight hours through the early morning hours (00:00-06:00 CST) and highest during the afternoon and early evening hours (14:00-18:00 CST). This diurnal cycling of CO_2 is likely caused by daily ventilation of the caves, or "cave breathing", which is a well know phenomenon in the study area. These patterns of airflow also occur even when no density-driven ventilation is expected to occur ($\rho_{cave} > \rho_{outside}$), suggesting that diurnal barometric pressure fluctuations, not density-driven flow, are the cause of diurnal cave ventilation in the study area. If density-driven flow were causing diurnal ventilation, there would likely be bi-directional air flow at the cave entrances as warmer cave air would rise out of the caves and be replaced by cooler atmospheric air.

3.5.1. Diurnal barometric ventilation

In the study area, cave air flow is dominated by barometric tides and generally flows out of the caves from early morning (06:00-09:00 CST) to late afternoon (15:00-18:00 CST) and then reverses direction, flowing into the caves from late afternoon to early morning. Barometric tides are a well know global phenomenon (Melchior, 1983; Wallace and Hobbs, 2006) that has been shown to affect cave meteorology (i.e. Sondag et al., 2003; Bourges et al., 2006). As barometric pressure increases, the pressure differential between the atmosphere and cave forces outside air with a lower CO_2 concentration (~385 ppm) into the cave, displacing and diluting the high-CO_2 cave air, causing a decrease in cave-air CO_2 concentrations. When barometric pressure decreases, the pressure differential is reversed and air flows out of the cave, drawing higher CO_2 air from deeper within the cave toward the entrance and causing cave-air CO_2 concentrations to increase. Hereafter this phenomenon is referred to as "barometric pumping" (after Perrier and Richon, 2010).

CO_2 concentrations measured at the entrances of cave WP and MR, with airspeeds measured simultaneously, offer more compelling and detailed evidence for barometric pumping (Table 2; Figure 15). During airspeed measurements, the CO_2 concentration of air near the entrance both caves were lowest just before outward airflow became sustained. The CO_2 concentration then steadily increased until cave airflow direction reversed. This continual increase of CO_2 is likely due to the exhalation of air sourced from deeper within the cave as time elapsed. When air began flowing into each cave, the CO_2 concentration at the entrance dropped to near atmospheric concentrations within five minutes, confirming that low-CO_2 outside air was indeed mixing with and displacing cave air.

The simultaneous deployment of three logging CO_2 meters within WP and two within IS further support the hypothesis that barometric pumping is the primary cause of diurnal CO_2 fluctuations. All stations throughout the length of caves WP and IS experienced significant diurnal CO_2 fluctuations, suggesting that cave ventilation is not limited to portions of a cave located near the entrance (Figure 11, Figure 12). The magnitude of CO_2 fluctuations, however, did increase with distance from the cave entrance. During times of airflow into caves, stations nearest to the entrance reached minimum CO_2 concentrations prior to stations located furthest from the entrance; whereas during times of exhalation, peak CO_2 concentrations were reached by deeper stations prior to those nearer to the entrance. This lag time in reaching minimum and maximum concentrations was more pronounced in IS where the stations are located a much greater distance from one another and from the cave entrance as compared to WP (Figure 7).

The influence of air density on CO_2 fluctuations appears to become larger over longer timescales. Cave-air CO_2 was typically weakly correlated with air density, but when a three-day running mean of density was taken, CO_2 was typically better correlated with air density (Figure 13; Figure 14). Contrasts between cave air and outside air density exerts a more significant control on cave ventilation during the cooler months, when outside air temperatures are usually near or lower than cave air temperatures. Barometric pressure seems to exert a more significant control on cave ventilation during the warmer months, when cave air is almost always more dense than outside air. This is supported by the greater correlation between cave-air CO_2 and air density during the cooler months and the greater correlation between cave-air CO_2 and barometric pressure during the warmer months (Figure 14).

3.5.2. Cave-specific controls on ventilation

All study caves except MR experienced seasonal fluctuations of cave-air CO_2 concentrations (Figure 9). The lack of seasonal cave-air CO_2 fluctuations in MR can be explained by efficient diurnal ventilation at the cave. Cave ventilation measurements at MR reveal that nearly 16 times the cave volume exited the cave during the nine-hour monitoring period. Assuming that ventilation is a daily phenomenon, it is likely that CO_2 concentrations in the subsurface near MR are not able to build up as the rate of CO_2 production in the soils overlying the area might be outpaced by the rate that CO_2 is expelled from the subsurface. In contrast to MR, less than one cave volume is expelled from WP and IS on the days that airspeed measurements were taken. If airspeed measurements taken at IS and WP are representative of diurnal ventilation at both caves, then it is reasonable to assume that the rate of CO_2 production near those caves is able to match or exceed the rate that CO_2 is expelled from the subsurface.

The large discrepancy in ventilation efficiency between MR and WP could be attributed to the physical characteristics of the stratigraphic units that the caves are located within (Figure 2). Much of MR is located within the Leached and Collapsed member, which is highly-permeable unit formed by the dissolution and subsequent collapse of the units that make up the member; thus, much of MR's passages are formed within the pore spaces of a large rubble pile. As a result, MR and the surrounding epikarst are well ventilated (Table 2). In contrast, WP is formed mostly within the Kirschberg member, which is known for more conduit-like cave development. This more conduit-like geometry leads to less efficient ventilation at WP (Table 2) as much of the airflow is focused within the cave passages and not through highly porous stratigraphic units like at MR.

The timing of diurnal CO_2 cycling is similar in all caves studied, but the magnitude of diurnal CO_2 fluctuations in the tourist caves (IS, and NBN) are much less than the magnitude of fluctuations in the undeveloped caves (MR and WP). This difference may be attributed to cave volume as the tourist caves have a much greater volume than the undeveloped caves (Table 1). As the volume of a cave increases, its surface area to volume ratio decreases, thus there is less surface area per unit volume of cave passage for CO_2 to enter into the cave as gaseous flow through fractures or degassing from drip water. As well, the vegetation and soil types and thicknesses in the study area are all similar (Table 1) and the study sites experience nearly identical climatic conditions, so it is likely that the amount of CO_2 production per unit area above each cave is similar. Due to the size of the cave footprints I expect the tourist caves to have a greater net flux of CO_2 from the soil zone compared to the undeveloped caves. However, the volume of the tourist caves relative to their footprint is much greater (Table 1), therefore the flux of CO_2 into the tourist caves, per unit volume, may actually be less than the flux of CO_2 into the undeveloped caves.

3.5.3. Subterranean airflow in karst settings

Airspeed measurements taken at WP and MR show that the caves ventilated at a rate of one full cave volume every 504 minutes and 34 minutes respectively during one continuous exhalation (Table 2). It is unlikely that the exiting cave air was replaced by air derived directly from the surface as there is only one entrance to each cave, no airflow reversals were detected and cave-air CO_2 concentration increased when barometric pressure decreased. As well, the barometric pressure above each cave is spatially uniform at any given time, thus any other unknown connections to the surface would experience similar pressure gradients as the entrances (i.e. would blow out). Exiting air must be replaced by air from another source. Likely, the exiting air was replaced by air

flowing into the cave through the network of fractures and conduits that are connected to the cave.

The subsurface in karst areas are filled with many interconnected fractures and cavities that act as conduits through which large quantities of water can flow. The incense tracer experiments suggest that the same is true for gasses, especially when a pressure gradient is present (i.e. fluctuating barometric pressure). The scent of incense was detected at Blowing Fern cave 16 minutes after lighting in Barker Ranch Cave. Assuming that the air took a straight flow path between Barker Ranch Cave and Blowing Fern Cave and that little dispersion or diffusion took place, the average velocity of airflow through the epikarst was 12.5 m/min. It is unlikely that the airflow between the caves was along a straight path and that little dispersion and diffusion took place; therefore the calculated velocity represents a lower limit of airspeed within the epikarst at the time of the experiment. Other underground air tracer experiments using smoke have been conducted near the study area in the central Texas region and confirm that air is able to move several meters laterally through the subsurface (Taucer and Munster, 2005).

Radon exhalation fluxes from the walls of a tunnel in the French Alps were correlated with barometric tides, suggesting that barometric pumping was driving advective transport of air from fractures into the tunnel (Richon et al., 2007). In almost every instance, CO_2 concentrations were higher in fractures and voids than in the cave passage that they connected to. Alone this would not be sufficient evidence to support the hypothesis; however, diurnally-cycling CO_2 concentrations, the air tracer experiment and the discrepancy between the cave volumes and the volumes of air exiting the caves all suggest that higher CO_2 air is flowing into the cave. The most likely source of this high CO_2 air is from the network cavities and fractures in the surrounding epikarst.

Because air is present in the caves at all times, it is reasonable to assume that the air expelled from the caves during diurnal cave ventilation is replaced by air from fractures and cavities that are connected to the caves. It is therefore possible to estimate the volume of ventilated epikarst void space using the volume of gas that is ventilated by the caves during one exhalation and the change in barometric pressure (Eq. 3-12). Because ventilation rates were only determined at WP and MR, this discussion is limited to those caves. The estimated volume of void space ventilated at the entrance to WP is 4.61×10^6 m^3 and the volume of void space ventilated at the entrance of MR is 2.19×10^6 m^3 (Eq. 3-12). These ventilated volumes are several orders of magnitude greater than the volume of the caves (Table 1). These calculations further suggest that the volume of epikarst affected by diurnal cave ventilation far exceeds the volume of the caves themselves, supporting the hypothesis that significant airflow occurs in the subsurface in the study area.

3.5.4 Conceptual model of cave ventilation

The following description and Figure 16 summarize a conceptual model of subterranean airflow in the study area. Barometric pumping caused by diurnally fluctuating barometric pressure is the primary control on ventilation of caves in the study area. The flow of air into and out of caves in the region is known to reverse twice every 24 hours (except when weather fronts or other disturbances move through the region) and these reversals coincide with daily maximum and minimum barometric pressure. In essence, caves in the region are "breathing" due to barometric pressure fluctuations, with "exhalations" from the caves occurring when barometric pressure is falling and air is pulled from the subsurface to replace the exhaled air. "Inhalations" then occur when barometric pressure rises, forcing air into the subsurface. This daily breathing causes airflow within the caves to act much like a piston. During inhalations, higher-CO_2 cave

air is displaced away from the entrance as low CO_2 atmospheric air is forced into the cave by rising barometric pressure. This influx of atmospheric air lowers the CO_2 concentrations within the cave and this effect is greater near the cave entrance. To accommodate the large volume of air entering the cave (which has a fixed accommodation volume), pre-existing cave air is forced into the network of fractures and cavities that connect the cave to the surrounding epikarst. During exhalations, falling barometric pressure sucks air from the cave, causing air to flow from deeper within the cave and from fractures and cavities to replace the volume of air that was ventilated. Because air deeper within the cave and from fractures and cavities has a higher concentration of CO_2, the concentration of CO_2 within the cave increases during the exhalation. The daily repetition of cave breathing leads to the significant diurnal cave-air CO_2 fluctuations that are typical of most studied caves in the region.

3.6. IMPLICATIONS

The results show that cave ventilation is both dynamic and prevalent, occurring on seasonal and diurnal timescales and that consideration should be given to these processes when interpreting paleoclimate based on speleothem proxies. Often, hiatuses in speleothem growth are assumed to indicate a decrease in rainfall, however, the possibility of non-growth or slower growth due to elevated cave-air CO_2 should be considered. Banner et al. (2007) found that seasonal changes in speleothem growth rate in three central Texas caves were controlled by cave-air CO_2 concentrations and not drip water availability. Other studies corroborate this finding in other regions through inferences based on water chemistry or cave air measurements (Baldini et al., 2008; Spotl et al., 2005). In settings where cave-air CO_2 fluctuates seasonally and drip water availability does not limit speleothem growth, it is possible that geochemical proxies for rain, temperature, etc might only preserve the cool-season record.

Perhaps the most exciting implication of this study is that some speleothems might yield very high resolution data. Seasonal or even daily hiatuses in growth might act as markers, allowing for higher temporal precision that would yield records with sub-annual resolution. An excellent candidate for such analysis would be a fast-growing speleothem that is fed by a drip source that is highly responsive to climatic conditions. A less hydrologically responsive drip would be less desirable for such an analysis as a long residence time might average out seasonal or shorter-term changes in drip water chemistry due to mixing and more extensive water-rock interaction.

Geomorphic changes, such as the opening and closing of cave entrances, might also affect cave ventilation patterns and subsequently, calcite deposition rates. Likely, most exchange between cave air and atmospheric air occurs through cave entrances, therefore, the opening or closing of a cave entrance will have a profound impact on cave ventilation, particularly in caves that have only one entrance. The closing of a cave entrance will essentially slow the exchange of air between the cave and atmosphere and lead to stagnation of the cave air and an increase in the concentration of CO_2. Persistent elevated CO_2 concentrations might inhibit calcite deposition, despite the presence of active drips, leading to a "gap" in the speleothem record that could be interpreted as a lack of drip water due to a drying event.

It is important to understand that cave meteorology is highly complex and can be affected by a multitude of variables. This study also highlights the variability in cave ventilation and CO_2 patterns, even in caves within a small geographic region like the study area. However the results do suggest that it is possible to make some inferences as to how cave ventilation varies based on cave characteristics. Cave volume was shown to be an important factor controlling the magnitude of CO_2 fluctuations, both seasonally and

diurnally. As well, distance from the cave entrance also impacts ventilation patterns significantly.

It is likely that the relative significance of the parameters affecting cave ventilation and CO_2 production vary by region, geology and cave system. However, further study in different settings might uncover some commonalities that could be applied widely to paleoclimate studies (e.g. James and Banner, 2010). In addition to determining if diurnal cave-air CO_2 fluctuations are a global phenomenon, future studies should also focus on constraining how CO_2 inputs vary based on climate, overlying vegetation and geological setting. As well, a better understanding of how drip water chemistry responds to diurnal, storm-scale and seasonal CO_2 fluctuations might help determine the extent of bias in the speleothem record or lead to better temporal resolution (i.e. seasonal or potentially daily) in climate reconstructions. Ultimately, it may be possible to develop a robust model capable of predicting the magnitude of CO_2 fluctuations in caves around the globe. Such models might also be combined with a geochemical model to predict the extent of bias in a speleothem record caused by cave-air CO_2 fluctuations.

Table 1. Characteristics of monitored caves and overlying soils. No r^2 value was calculated for DP as there are only two stations in the cave. Asterisk denotes that r^2 value is calculated for average CO_2 and depth from surface.

Cave Name	Cave Volume (m^3)	Footprint/ Volume	Overlying Soil Thickness & <Stdev>	USDA Soil Type	Tourist Cave	Storm-washed Debris	Min/Max CO_2 (ppm)	r^2 Average CO_2 Distance From	Transect Length (m)
Inner Space Caverns (IS)	>100 000	0.03	0.41 <0.18>	Silty clays & stony clays	Yes	None	400/7,600	0.87	450
Natural Bridge Caverns North (NBN)	>100 000	0.03	0.34 <0.26>	Stony clay & gravely clay loam	Yes	None	370/9,500	0.79	200
Natural Bridge Caverns South (NBS)	>100 000	0.04	0.33 <0.19>	Stony clay & gravely clay loam	Yes	None	470/38,000	0.25	400
Whirlpool Cave (WP)	22 000	0.67	0.31 <0.22>	Stony clay loam	No	None	420/22,000	0.84	125
Maple Run Cave (MR)	450	0.09	0.42 <0.14 >	Stony clay loam	No	Little	570/23,000	0.05 0.29*	42
District Park Cave (DP)	100	0.15	0.4 <0.17>	Stony clay loam	No	Significant	500/31,000	n/a	5

Table 2. The volume of air ventilated from WP and MR during one cave exhalation.

Ventilation Measurements at WP		**Ventilation Measurements at MR**	
Measurement Time (CST)	Volume ventilated (m^3)	Measurement Time (CST)	Volume ventilated (m^3)
8:15	Sustained outward airflow begins	8:45	Sustained outward airflow begins
8:50	1,598	9:15	1,151
10:55	5,817	11:47	2,173
13:10	4,049	13:55	3,964
15:05	3,892	15:00	1,656
15:50	5,588	17:20	569
16:15	Sustained outward airflow ends	17:30	Sustained outward airflow ends
Volume of air ventilated	20,944 m^3	**Volume of air ventilated**	9,513 m^3
Cave Volume	22,000 m^3	**Cave Volume**	600 m^3
Vetilation Rate (min to ventilate full cave volume)	504.3	**Vetilation Rate (min to ventilate full cave volume)**	33.5

Table 3. Correlation between CO_2 concentrations at monitoring sites and atmospheric temperature and pressure.

Station ID	Begin Date	End Date	r^2 CO_2 and Temperature	r^2 CO_2 and Pressure
ISLM	11/18/07	10/8/07	0.16	-0.16
ISLM	1/14/08	2/7/08	0.31	-0.35
ISLM	2/18/08	3/28/08	0.54	-0.41
ISLM	4/25/08	7/25/08	0.35	-0.36
ISLM	9/23/08	10/15/08	0.13	-0.36
ISST	11/30/07	12/18/07	0.61	-0.41
ISST	2/4/08	5/8/08	0.21	-0.13
ISST	6/5/08	7/25/08	-0.21	-0.29
ISST	9/23/08	1/23/09	0.43	-0.18
MR3	11/14/07	12/7/07	0.21	-0.42
MR3	1/15/08	2/8/08	0.51	-0.62
MR3	8/19/08	10/24/08	0.41	-0.46
MR3	9/11/08	9/21/08	0.34	-0.5
WP7	10/23/08	11/8/08	0.41	-0.37
WP2	8/17/09	9/21/09	0.26	-0.46
WP5	8/17/09	9/21/09	0.24	-0.5
WP7	8/17/09	9/21/09	0.18	-0.56

Table 4. Correlation between cave air CO_2 and outside temperature and pressure at WP2, WP5 and WP7 from 9/18/2009 to 9/20/2009.

Station ID	r^2 CO_2 and Temperature	r^2 CO_2 and Pressure	Distance from entrance (m)
WP2	0.26	-0.46	20
WP5	0.24	-0.5	60
WP7	0.18	-0.56	100

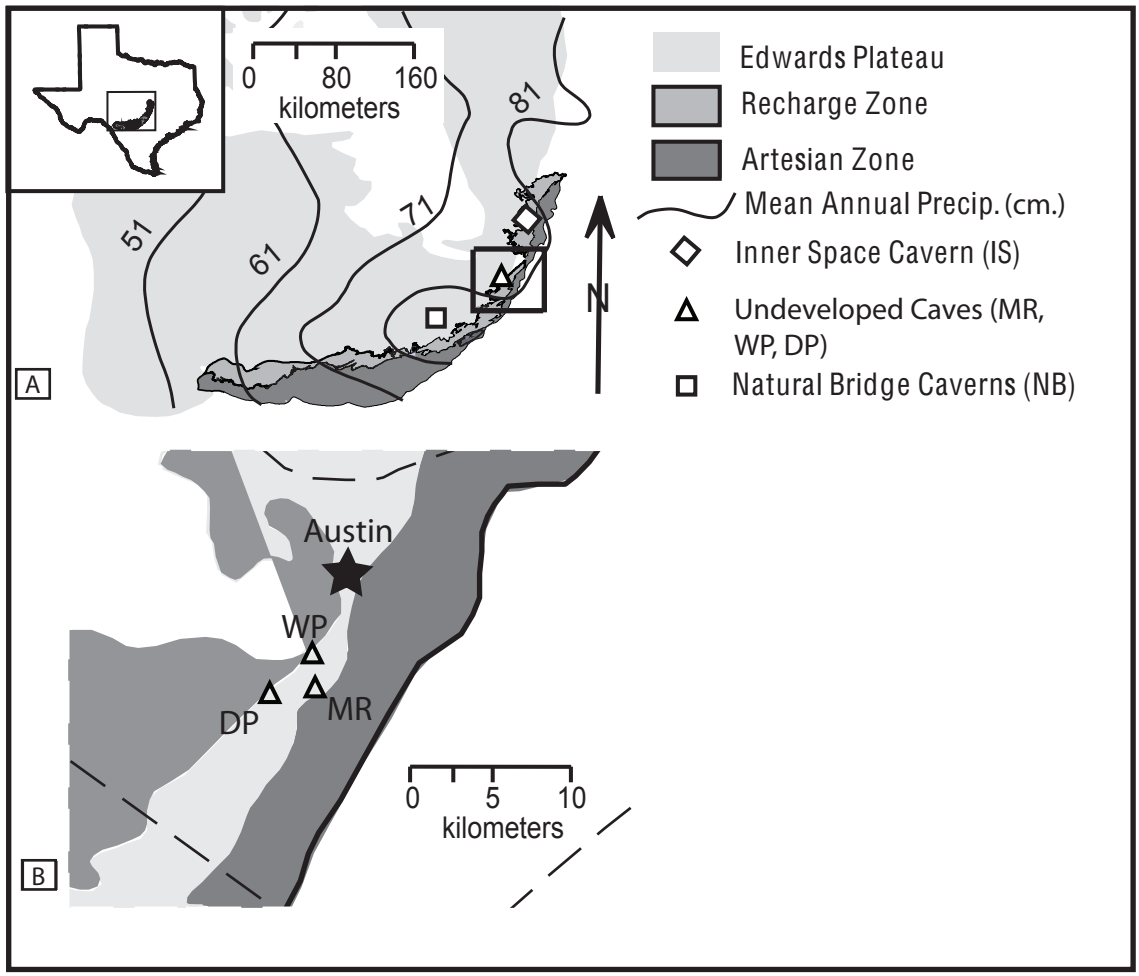


Figure 1. Map of cave locations on the Edwards plateau in central Texas, USA.

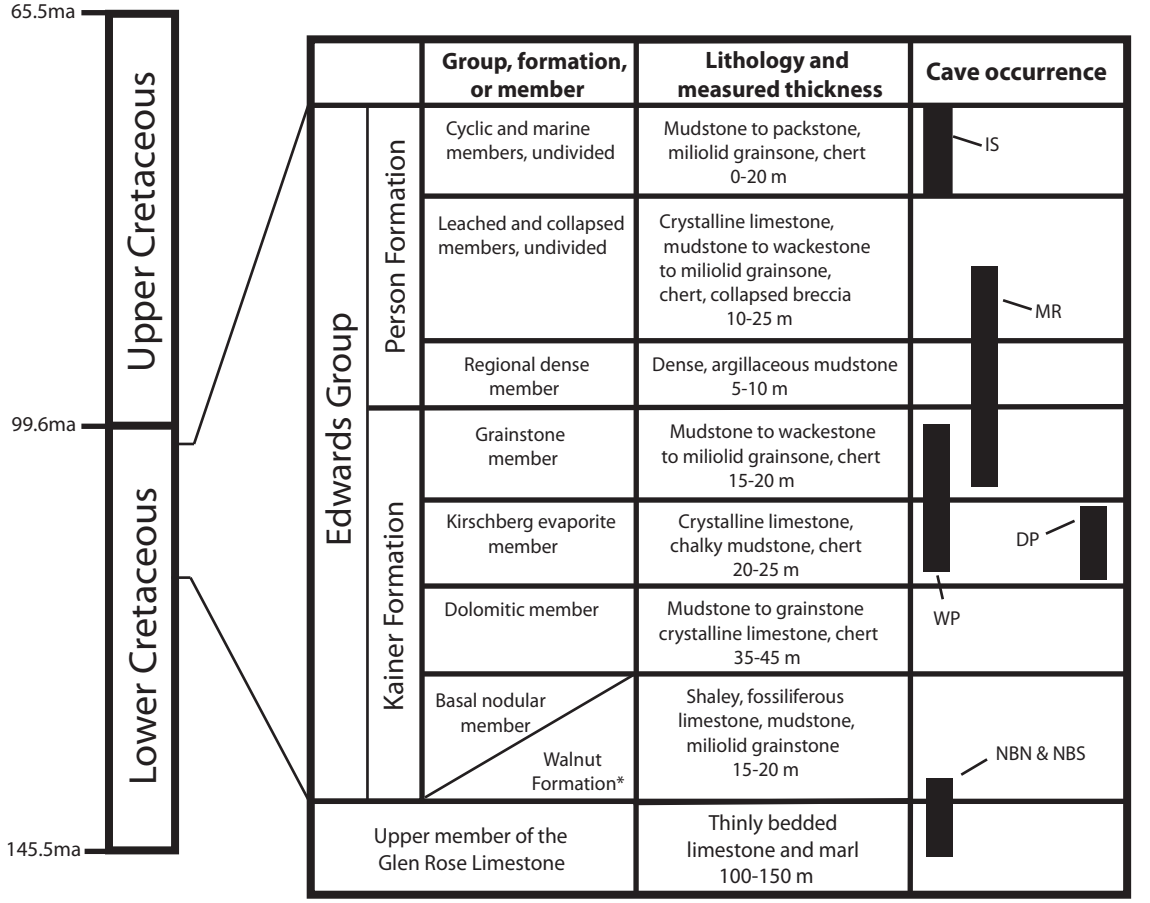


Figure 2. Hydrostratigraphic section of the study area showing the intervals of occurrence of the caves of this study. The undeveloped caves (MR, DP and WP) are formed within several members of the Kainer and Person Formations. Note that MR and WP are formed in more than one member. NBN and NBS are formed in the same member adjacent to one another. Adapted from Maclay and Small (1976), Kastning (1983) and Small et al. (1996). *Note that the Basal Nodular is not present at Natural Bridge Caverns.

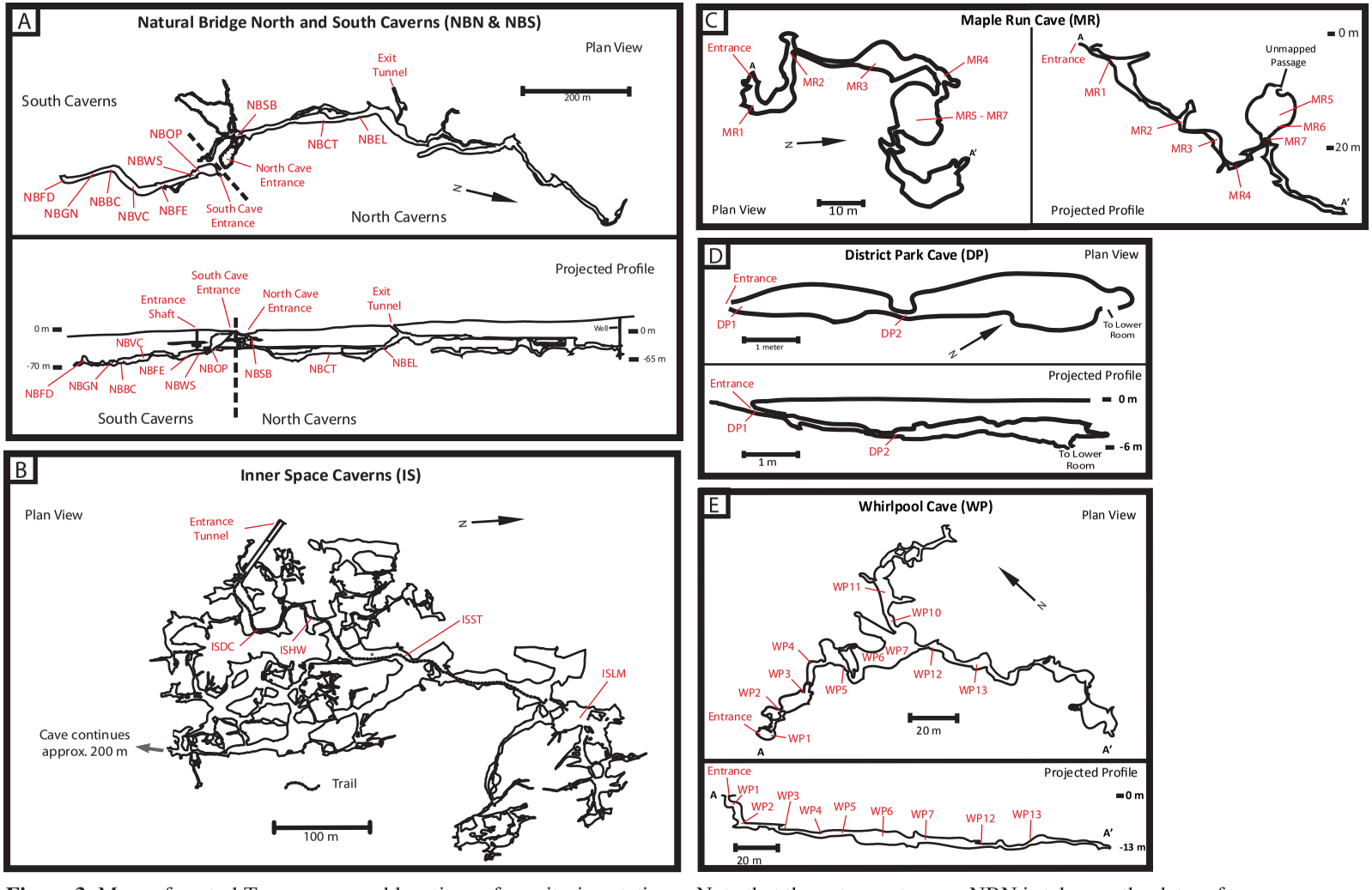


Figure 3. Maps of central Texas caves and locations of monitoring stations. Note that the entrance to cave NBN is taken as the datum for indicated depths for both NBN and NBS. Cave entrances are taken as the datum for all other depths reported. IS map adapted from Atkinson (2003), NBN and NBS maps adapted from Atkinson (2004), MR map adapted from Scott (2000), WP map adapted from Russell (1979) and DP map adapted from Russell (1988).

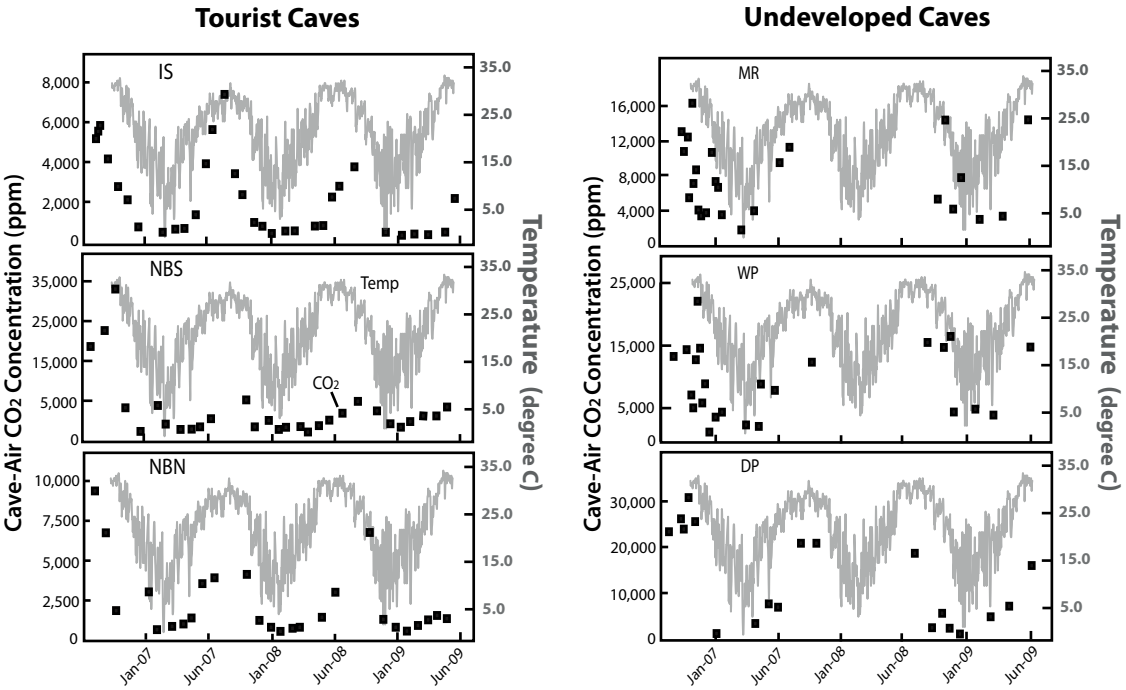


Figure 4. Time series of weighted mean cave-air CO_2 concentration (black squares) measured during each transect of tourist and undeveloped caves and outside air temperature (gray solid lines). Instrument error (5% of measurement or 50 ppm) is smaller than symbols used to represent CO_2 concentrations. Air temperature was measured at a National Climate Data Center weather station located in Austin, Texas (COOP ID: 410428; www.ncdc.noaa.gov).

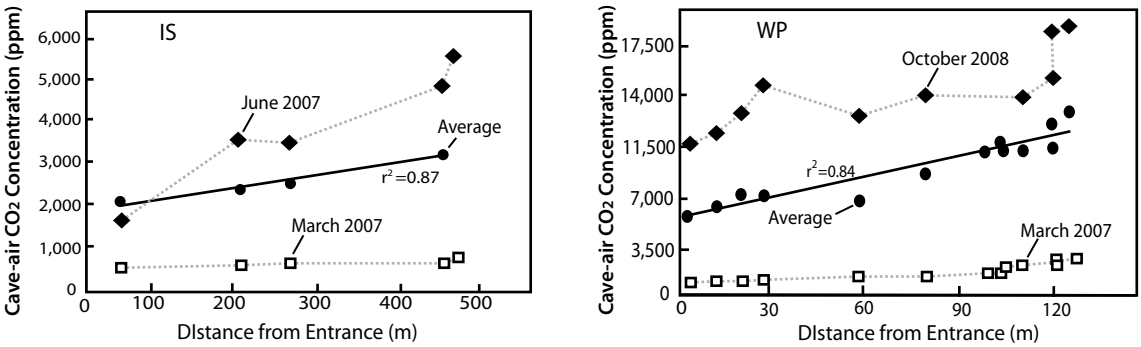


Figure 5. Representative warm and cool season CO_2 transects at one tourist and one undeveloped cave (IS & WP). Mean CO_2 concentration measured at each station during study. Warm season values denoted by solid diamonds (◆), cool season transects denoted by un-filled squares (▫) and mean values denoted by solid circles (●).

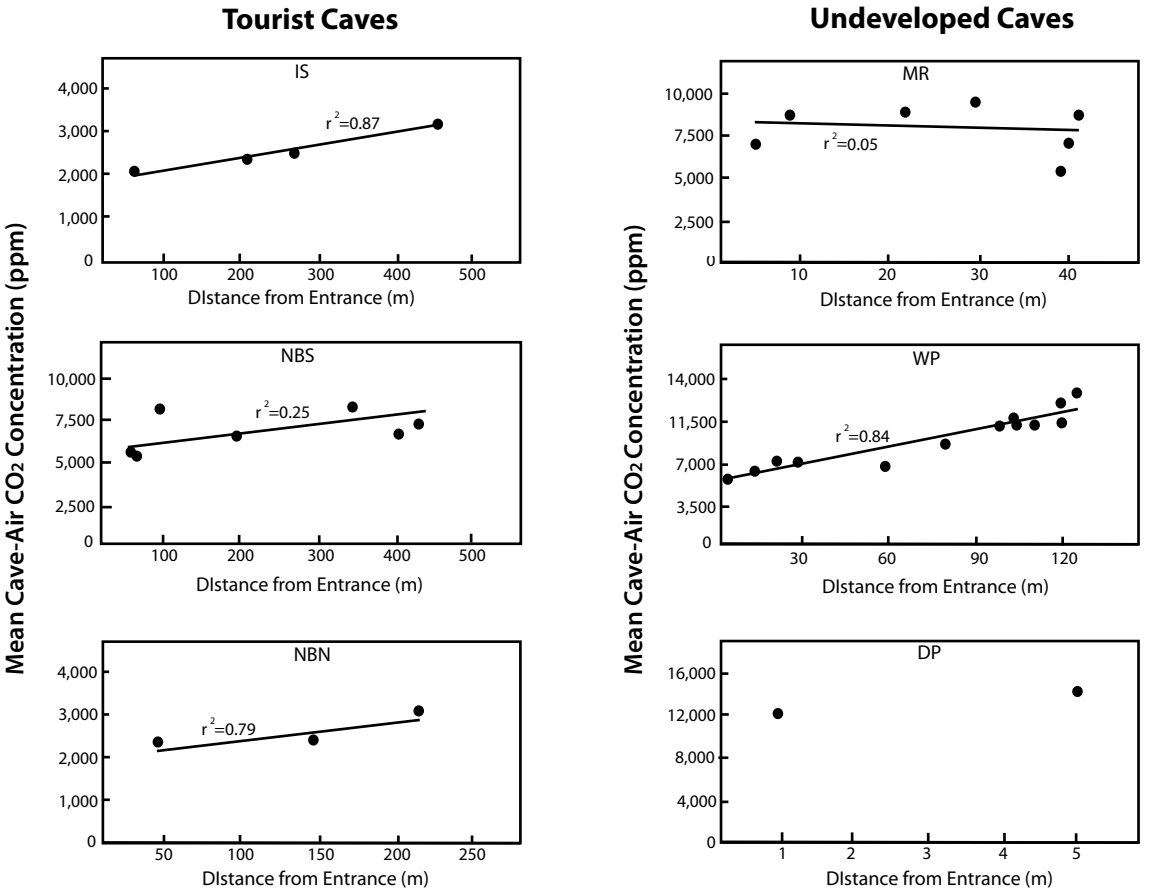


Figure 6. Mean CO_2 concentration measured at each station versus distance from the cave entrance. No r^2 for DP, as there are only two stations within the cave.

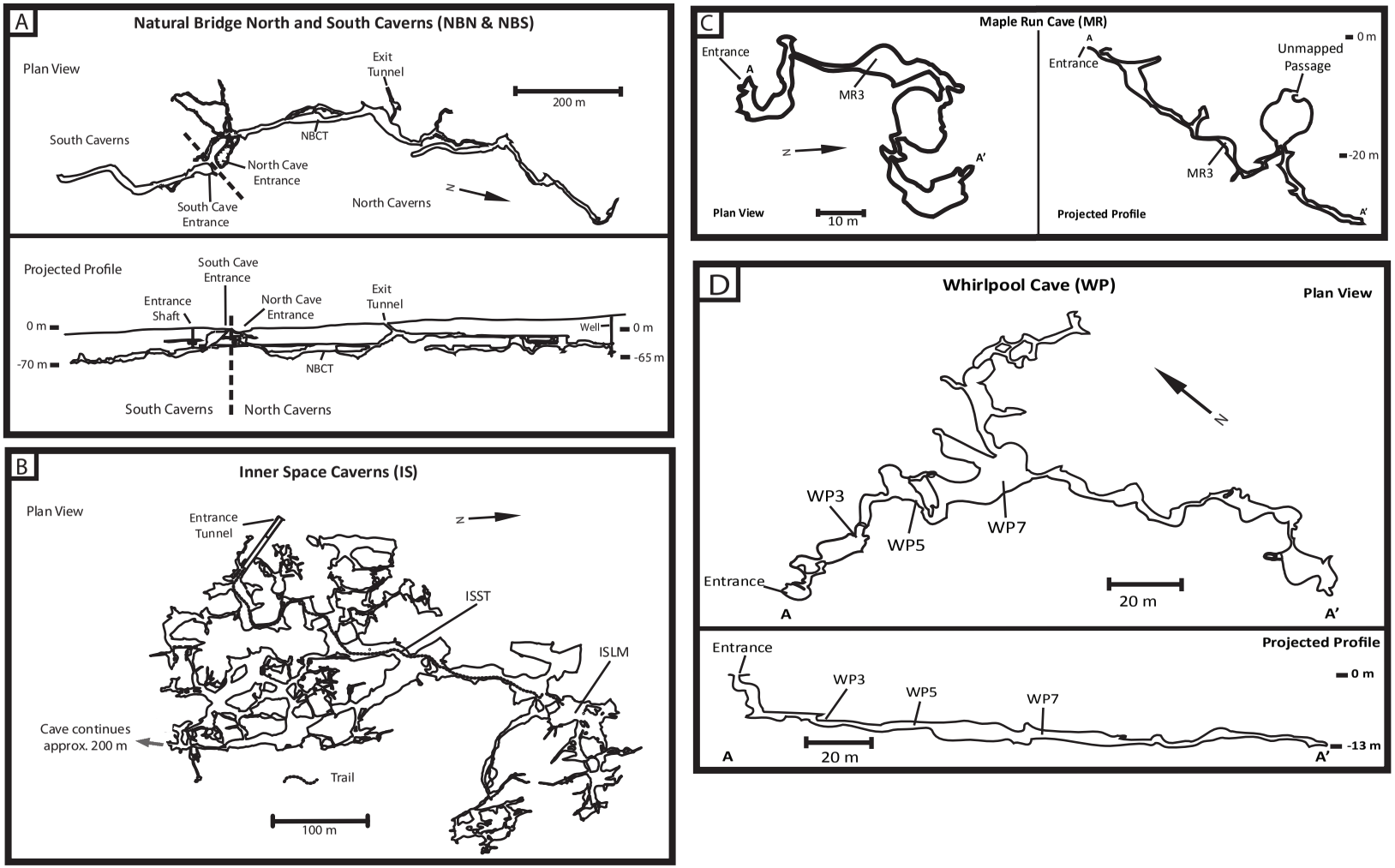


Figure 7. Locations of CO_2 logging stations.

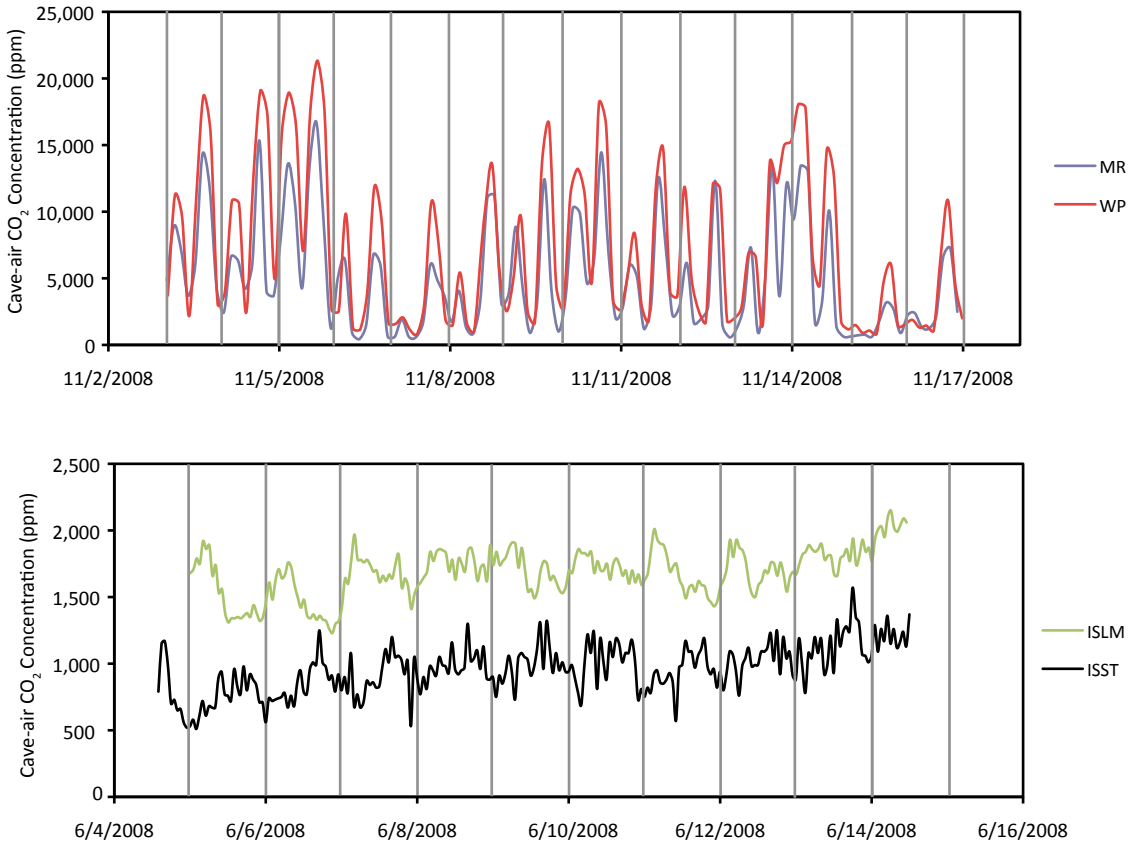


Figure 8: Representative diurnal CO_2 fluctuations in the study caves. Note that the smaller volume undeveloped caves (MR & WP) experience much larger diurnal CO_2 fluctuations than IS (ISST & ISLM). All tick marks and vertical gray lines represent midnight on the day indicated.

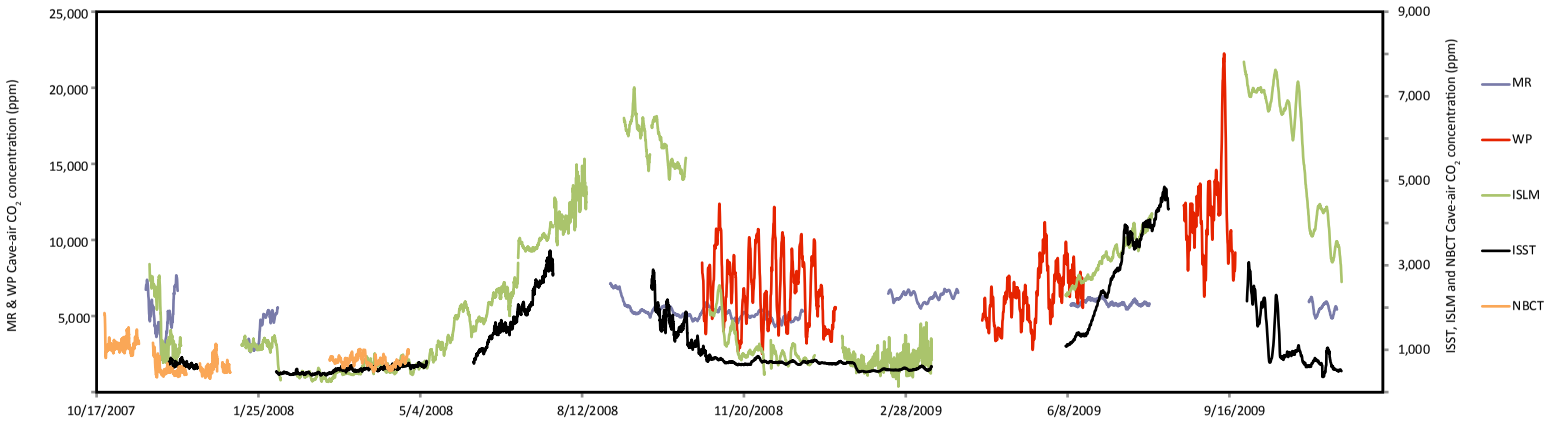


Figure 9. CO_2 concentrations at all stations throughout the duration of the study. All caves show strong seasonal CO_2 fluctuations except MR. Note that a three-day running average is shown to remove short-term fluctuations (i.e. diurnal and storm events). Note that nearly 30,000 data points are represented.

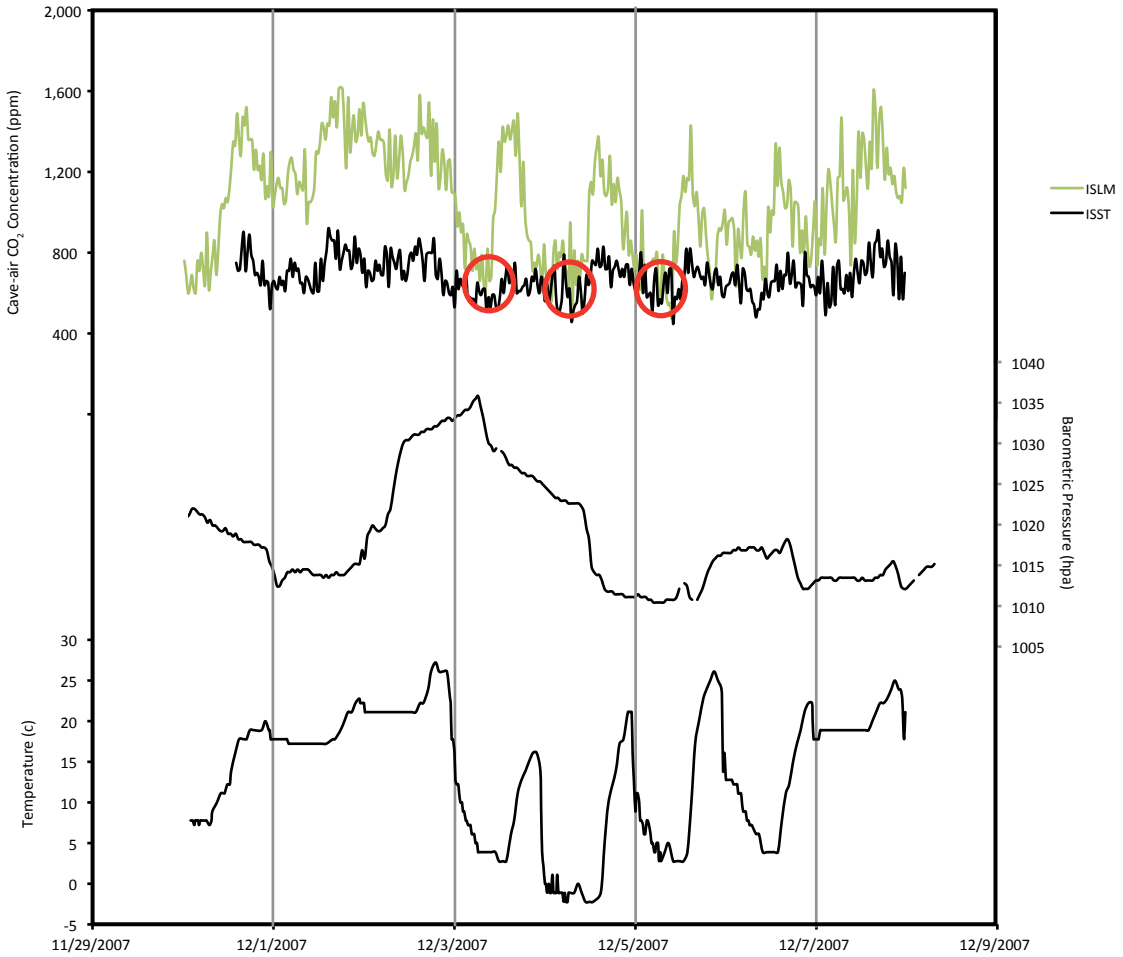


Figure 10. Representative storm-event ventilation in Inner Space Cavern. Note that the concentration of CO_2 at ISLM decreased to the same concentration as ISST on several occasions (circled in red), indicating that cave ventilation has become strong enough to ventilate ISLM even though it is nearly 200 meters further from the entrance than ISST. Such ventilation patterns are typical in the study area when large fluctuations in temperature and barometric pressure occur. Such fluctuations are typically associated with storms and cold fronts. All tick marks and vertical gray lines represent midnight on the day indicated.

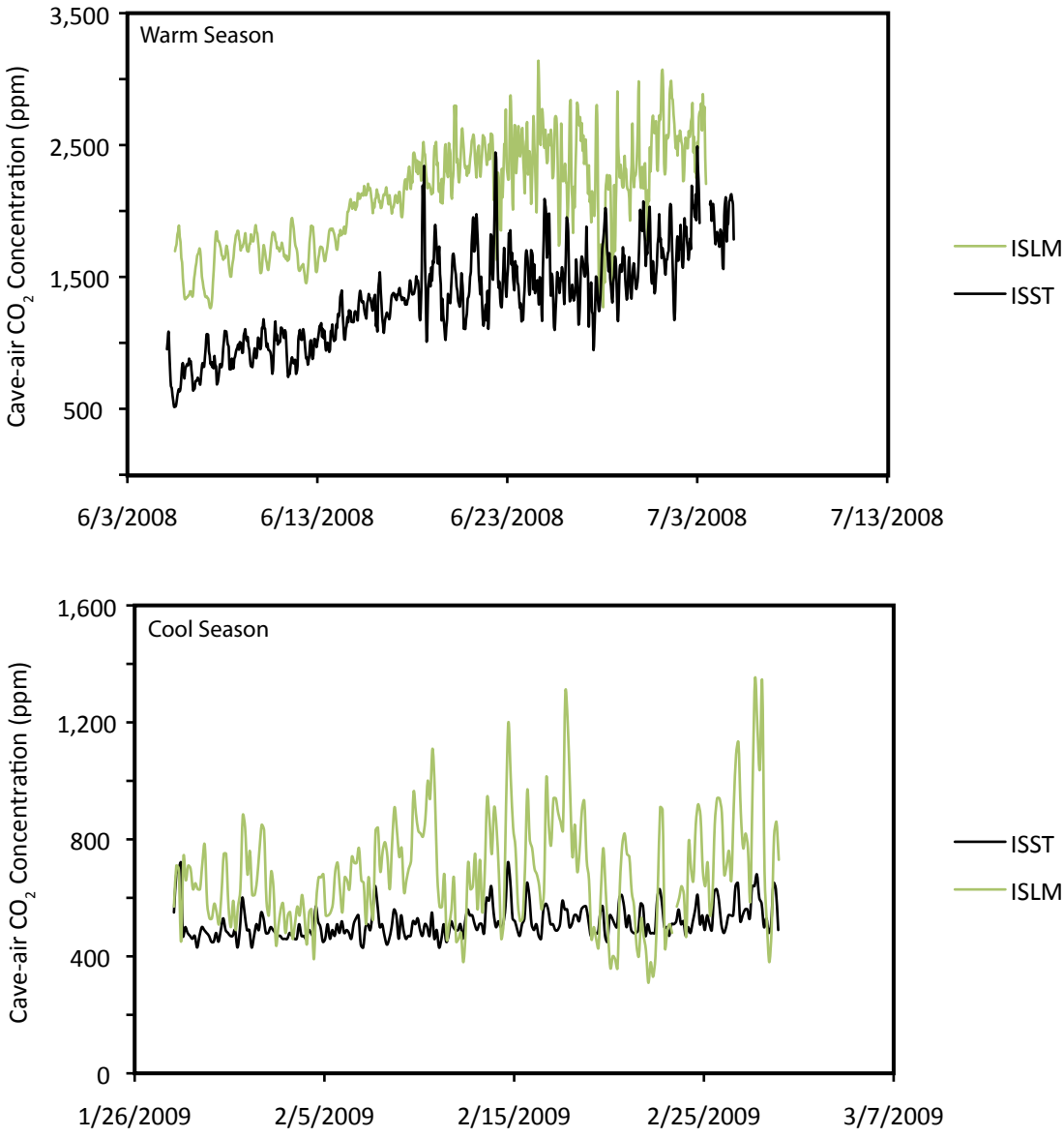


Figure 11. Representative cool and warm season CO_2 concentrations in Inner Space Cavern showing that CO_2 is elevated at ISLM, the deeper station. CO2 levels are not as elevated at ISLM relative to ISST during the cool season. Cave air CO_2 concentration is positively correlated with distance from the cave entrance in all caves except Maple Run.

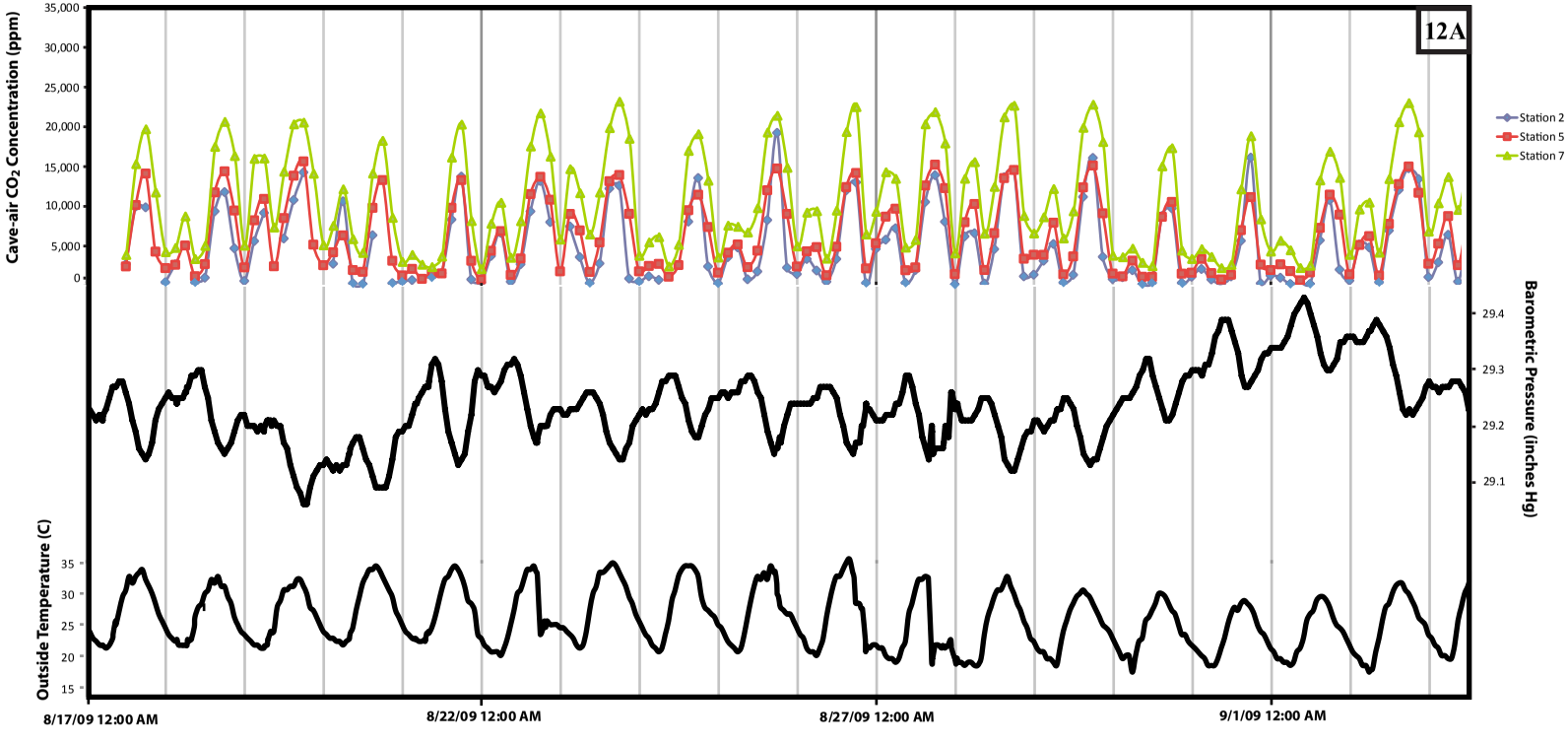
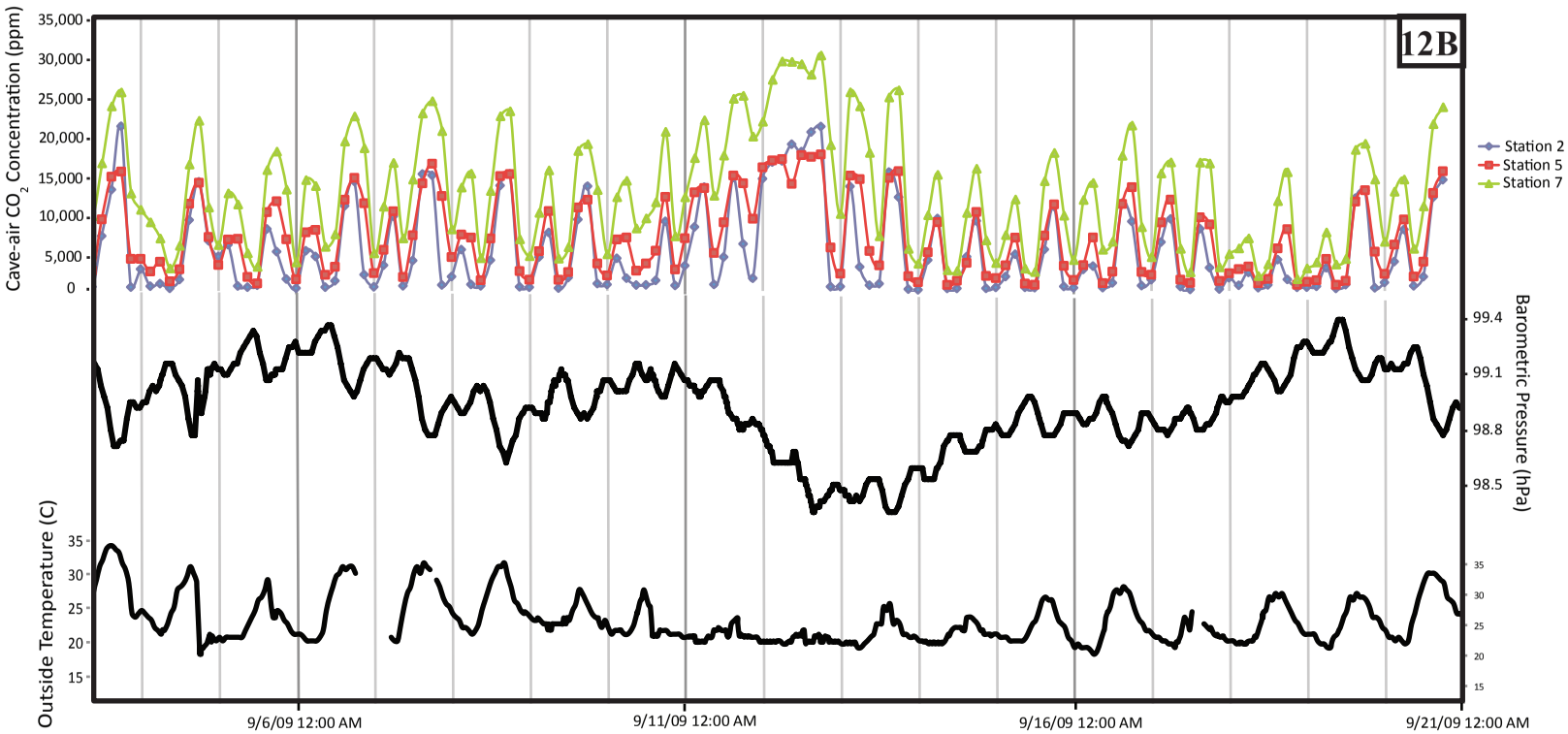


Figure 12A & 12B. Surface air pressure and temperature and cave air CO_2 concentrations at WP2, WP5 and WP7 located 12, 60 and 100 meters from the cave entrance respectively. Large diurnal CO_2 fluctuations are typical in Whirlpool Cave and are better correlated with barometric pressure than outside temperature. Note that CO_2 concentrations generally increase with increasing distance from the cave entrance. Figure 12 A & 12B are a continious time series.


12B
Cave-air CO_2 Concentration (ppm)
35,000
30,000
25,000
20,000
15,000
10,000
5,000
0
Station 2
Station 5
Station 7
Barometric Pressure (hPa)
99.4
99.1
98.8
98.5
Outside Temperature (C)
35
30
25
20
15
9/6/09 12:00 AM
9/11/09 12:00 AM
9/16/09 12:00 AM
9/21/09 12:00 AM

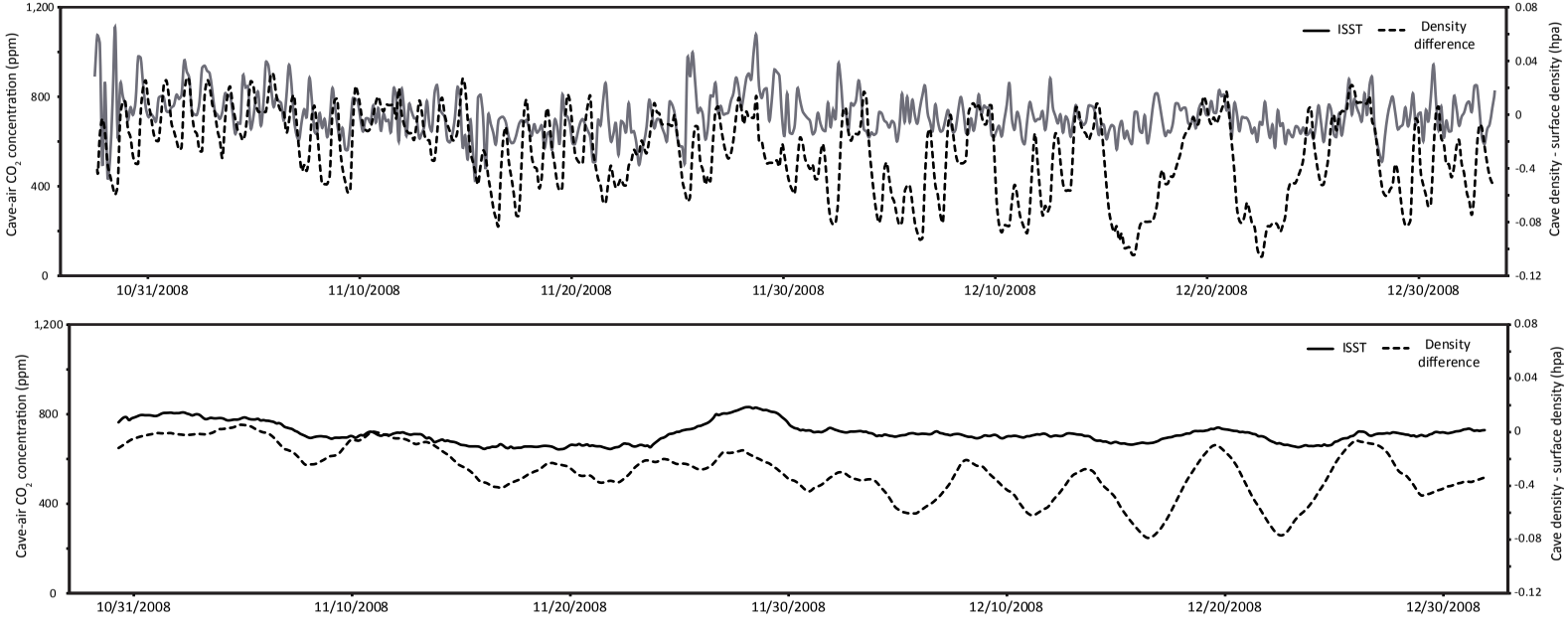


Figure 13A through 13D. Top panels- cave air CO_2 concentrations and cave air density-outside air density at ISST (a), ISLM (b), MR3 (c) and WP7 (d). Bottom panels show a three-day running average of cave air CO_2 concentrations and cave air density-outside air density. Note that when cave air density is less than the outside air density (cave air density-outside air density < 0) density driven ventilation is likely but there is a weak correlation between cave air CO_2 and density (top panels). When a three-day running average is taken, there is a strong correlation between cave air CO_2 and density (bottom panels).

Figure 13B:

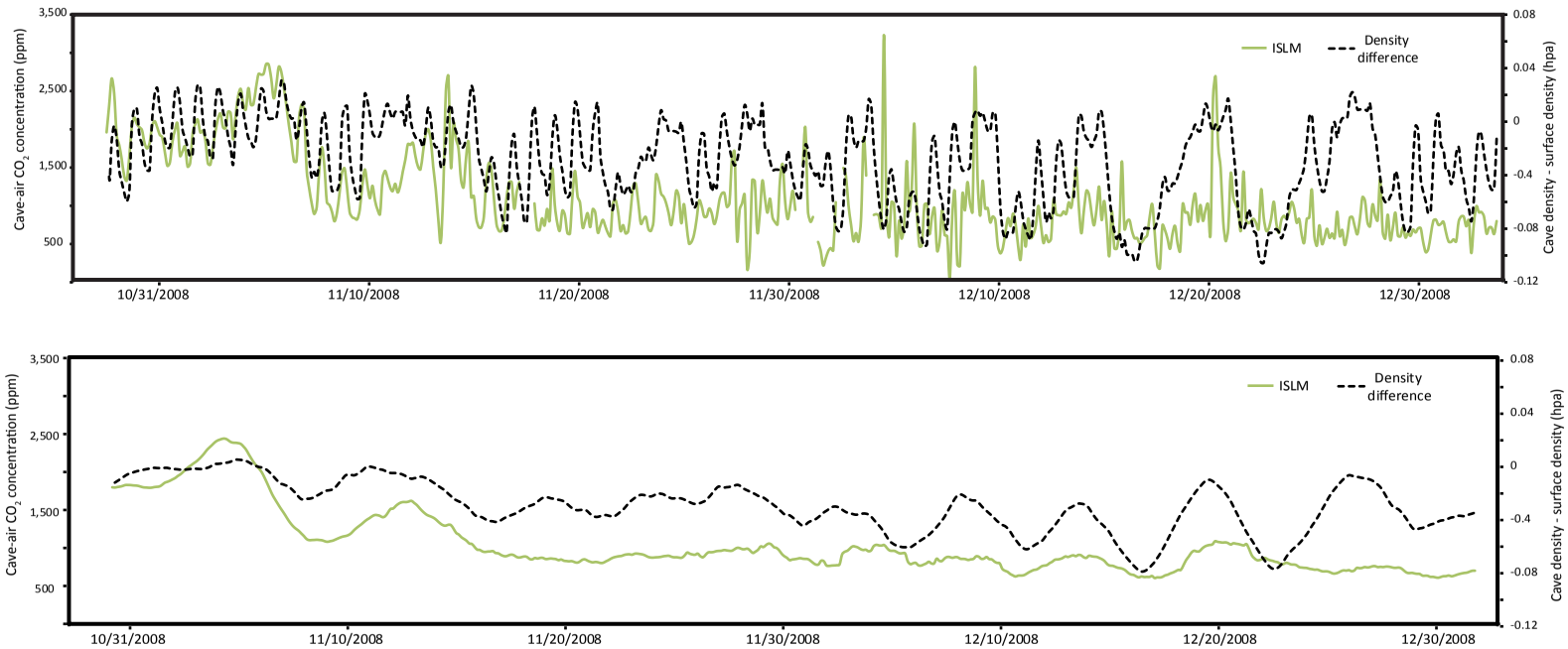

3,500
2,500
1,500
500
Cave-air CO_2 concentration (ppm)
0.08
0.04
0
-0.4
-0.08
-0.12
Cave density - surface density (hpa)
ISLM
Density difference
10/31/2008
11/10/2008
11/20/2008
11/30/2008
12/10/2008
12/20/2008
12/30/2008

Figure 13C:

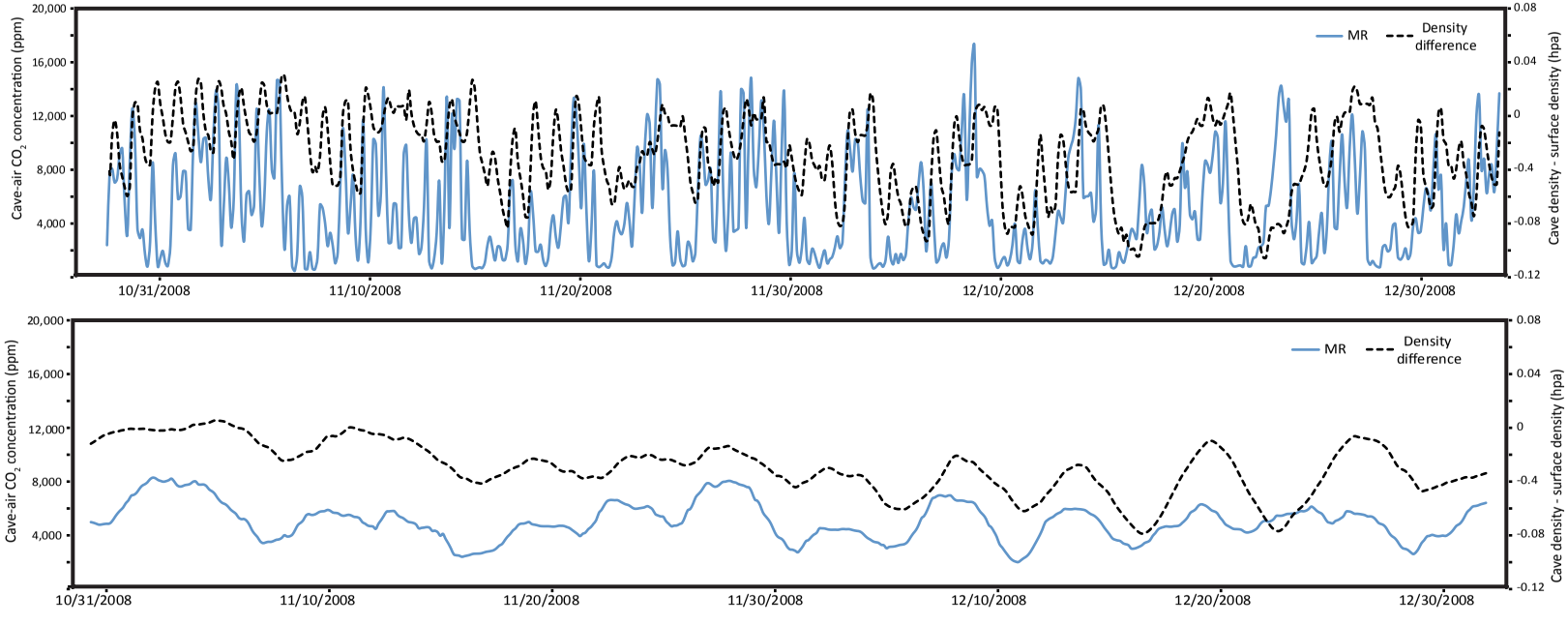
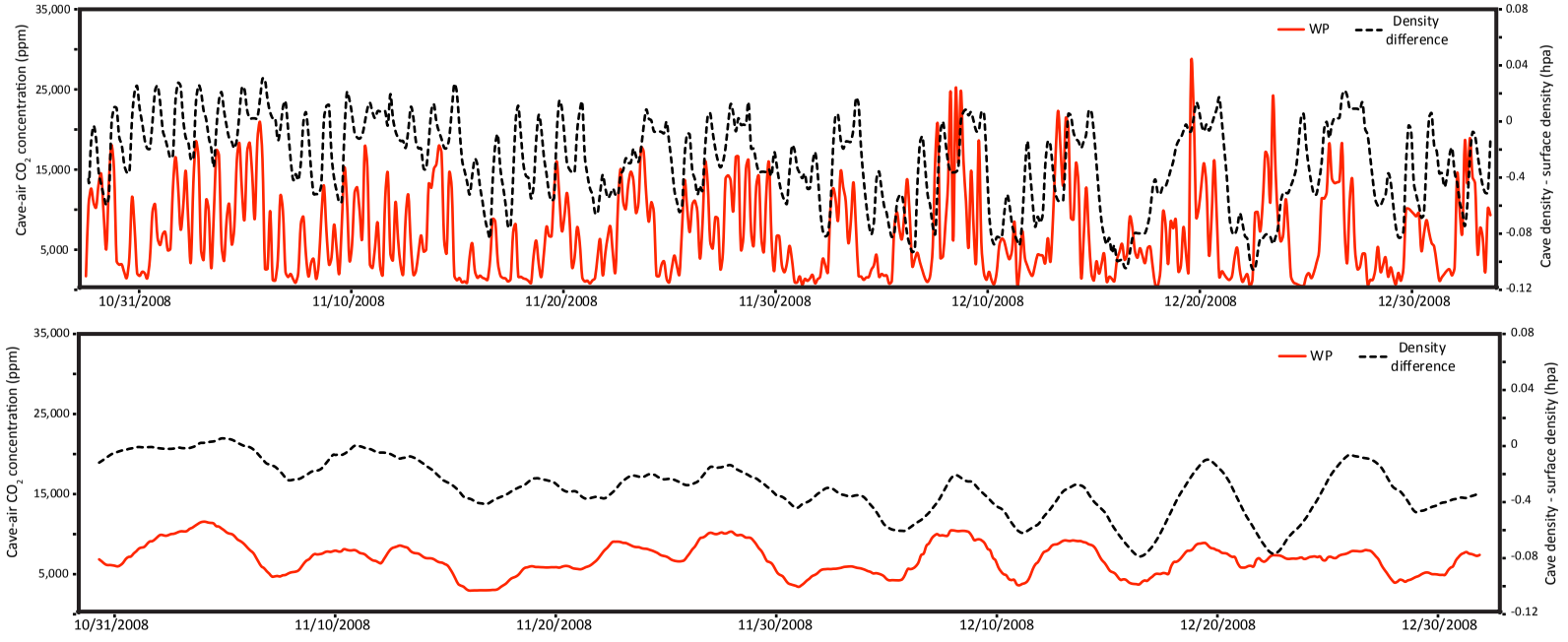

Cave-air CO_2 concentration (ppm)
20,000
16,000
12,000
8,000
4,000
0.08
0.04
0
-0.4
-0.08
-0.12
Cave density - surface density (hpa)
MR
Density difference
10/31/2008
11/10/2008
11/20/2008
11/30/2008
12/10/2008
12/20/2008
12/30/2008

Figure 13D:


35,000
25,000
15,000
5,000
Cave-air CO_2 concentration (ppm)
WP
Density difference
0.08
0.04
0
-0.4
-0.08
-0.12
Cave density - surface density (hpa)
10/31/2008
11/10/2008
11/20/2008
11/30/2008
12/10/2008
12/20/2008
12/30/2008

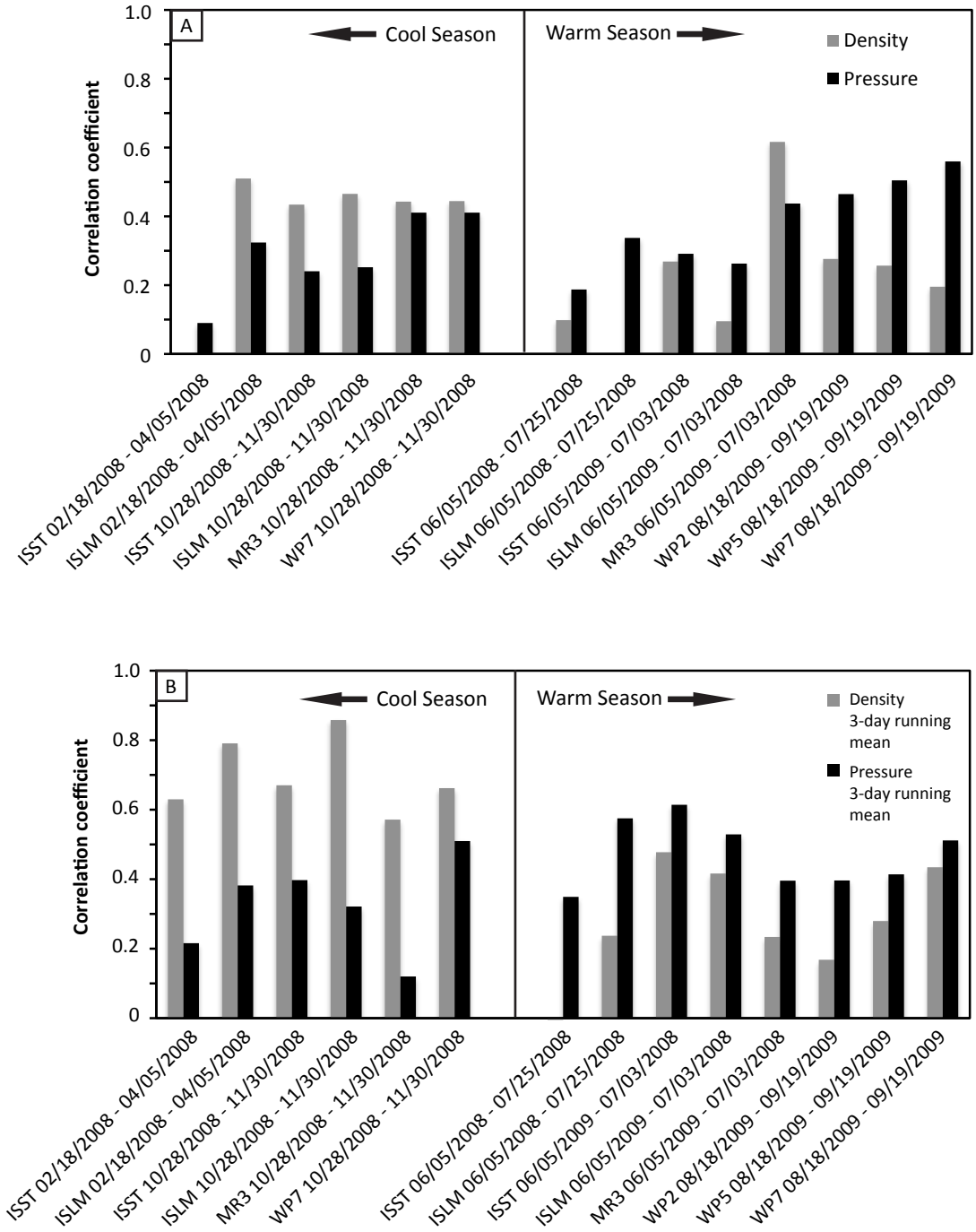


Figure 14. Panel A- Correlation between CO_2 concentrations at monitoring sites and air density and barometric pressure. Panel B- Correlation between three-day running mean of CO_2 concentrations at monitoring sites and three–day running mean of air density and barometric pressure. Note that barometric pressure is more strongly correlated with CO_2 concentrations in the warmer months and density is more strongly correlated with CO_2 concentrations during the cooler months. All values are considered to be statistically significant ($p > 0.05$)

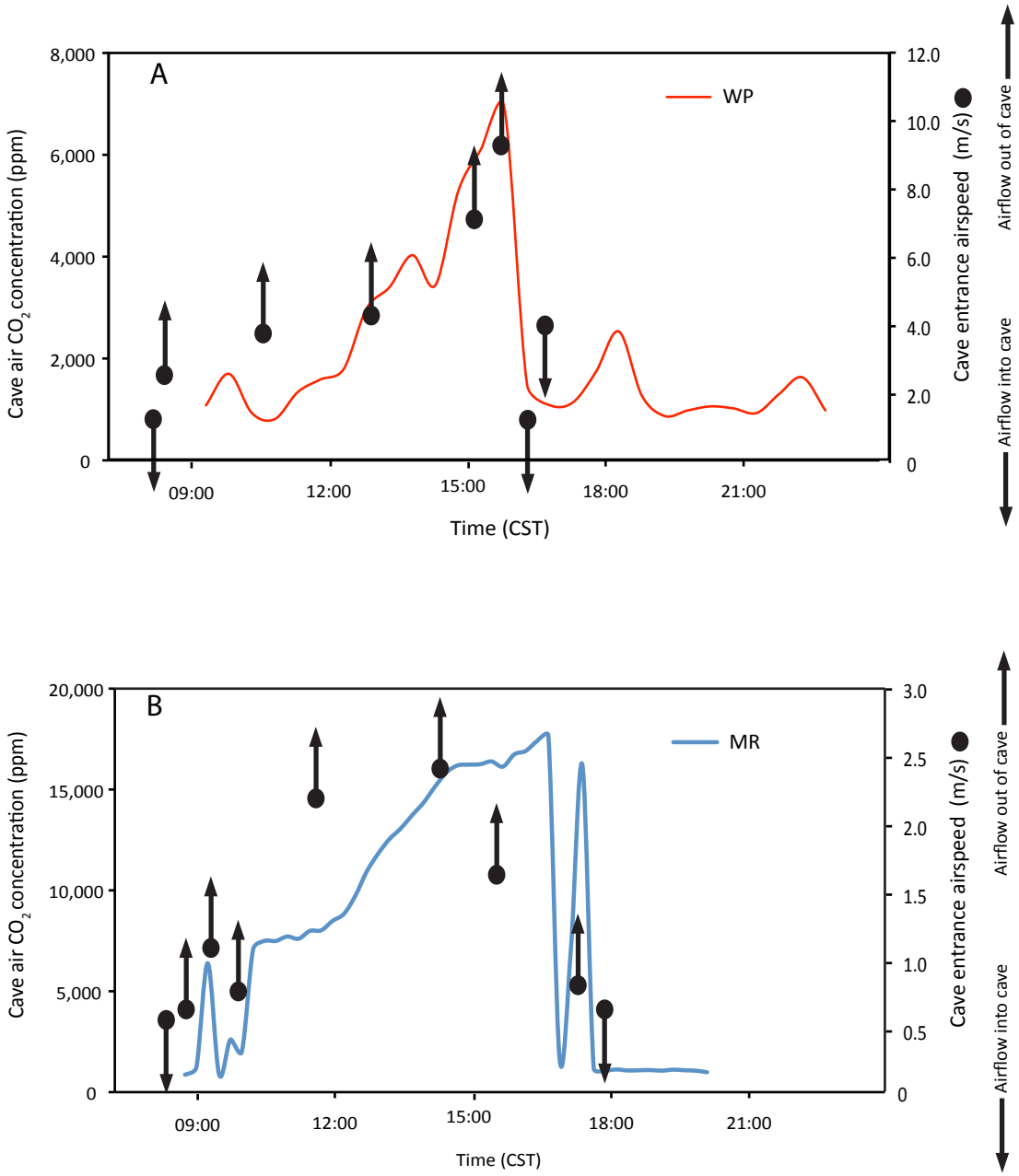


Figure 15. The concentration of CO_2 and airspeeds measured at the entrances of Whirlpool Cave (A) and Maple Run Cave (B) during airspeed measurements. Note that airspeeds at Whirlpool Cave are much higher than airspeeds at Maple Run as the entrance to Whirlpool Cave has a much smaller area.

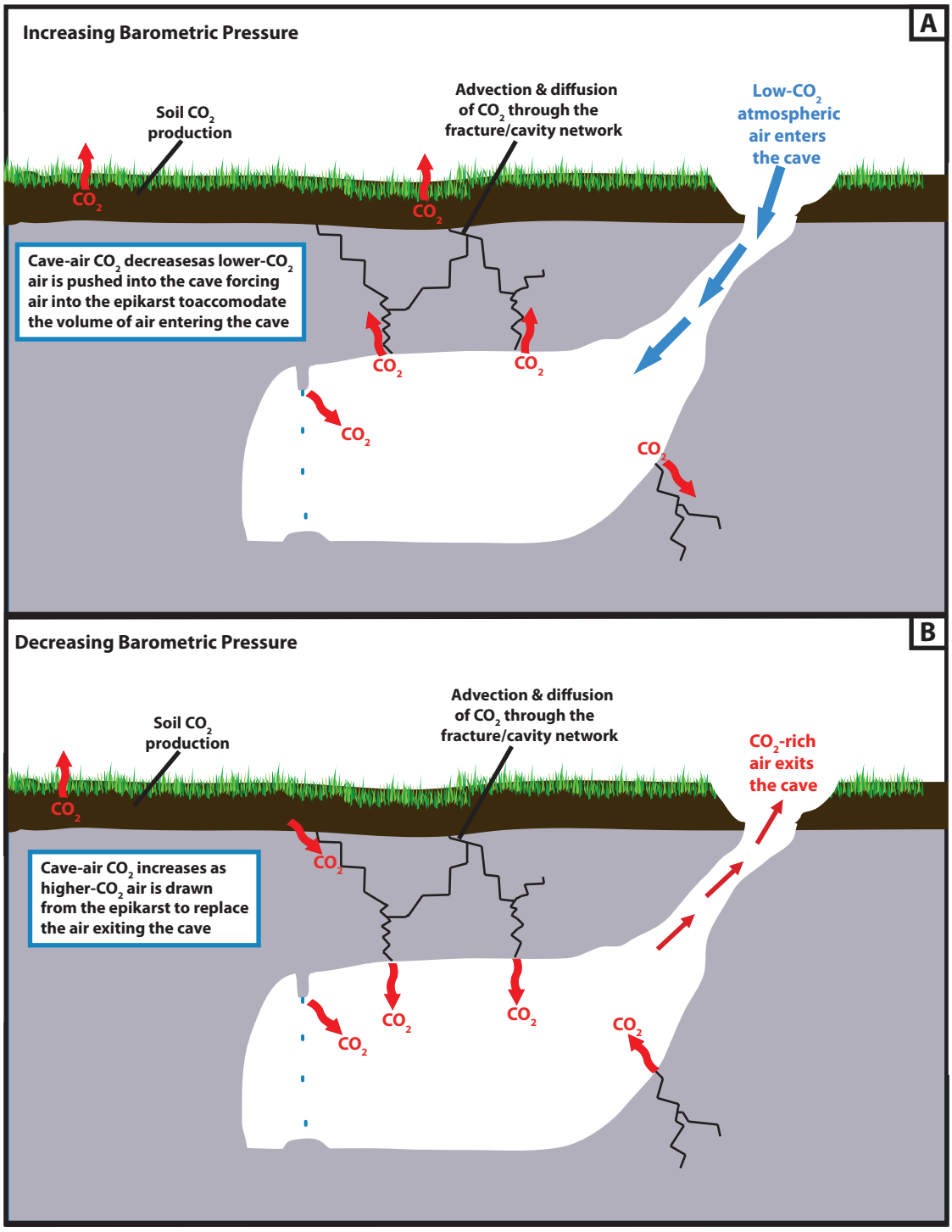


Figure 16. Conceptual model of subterranean airflow and CO_2 flux in the study area.

APPENDIX A. METHODS AND SITE DESCRIPTIONS

CARBON DIOXIDE METERS TECHNICAL SPECIFICATIONS

Carbon dioxide concentrations were measured with Vaisala CARBOCAP hand-held carbon dioxide meters and Telaire 7001 hand-held carbon dioxide meters. Both types of meters utilize infrared absorption technology to measure the carbon dioxide concentration of air as it diffuses through the measurement chamber. The Vaisala and Telaire meters were frequently compared to one another to ensure that they gave the same readings (within instrument error) when placed side-by-side in the field or when zero-point accuracy checks were performed.

Vaisala Carbon Dioxide Probe

Accuracy of the probe is ±20 ppm CO_2 or 2% of the reading, whichever is larger, which is well below the magnitude of cave-air CO_2 fluctuations in the study area (Figure 4; Figure 8). The temperature dependence of the probes is 0.1% of the full scale/°C (reference 25°C) however, the logging units allow for temperature corrections to be made at the time of measurement. The average cave air temperature measured in the tourist caves was used as the correction temperature. Cave air temperatures do not vary significantly on an annual basis and deployments were typically less than two months in duration; therefore the actual bias due to temperature fluctuations is likely less than the factory specifications given above. The pressure dependence of the probes is 0.15% of the reading/hPa (reference 1013 hPa). Typical diurnal surface barometric pressure fluctuations in the study area were only a few hPa. Error induced by barometric pressure

fluctuations are negligible with respect to the magnitude of diurnal and seasonal cave-air CO_2 fluctuations. The long-term stability of the meters is <± 5% of the full scale/2 years and all meters were factory recalibrated at least every two years and many every year. The meter operating temperatures are -20 to 60°C and the operating pressures are 700 to 1300 hPa. The meters were well within theses operating conditions at all times during the study. The meters are capable of operating in 1 to 100% relative humidity (non-condensing), however the cave atmospheric conditions typically were condensing. To reduce errors due to condensation on the probe tips, special membrane sleeves (Vaisala part number GM45168SP) were placed over the probe tips to exclude moisture. These sleeves did reduce erroneous readings due to condensation, however were not 100% effective. Erroneous data removal was performed according to the procedures detailed in chapter three. Vaisala meters were placed inside a specially designed housing to protect against rodent damage and the treacherous trips through the undeveloped caves (Figure A1). The Vaisala CO_2 meters were used exclusively for diurnal and short-term monitoring.

Telaire 7001 Handheld Carbon Dioxide Meter

The accuracy of the Telaire 7001 Handheld Carbon Dioxide Meter is ±50 ppm or 5% of the reading, whichever is greater. This error is negligible when compared to seasonal cave air CO_2 fluctuations measured during transects of the caves. Data from the Telaire meters was not used for diurnal or other short-term determinations of CO_2 variability. Temperature and pressure dependence is ±0.1% of the reading or ±2 ppm (referenced at 25°C) whichever is greater and 0.13% of the reading/mm Hg respectively.

Error introduced by temperature and pressure dependence is negligible compared to the magnitude of the seasonal cave-air CO_2 fluctuations. Annual drift is ±20 ppm, but the meter was calibrated several times per year according to the manufacturer instructions.

METER CALIBRATION AND QUALITY CONTROL

All meters were calibrated in accordance with or more frequently than the suggested calibration intervals provided by their respective manufacturers. All Vaisala meters were factory recalibrated as suggested by the manufacturer. The Telaire 7001 meters were recalibrated in-house using standard reference gases (10,000 ppm CO_2) or nitrogen gas (0 ppm CO_2) according to the manufacturers specifications. The meters were placed in a large Ziploc bag that was sealed except for a small hole near the top to allow the reference gas or nitrogen gas to flow out of the bag. To ensure that all room air was flushed from the bag, nitrogen gas was allowed to flow through the bag for 5 minutes before calibration began. The Telaire meters were then calibrated according to manufacturers instructions.

Accuracy Verification

Periodic zero-point accuracy checks were performed on all meters using nitrogen gas and the calibration apparatus discussed above. Any Vaisala meter giving erroneous readings (>±100ppm of the reference gas) was sent for factory repair and/or recalibration. All Telaire 7001 meters giving erroneous readings (>±100ppm of the reference gas) were recalibrated in-house and retested for accuracy.

Meter maintenance/repair protocol

All Vaisala meters were removed from the caves for data acquisition, accuracy verification and maintenance. During removal and storage, meter cases were left open to allow air-drying of the meter components and protective casing. The Telaire 7001 meters were stored out of their cases to allow air-drying. Desiccant packs were replaced every time Vaisala meters were removed from the caves (approximately every 4-6 weeks) and the cases were inspected for cracks or leaks that might allow moist cave air to come into contact with the meter circuitry.

CAVE AIR CARBON DIOXIDE MEASUREMENTS

Due to the ruggedness of the undeveloped caves, it was impractical to wear CO_2 scrubbing respirators or other devices that remove exhaled CO_2 from where measurements were being taken. To account for operator bias, several experiments were performed to estimate this impact. Upon arriving at a measurement site, the initial CO_2 concentration was recorded. To determine if there was a rise in CO_2 concentration as a result of respiration, CO_2 concentrations were measured after a waiting period of five minutes. This experiment was repeated at several sites within each undeveloped cave. No increase in CO_2 concentration greater than the instrument error (±50 ppm) was measured and occasionally, small decreases (20-30 ppm) within instrument error were observed. Measurements reported here were typically recorded within two to three minutes of arrival at each site and no measurements were taken after spending five minutes at a site. Based on this protocol, and the magnitude of seasonal cave-air CO_2

fluctuations observed, operator CO_2 inputs are considered insignificant relative to the data presented in this study.

All Vaisala meters were deployed so that probe tips were at lease 20 cm from any surface. To ensure that ambient cave-air CO_2 concentrations were measured, Vaisala meters were not deployed within 0.5 m of open fractures or active drips as CO_2 advection/diffusion or degassing near these features might be sufficiently strong to elevate the immediate area concentration well above ambient cave-air CO_2 concentrations. To lessen the impact of visitor respiration on measured CO_2 concentrations, Vaisala meters were deployed at least 5 meters from pathways in the tourist caves.

Nearly 30,000 carbon dioxide measurements taken by the Vaisala meters and over 100,000 weather measurements taken at three NCDC weather stations are reported here. As it is not practical to present these data in the print copy of this manuscript, the data is available on a compact disc that has been included with the physical copy of this thesis that is retained by the Walter Geology Library at the University of Texas at Austin.

SITE DESCRIPTIONS

See Figure A2 for detailed cave maps showing monitoring site locations.

Inner Space Cavern

Inner Space Cavern is a tourist cave located approximately 40km north of Austin TX in Georgetown TX (www.myinnerspacecavern.com). We estimate that Inner Space Cavern receives several hundred to a few thousand visitors each day depending on the

season; however, management does not release the exact number of visitors. Interstate Highway 35 overlies part of the cave, however the hydrogeology and spatial distribution of CO_2 concentrations in the cave suggest that the highway does not have a significant impact on the cave-air CO_2.

Inner Space Cavern – Drapery Column (ISDC)

This site is located approximately 75m from the cave entrance and approximately 15m below the surface. The passage here is approximately 2m tall and 6m wide. Only spot measurements were taken here using the Telaire 7001 meter. Measurements were taken from the edge of the tourist trail, typically in the mornings before the cavern opened to the public.

Inner Space Cavern – Hallway Drip (ISHW)

This site is located approximately 220m from the cave entrance and approximately 17m below the surface. The passage here is approximately 2m tall and 2m wide. Only spot measurements were taken here using the Telaire 7001 meter. Measurements were taken from the edge of the tourist trail, typically in the mornings before the cavern opened to the public.

Inner Space Cavern – Flowing Stone of Time (ISST)

This site is located approximately 260m from the cave entrance and approximately 19m below the surface. This site is located in a large room approximately 30m long, 20m wide and 10m tall. A Vaisala meter was deployed behind a large flowstone formation approximately 5m from the tourist trail. Spot measurements were taken approximately 10m from ISST using the Telaire 7001 meter, typically in the mornings before the cavern opened to the public.

Inner Space Cavern – Lake of the Moon (ISLM)

This site is located approximately 460m from the cave entrance and approximately 20m below the surface. This site is located in a smaller room approximately 15m long, 10m wide and 3m tall. A Vaisala meter was deployed approximately 10m from the tourist trail. Spot measurements were taken within 2m of the Vaisala meter location using the Telaire 7001 meter, typically in the mornings before the cavern opened to the public.

Natural Bridge Caverns

Natural Bridge Caverns is a tourist cave located approximately 60km south of Austin TX near San Antonio TX (http://www.naturalbridgecaverns.com). Natural Bridge is divided into two caves, Natural Bridge North Cave and Natural Bridge South Cave. Natural Bridge Caverns receives several hundred to a few thousand visitors each day depending on the season; however, management does not release the exact number of cavern visitors. The caverns are named for a beautiful natural bridge that spans the entrance of the North Cave. The caverns are overlain partly by a parking lot and visitor's center, but natural cover overlies much of the caverns.

Natural Bridge North Cave – Switchback Drip (NBSB)

This site is located along a series of man-made switchbacks approximately 50m from the sealed cave natural entrance and is approximately 20m below the land surface. Only spot measurements were taken here using the Telaire 7001 meter. Measurements

were taken from the edge of the tourist trail, typically in the mornings before the cavern opened to the public.

Natural Bridge North Cave – Castle Table Top (NBCA)

This site is located approximately 200m from the sealed cave natural entrance and approximately 40m below the land surface. A Vaisala meter was deployed approximately 5m from the tourist trail. Spot measurements were taken within 5m of the Vaisala meter location using the Telaire 7001 meter, typically in the mornings before the cavern opened to the public.

Natural Bridge North Cave – Emerald Lake (NBEL)

This site is located approximately 240m from the sealed cave natural entrance and approximately 20m below the land surface. Only spot measurements were taken here using the Telaire 7001 meter. Measurements were taken from the edge of the tourist trail, typically in the mornings before the cavern opened to the public.

Natural Bridge South Cave – Off Path (NBOP)

This site is located approximately 50m from the sealed cave entrance and approximately 40m below the land surface. Only spot measurements were taken here using the Telaire 7001 meter. Measurements were taken from the edge of the tourist trail, typically in the mornings before the cavern opened to the public.

Natural Bridge South Cave – End of Path (NBEP)

This site is located approximately 55m from the sealed cave entrance and approximately 40m below the land surface. Only spot measurements were taken here

using the Telaire 7001 meter. Measurements were taken from the edge of the tourist trail, typically in the mornings before the cavern opened to the public.

Natural Bridge South Cave – Wellshaft (NBWS)

This site is located approximately 60m from the sealed cave entrance and approximately 50m below the land surface. Only spot measurements were taken here using the Telaire 7001 meter. Measurements were taken from the edge of the tourist trail, typically in the mornings before the cavern opened to the public. This room has been modified with a concrete floor and benches.

Natural Bridge South Cave – Fried Egg Drip (NBFE)

This site is located beyond the developed tourist trail approximately 80m from the sealed cave entrance and approximately 60m below the land surface. Only spot measurements were taken here using the Telaire 7001 meter.

Natural Bridge South Cave – Volcano Drip (NBVC)

This site is located beyond the developed tourist trail approximately 170m from the sealed cave entrance and approximately 60m below the land surface. Only spot measurements were taken here using the Telaire 7001 meter.

Natural Bridge South Cave – Box Canyon (NBBC)

This site is located beyond the developed tourist trail approximately 200m from the sealed cave entrance and approximately 65m below the land surface. Only spot measurements were taken here using the Telaire 7001 meter.

Natural Bridge South Cave – Granola Drip (NBGN)

This site is located beyond the developed tourist trail approximately 210m from the sealed cave entrance and approximately 65m below the land surface. Only spot measurements were taken here using the Telaire 7001 meter.

Natural Bridge South Cave – Fault Drip (NBFT)

This site is located beyond the developed tourist trail approximately 240m from the sealed cave entrance and approximately 70m below the land surface. Only spot measurements were taken here using the Telaire 7001 meter.

District Park Cave

District Park Cave is located in Dick Nichols District Park in South Austin, Texas. The exact location of the cave will not be given for safety and conservation reasons. The cave is overlain by natural cover and is located in a stand of vegetation dominated by mature Juniper and Oak trees and some smaller bushes and grasses. This cave captures a small amount of storm-washed debris after heavy rainfall. BECAUSE HIGH LEVELS OF CARBON DIOXIDE ARE COMMON IN THIS CAVE, IT SHOULD ONLY BE ACCESSED BY EXPERIENCED CAVERS WHO ARE IN GOOD PHYSICAL CONDITION.

District Park 1 (DP1)

This site is located at the entrance of the cave and measurements are taken directly below the overhanging lip of the cave entrance. Only spot measurements were taken at this station.

District Park 2 (DP2)

This site is located approximately 10m from the entrance and is approximately 3m below the ground surface. Crawling through a 5m long passage accesses this site. Measurements were taken adjacent a locked metal gate that prevents unauthorized access to the deeper portions of the cave. Only spot measurements were taken at this station.

Maple Run Cave

Maple Run cave is located in South Austin, TX in the Goat Cave Karst Preserve. Maple run is overlain by natural cover and is located in a stand of Cedar and Juniper trees. Although Maple Run is gated, the exact location of the cave will not be given due to safety concerns and previous successful attempts to defeat the gate that resulted in vandalism to the cave. This cave is very treacherous and portions of the cave require short vertical climbs without rock climbing equipment, long crawls through very small passages, and large loose rocks that could pose a crushing hazard. THIS CAVE SHOULD ONLY BE ACCESSED BY EXPERIENCED CAVERS WHO ARE IN GOOD PHYSICAL CONDITION AND HAVE A STRONG KNOWLEDGE OF THE CAVE PASSAGES AND HAZARDS CONTAINED THEREIN.

Maple Run Entrance (MRE)

This site is located approximately 0.5m from the cave entrance just inside a large locked gate that deters unauthorized access to the cave. Only spot measurements were taken at this station.

Maple Run 1 (MR1)

This site is located approximately 5m from the cave entrance and approximately 2m below the ground surface, at the edge of a 3m pit. Crawling from the entrance through a small room accesses this site. Only spot measurements were taken at this station.

Maple Run 2 (MR2)

This site is located approximately 30m from the cave entrance and approximately 10m below the ground surface, just before a very tight crawlway (approximately 0.2m tall). Crawling through a very small passage at the base of the pit near MR1 accesses this site. Only spot measurements were taken at this station.

Maple Run 3 (MR3)

This site is located in a small room approximately 22m from the cave entrance and approximately 15m below the ground surface. The room is approximately 5m tall, 5m long and 3m wide. Crawling through a very small 10m long passage near MR2 accesses this site. Vaisala meters were deployed on a small ledge along the east side of the room. Spot measurements were taken in the center of the room.

Maple Run 4 (MR4)

This site is located in a small room approximately 45m from the cave entrance and approximately 20m below the ground surface. The room is approximately 1m tall, 5m long and 2m wide. Crawling through a very small passage at the base of a pit just northwest of MR3 accesses this site. Only spot measurements were taken at this station.

Maple Run 5-7 (MR5, MR6, MR7)

These sites are located in a large room approximately 70m from the cave entrance and approximately 20m below the ground surface. The room is spherical in shape and is approximately 10m in diameter. From MR4 crawling through a very small passage to the south and then climbing a 10m vertical face access this site. MR5 is located at the top of a large rubble pile and MR6 and MR7 are located 1m and 2m below MR5. Only spot measurements were taken at these stations. These sites were not accessible after January 2009 due to the rescue of a spelunker (by local cavers) that required the collapsing of the passage leading to MR5-7.

Whirlpool Cave

Whirlpool Cave is located in the Whirlpool Cave Preserve in South Austin, TX approximately 40m to the East of Loop 1. Although the physical dangers in this cave are not as great as in Maple Run, the cave passages are somewhat confusing and persons without a good knowledge of the cave can become lost quite easily. There are some tight passages within this cave and a few loose rocks that may become dislodged and cause injury. THIS CAVE SHOULD ONLY BE ACCESSED BY EXPERIENCED CAVERS WHO ARE IN GOOD PHYSICAL CONDITION AND HAVE A STRONG KNOWLEDGE OF THE CAVE PASSAGES AND HAZARDS CONTAINED THEREIN.

Whirlpool 1 (WP1)

This site is located approximately 5m from the entrance in the center of a small room that is approximately 5m in diameter. Only spot measurements were taken at this site.

Whirlpool 2 (WP2)

This site is located in a small room that is approximately 3m in diameter and located approximately 15m from the cave entrance. Measurements were taken at the edge of a 1m drop leading to the next room of the cave. This site is accessed by crawling down a tight corkscrewing passage to the south of WP1. A Vaisala meter was deployed here for a short time and spot measurements were taken here.

Whirlpool 3 (WP3)

This site is located in a small room that is approximately 6m in diameter and located approximately 20m from the cave entrance. Measurements were taken near a small natural bridge over a passage leading to the next room of the cave. Only spot measurements were taken at this site.

Whirlpool 4 (WP4)

This site is located approximately 45m from the cave entrance. Measurements were taken at the mouth of a smaller passage leading to the next room of the cave. Only spot measurements were taken at this site.

Whirlpool 5 (WP5)

This site is located in a small room that is approximately 2m in diameter and located just to the north of the trail approximately 60m from the cave entrance. Measurements were taken on a small rock shelf inside the small room. A Vaisala meter was deployed near this station for a short time and spot measurements were taken here.

Whirlpool 6 (WP6)

This site is located approximately 70m from the cave entrance. Measurements were taken at the mouth of a smaller passage as it emerges into the Travis County Room, the largest room in the cave. Only spot measurements were taken at this site.

Whirlpool 7 (WP7)

This site is located in the center of the Travis County Room, the largest room in the cave. A Vaisala meter was deployed here. Due to tampering and condensation on the probe tip, only limited data is available for this site. Spot measurements were taken here.

Whirlpool 8 & 9 (WP8, WP9)

These sites are located in a small crawlway at the east end of the Travis County Room (WP7). These sites consist of small cavities that were monitored until August 2008.

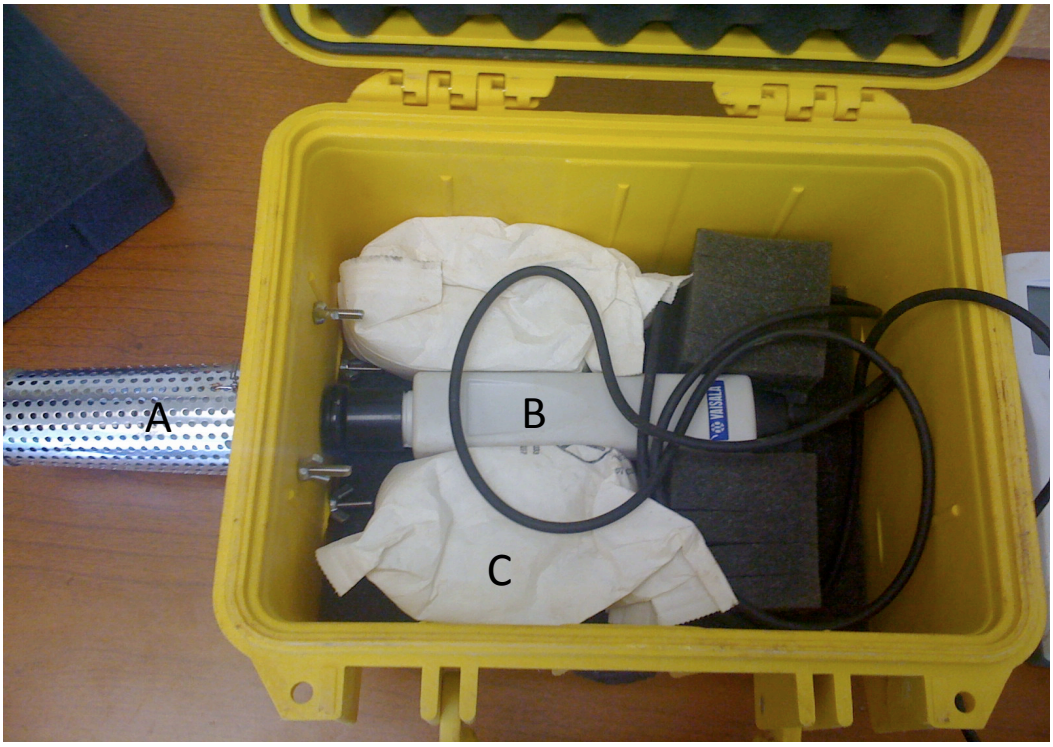
Whirlpool 10 & 11 (WP10, WP11)

These sites are located in a small crawlway approximately 120m and 130m from the cave entrance respectively. This crawlway branches off from the north of the Travis County Room. Only spot measurements were taken at these sites.

Whirlpool 12 & 13 (WP12, WP13)

These sites are located in a small crawlway approximately 120m and 130m from the cave entrance respectively. This crawlway branches off from the southeast of the Travis County Room. Only spot measurements were taken at these sites.

Figure A1. Vaisala logging carbon dioxide meter protective housing. A) metal mesh protecting probe tip where measurements are taken, B) carbon dioxide probe, C) desiccant pack, D) datalogger and measurement readout and E) water proof Pelican camera case. Note that desiccant packs were changed, data was acquired and the meter was tested for accuracy after each deployment. A small hole was drilled in the Pelican case to allow the probe tip to stick out and a small amount of silicone was used to seal the hole.



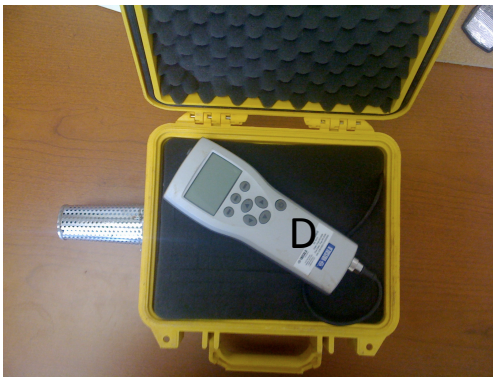
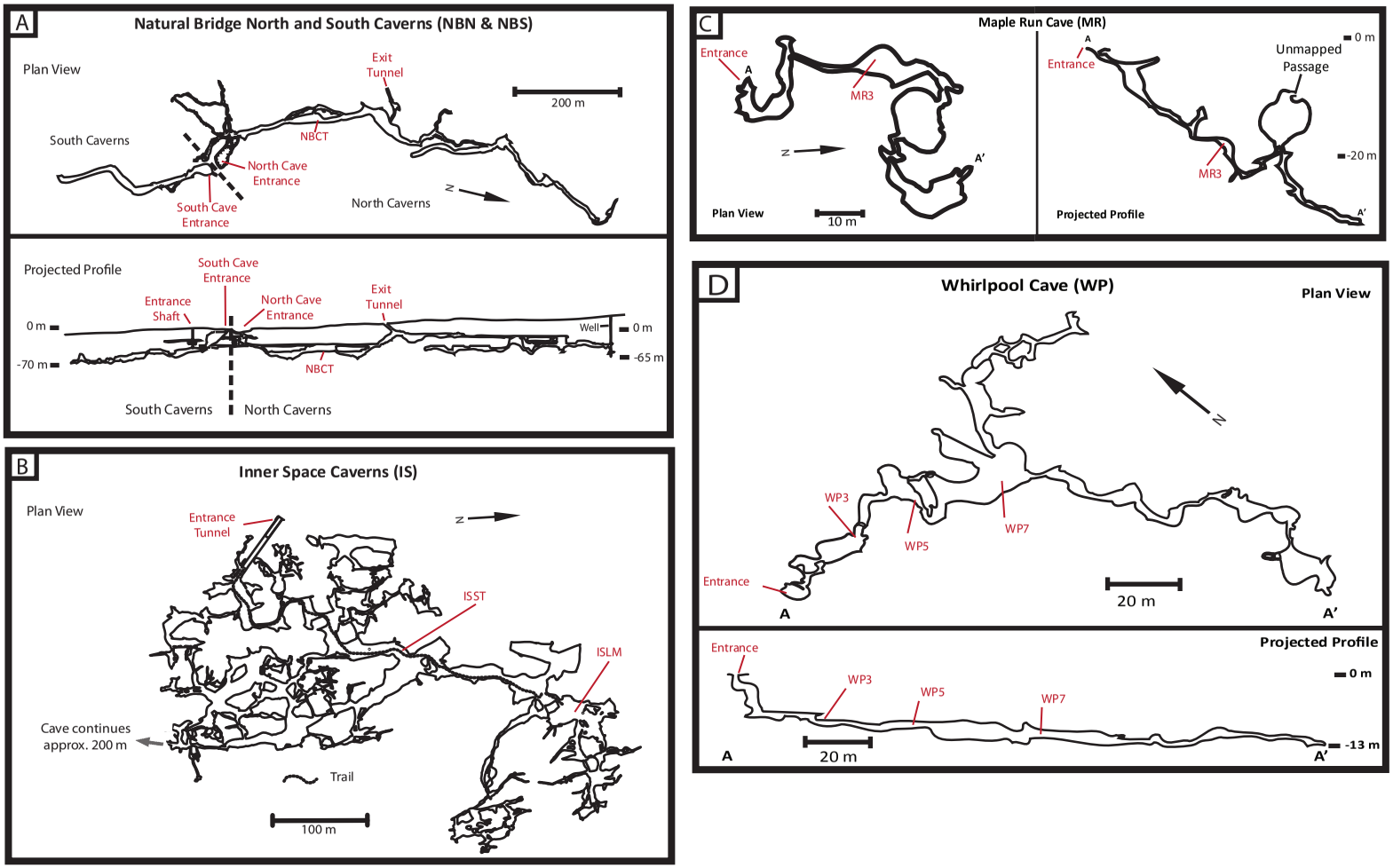




Figure A2. Locations of CO_2 logging stations.



APPENDIX B. DATA ANALYSIS

All measurements taken during transects of the undeveloped caves are given in Table B1 and the tourist caves in Table B2. The Vaisala logging carbon dioxide meters yielded over 30,000 data points and thus are not presented in the text of this document, but on a compact disk in the physical copy of this document in Portable Document (.pdf) format.

CORRELATION ANALYSIS

MATLAB version R2008b (MathWorks, Inc.) was used to determine the strength of correlation between cave air carbon dioxide and barometric pressure, outside temperature, and the difference between cave and outside air densities (density calculations given in Chapter Three of this manuscript). The following are step-by-step procedures used for the calculations:

1. All data series were normalized to synchronous time steps using the "Interpolate" curve fitting command in Kaleidagraph 4.0.4 software (Synergy Software). Interpolated curves were compared to actual data and no differences were detected.

2. The fitted parameters were saved as individual .txt files for greatest MATLAB compatibility.

3. Text files were imported to the MATLAB workspace and renamed without the .txt extension.

4. Correlation coefficients were calculated using the "corrcoef" command in MATLAB (see below for example).

5. Correlation values are output in the workspace as a matrix in the order specified in the .m file

Example of MATLAB input code

```
%calculating correlation coefficients between CO2, temp, and pressure
for
%Maple Run
ct08=corrcoef(mrco208192008,mrtemp08192008);
cp08=corrcoef(mrco208192008,mrpress08192008);
pt08=corrcoef(mrpress08192008,mrtemp08192008);

%Combining R's to a single matrix for month of variable name
Aug = [ct08(1,2);cp08(1,2);pt08(1,2)];

ct11=corrcoef(mrco211142007,mrtemp11142007);
cp11=corrcoef(mrco211142007,mrpress11142007);
pt11=corrcoef(mrpress08192008,mrtemp08192008);

Nov = [ct11(1,2);cp11(1,2);pt11(1,2)];

ct01=corrcoef(mrco201152008,mrtemp01152008);
cp01=corrcoef(mrco208192008,mrpress01152008);
pt01=corrcoef(mrpress01152008,mrtemp01152008);

Jan = [ct01(1,2);cp01(1,2);pt01(1,2)]
```

VENTILATION VOLUME CALCULATIONS

The volume of air ventilated from Maple Run Cave and Whirlpool cave during one continuous exhalation event was calculated. Measurements were taken before outward airflow was detected but only values measured during sustained outward airflow were used for volume calculations. The volume of air exiting the cave was calculated as follows:

1) Volume = airspeed * area of entrance

At least three measurements were taken every two hours for the duration of sustained outward airflow. The average of the measurements taken during each time

interval was used to calculate the volume of air exiting the cave during that time interval. Finally the calculated volumes were summed to determine the total volume of air exiting the caves during the measurement periods. Table B1 summarizes these calculations.

Table B1. Cave air CO_2 concnetrations in the undeveloped caves

Station	Cave Air CO_2 (ppm)									
	08/03/06	09/13/06	09/24/06	10/01/06	10/07/06	10/11/06	10/18/06	10/25/06	11/02/06	11/15/06
WP1	10800	14300	555	1012	13100	18200	9154	1186	966	423
WP2	10300	14500	2668	1521	13600	19000	10300	2091	1652	698
WP3	12300	13100	3215	1588	14600	19800	10900	2426	1519	788
WP4	12700	15800	3475	1759	15100	20000	11500	2682	2305	795
WP5	14000	8700	2281	1841	12500	18500	9400	2870	2875	1097
WP6	16700	11500	6870	1951	9800	19800	12100	3497	7812	1124
WP7	16100	12600	6888	5048	11300	21500	14200	8067	9298	1180
WP8	18400	12900		4780	11800	22200	15000	8050	10000	1134
WP9	15300	12800	10400	4903	10300	21600	14200	8535	10500	1596
WP10	12900	11300	11200	5289	10500	21800	12000	4920	10400	1352
WP11		12300	10600	4480	10500	19300	13700	7113	9900	1549
WP12		14400	7750	8555	12800	20400	16000	6720	12200	1233
WP13		14600	9928	10100	13300	22800	17800	4221	13800	1606

Station	Cave Air CO_2 (ppm)									
	12/02/06	12/21/06	03/01/07	04/07/07	04/12/07	05/22/07	10/13/07	08/04/08	09/16/08	10/23/08
WP1	747	419	487	2490	6010	2893	8076	8600	10300	11640
WP2	1214	1233	958	2823	6593	3597	8080	9980	10900	12360
WP3	1177	1179	1149	2507	6969	9093		10550	11100	13100
WP4	1814	1353	1502	2844	7224	4263	10100	12050	11800	14420
WP5	2626	2369	1553	2978	6884	4547	9731	11080	9900	12580
WP6	2650	2465	1980	3033	7491	5436	11300	12650	14200	13860
WP7	4654	5197	2284	3262	8981	8422	12000	15300	15300	16960
WP8	5581	6907	2625		9457	8442	14100			
WP9	5210	6560	3147		9463	7038	11700			
WP10	5605	7270	3013		9519	5637	10900	16220	12300	12700
WP11	4021	5656	3272		6255	6788	11100	13300	12200	13190
WP12	3460	4868	2777		10100	10100	13100	17850	14100	17350
WP13	3891	6314	2916		10700	12000	14700	20940	16000	17790

Table B1. Cave air CO_2 concnetrations in the undeveloped caves

Station	Cave Air CO_2 (ppm)						
	11/08/08	11/15/08	12/15/08	02/26/09	04/14/09	07/01/09	08/11/09
WP1	5770	2180	434	525	760	7980	2151
WP2	6010	3002	567	1397	1720	8190	2584
WP3	7230	3339	665	1624	2100	8660	2725
WP4	7550	3757	702	2223	2900	9334	3026
WP5	7700	3903	753	2723	3090	9648	3451
WP6	8220	4490	1811	3201	3110	11100	4714
WP7	8960	6002	3200	5062	3230	13900	6320
WP8				5322			
WP9				5204			
WP10			4101	4538	5990	12700	6906
WP11			4302	4834	6120	13000	7182
WP12			7320	8174	5090	19100	9931
WP13			10010	9920	6010	20000	12300

Station	Cave Air CO_2 (ppm)									
	9/6/06	9/13/06	9/22/06	9/27/06	10/7/06	10/11/06	10/18/06	10/25/06	11/2/06	11/15/06
Entrance	8110	11900	8528	12000	1627	14800	14800	6386	1852	358
MR1	9140	12700	8994	12100	3234	14200	6944	7044	2300	625
MR2	10200	13700	10300	13200	7157	23900	7862	8934	3339	2221
MR3	11400	13600	11100	13800	8202	16900	8506	9185	3658	2724
MR4	12400		19400	14100	6621	17500	9675	9952	6944	2770
MR5			6800	8600	2750	10300	4190	7752	3084	4556
MR6			10600	11600	3655	15300	5640	8752	3954	5295
MR7			8700	13400	6345		6665	9310	4320	5608

Table B1. Cave air CO_2 concnetrations in the undeveloped caves

Station	Cave Air CO_2 (ppm)									
	12/2/06	12/15/06	12/21/06	3/1/07	4/7/07	6/21/07	8/30/07	9/8/08	9/24/08	10/24/08
Entrance	3163	8292	6452		358	3550	8607		3291	
MR1	2978	8285	6071	2992	566	3698	9061	10600	3974	13400
MR2	3558	10000	7258	4141	574	3549	10300	12500	4469	15000
MR3	3803	10300	7923	7981	941	3910	10400	Batteries	5332	14800
MR4	3979	15700	8023	8482	866	5208	11100	Died	6868	14700
MR5	2976	8300	5796	7353	2869	3266	7459		5268	
MR6	4072	10500	7483	7880	2901	3515	8070		4443	
MR7	4387	11500	8644	8072	3117	5020	10600		6840	

Station	Cave Air CO_2 (ppm)				
	1/4/09	2/7/09	4/10/09	6/3/09	7/25/09
Entrance	880	6100	500	2790	7080
MR1	2382	7090	1200	2982	9208
MR2	3198	7740	1300	3800	12600
MR3	3660	7880	1380	3940	18900
MR4	3988	8100	4390	4430	20800
MR5	3008				
MR6	3470				
MR7	3600				

Station	Cave Air CO_2 (ppm)									
	7/31/06	9/6/06	9/13/06	9/27/06	10/7/06	10/8/06	10/11/06	10/18/06	12/21/06	4/12/07
DP1	14700	17600	23400	29800	14400	19800	9570	17000	516	1256
DP2	24800	27300	24200	31000				26700	1149	3517

Table B1. Cave air CO_2 concnetrations in the undeveloped caves

Station	Cave Air CO_2 (ppm)									
	5/22/07	6/21/07	8/30/07	10/15/07	8/4/08	9/24/08	10/24/08	11/15/08	12/15/08	3/22/09
DP1	7140	4050	17000	17000	15900	1376	4648	1780	410	800
DP2	7573	7223	21300	21300	19120	2445	5586	2230	690	4100

Station	Cave Air CO_2 (ppm)	
	6/3/09	7/25/09
DP1	2042	6875
DP2	8032	16200

Table B2. Cave air CO_2 concnetrations in thetourist caves

Station	Cave Air CO_2 (ppm)									
	8/10/06	9/12/06	10/13/06	11/10/06	12/10/06	2/21/07	3/30/07	4/27/07	5/29/07	6/29/07
ISDC	4640	3045	1395	1564		483	635	671	1131	3803
ISHW	4767	3092	810	1459	640	496	678	788	1008	3818
ISST	5282	4141	1174	1705	750	501	655	843	1109	3623
ISLM	5300	6417	7584	3778	907	572	757	684	2287	4507

Station	Cave Air CO_2 (ppm)									
	7/19/07	8/24/07	9/22/07	10/21/07	11/18/07	12/11/07	1/9/08	2/17/08	3/16/08	5/15/08
ISDC	5788		3763	1805	1014	521	451	483	560	949
ISHW	5573	7320	2013	1469	1174	740	486	561	539	597
ISST	5452	7369	2772	2150	866	602	488	631	593	829
ISLM	5793		5200	4188	2644	1398	401	631	600	930

Station	Cave Air CO_2 (ppm)									
	6/5/08	7/3/08	7/25/08	9/6/08	12/14/08	2/15/09	3/17/09	4/26/09	5/17/09	6/17/09
ISDC	770	2198	1596	1681	380	411	417	383		1578
ISHW	733	1551	2910	3551	413	398	392	405	382	892
ISST	1021	1793	2532	3235	411	368	691	452	450	1178
ISLM	928	3162	3731	5905	477	446		883	762	1961

Station	Cave Air CO_2 (ppm)									
	6/12/06	7/18/06	8/26/06	9/24/06	12/3/06	1/20/07	2/10/07	3/24/07	4/23/07	5/15/07
NBSB	3997	7102	9230	4016	432	802	451	582	768	1197
NBCA	4107	7098	9270	6385	402	2774	472	830	821	1307
NBEL	4340	6721	9302	9473		4368	621	927	1047	1315

Station	Cave Air CO_2 (ppm)									
	6/14/07	7/17/07	9/19/07	10/13/07	11/20/07	12/19/07	1/7/08	2/16/08	3/8/08	4/6/08
NBSB	3427	5367	6485	3637	1097	686	425	860	653	803
NBCA	3400	4928	6711	4223	962	718	478	720	659	785
NBEL	3549	1238	7488	4330	1204	665	525	412	785	877

Table B2. Cave air CO_2 concnetrations in thetourist caves

Station	Cave Air CO_2 (ppm)									
	5/6/08	6/10/08	7/8/08	7/22/08	9/14/08	10/20/08	11/23/08	1/15/09	2/7/09	3/8/09
NBSB	1510	2910	3275	6155	6328	1166	789	374	542	800
NBCA	1211	2699	3404	5955	6430	1112	644	394	549	686
NBEL	1307	3130	3537	6427	7232	1314	734	406	675	837

Station	Cave Air CO_2 (ppm)	
	4/11/09	5/5/09
NBSB	961	871
NBCA	849	876
NBEL	1215	1014

Station	Cave Air CO_2 (ppm)									
	6/12/06	7/18/06	8/26/06	9/24/06	10/22/06	12/3/06	1/20/07	2/10/07	3/24/07	4/23/07
NBOP	5224	20900	22900	31000	1499	605	670	2958	671	1122
NBEP	9208	20500	23600	32800	1549	711	2525	1272	836	2113
NBWS	7755	19100	23500	33300	1670	916	4824	1500	1005	1013
NBFE	7903	20000	23300	34900	2244	1148	15100	1648	1185	1077
NBVC	8710	16000	23800	35600	2621	1068	19300	4312	1523	1557
NBBC	10000	22500	24500	35800	2816	1100	28200	4158	1630	1478
NBGN	21000	24300	25600	36900	2857	1130	5364	4158	1922	1507
NBFT	11300	18500	25800	38200	5962	1135		1878	2234	1603

Station	Cave Air CO_2 (ppm)									
	5/15/07	6/14/07	7/17/07	8/17/07	9/19/07	10/13/07	11/20/07	12/19/07	1/7/08	2/16/08
NBOP	845	1450	1879	5979	6218	1807	940	701	793	707
NBEP	2441	4244	4182	9827	7946	1906	2236	1224	1658	1281
NBWS	1778	3292	1756	9900	8074	1914	2718	1251	1654	1873
NBFE	1829	13500	1520	9800	8148	2000	5012	1360	1801	1613
NBVC	2191	3948	2300	10000	8507	2253	3449	1494	2029	2686
NBBC	2334	4066	2577		8265	2415	3506	1608	2332	2176
NBGN	2250	4297				2346	3444	1531	2301	1918
NBFT	2523	4092				2540	4038	2336	3001	3032

Table B2. Cave air CO_2 concnetrations in thetourist caves

Station	Cave Air CO_2 (ppm)									
	3/8/08	4/6/08	5/6/08	6/10/08	7/8/08	7/22/08	9/14/08	10/20/08	11/23/08	1/15/09
NBOP	633	738	1184	1959	1884	3110	3571	1643	1245	494
NBEP		1978		9400	6440	4721	4802	1987	4492	470
NBWS	606	1731	2945	3622	3813	5474	4324	2100	1802	467
NBFE	1087	3171	10000	3904	6016	15600	9600	3237		489
NBVC	1232	2333	3095	4459	4475	6078	5855	2638	1993	570
NBBC	818	2449	3523	4815	4691	6216	6114	3049	1974	551
NBGN	858	2560	3650	4646	4753	6205	6266	3100	2592	565
NBFT	1483	3255	4780	5642	5861	8200	7107	4319	2745	1035

Station	Cave Air CO_2 (ppm)			
	2/7/09	3/8/09	4/11/09	5/5/09
NBOP	671	762	833	829
NBEP	833	1465	1366	1609
NBWS	901	1318	1849	2370
NBFE	963	1916	6671	3112
NBVC	1217	2252	1428	2841
NBBC	1376	2379	1589	2996
NBGN	1376	2372	1553	3118
NBFT	2144	3171	2058	3813

Table B3: Airspeed measurements and volume of air ventilated from Whirlpool Cave
Area of openings at cave entrance: 0.06m^3

Measurement Time (CST)	Measured Speed (m/s)	Measured Volume (m^3/s)	Time Interval	Volume Ventilated (m^3)
8:15	Sustained outward airflow begins			
8:35	2.79	0.3786		
8:45	3.69	0.4997	08:15-09:15	1598
8:50	1.99	0.2695		
8:55	3.62	0.4906		
9:00	4.29	0.5815		
10:45	3.17	0.4301		
10:55	3.80	0.5149	09:15-12:00	5817
11:05	6.04	0.8177		
13:00	3.58	0.4846		
13:10	2.64	0.3574	12:00-14:00	4049
13:20	6.24	0.8450		
15:00	5.77	0.7814		
15:05	9.28	1.2568	14:00-15:00	3892
15:10	8.90	1.2054		
15:45	8.72	1.1811		
15:50	9.66	1.3083	15:00-16:00	5588
15:55	9.12	1.2356		
16:00	Sustained outward airflow ends			
			Total Volume Ventilated:	20943m^3

Table B3: Airspeed measurements and volume of air ventilated from Maple Run Cave
Area of openings at cave entrance is 0.19m^3

Measurement Time (CST)	Measured Speed (m/s)	Measured Volume (m^3/s)	Time Interval	Volume Ventilated (m^3)
8:35	Sustained outward airflow begins			
8:45	0.63	0.1195		
9:00	1.03	0.1964	08:35 - 10:32	1151
9:15	1.12	0.2135		
9:30	1.21	0.2305		
9:45	0.72	0.1366		
11:35	2.19	0.4184		
11:45	2.01	0.3842	10:33 - 12:01	2173
11:50	2.15	0.4098		
11:55	2.10	0.4013		
12:00	2.32	0.4440		
13:50	2.41	0.4611		
13:55	2.37	0.4525	12:02 - 14:28	3964
14:00	2.32	0.4440		
14:55	1.30	0.2476		
15:00	1.56	0.2988	14:29 - 16:10	1656
15:05	1.43	0.2732		
17:15	0.80	0.1537		
17:20	0.76	0.1452	16:11 - 17:25	569
17:25	0.45	0.0854		
17:26	Sustained outward airflow ends			
			Total Volume Ventilated:	9513m^3

Table B4. Soil depths above the study caves measured by driving a 0.25 in rebar stake into the soil until refusal. Measurements were taken above the caves along straight line transects at 10 meter intervals.

Cave	Starting Coordinate UTM	Transect Direction	Interval (m)	Depth (cm)	Depth (cm)	Depth (cm)	Depth (cm)	Depth (cm)	Depth (cm)	Depth (cm)	Avg. Depth (cm)	Stdev (cm)
DP	14R 609850 3342950	NE	10	25	28	26	42	0*	73	39		
DP	14R 609850 3342910	NE	10	64	58	21	18	49	57	48		
DP	14R 609850 3342843	NE	10	29	61	22	15	54	29	36	37.8	18.9
WP	14R 610980 3343261	E	10	22	29	42	35	33	28	26		
WP	14R 610980 3343216	E	10	17	21	21	15	8	100	75		
WP	14R 610980 3343175	E	10	7	29	17	37	31	14	44	31.0	21.7
MR	14R 611073 3341547	NE	10	63	65	60	46	39	42	20		
MR	14R 611070 3341549	NE	10	23	59	38	59	53	24	24		
MR	14R 611074 3341564	NE	10	44	37	52	24	41	32	35	41.9	14.4
NBS	14R 563516 3284810	NE	10	24	14	25	14	29	51	47		
NBS	14R 563583 3284668	NE	10	20	21	33	37	53	20	80		
NBS	14R 563593 3284590	NE	10	30	42	73	18	21	20	44		
NBS	14R 563634 3284550	NE	10	0*	23	22	22	40	36	37	32.0	17.6
NBN	14R 563420 3285109	NE	10	19	31	29	0*	0*	56	52		
NBN	14R 563488 3285028	NE	10	35	72	38	22	23	0*	21		
NBN	14R 563559 3284954	NE	10	21	0**	0**	36	0**	0**	30	23.1	20.9
IS	14R 626049 3387012	N	10	27	33	29	23	44	23	36		
IS	14R 626029 3386929	NE	10	21	22	30	23	39	22	20		
IS	14R 625997 3386807	NE	10	24	19	37	26	25	30	28		
IS	14R 625787 3386818	NE	10	18	9	51	17	13	13	24	26.2	10.2

*Bedrock exposed at surface

**Asphalt parking lot

REFERENCES

Amundson, R.G. and Smith, V.S., 1988. Annual cycles of physical and biological properties in an uncultivated and an irrigated soil in the San Joaquin Valley of California. Agriculture, Ecosystems and Environment 20, 195-208.

Baker, A., Smart, P.L., and Ford, D.C., 1993. Northwest European palaeoclimate as indicated by growth frequency variations of secondary calcite deposits: Palaeogeography, Palaeoclimatology, Palaeoecology 100, 291–301.

Baldini, J.U., Baldini, L.M., McDermott, F., Clipson, N., 2006. Carbon dioxide sources, sinks, and spatial variability in shallow temperate zone caves: Evidence from Ballynamintra Cave, Ireland. Journal of Cave and Karst Studies 68, 4-11.

Baldini, J.U., McDermott, F., Hoffmann, D.L., Richards, D.A. and Clipson, N., 2008. Very high-frequency and seasonal cave atmosphere PCO_2 variability: Implications for stalagmite growth and oxygen isotope-based paleoclimate records. Earth and Planetary Science Letters 272, 118-129.

Banner, J.L., Gilfoyle, A., James, E., Stern, L.A. and Musgrove, M., 2007. Seasonal variations in modern speleothem calcite growth in central Texas, U.S.A. Journal of Sedimentary Research 77, 615-622.

Batiot-Guilhe, C., Seidel, J., Jourde, H., Herbrard, O. and Bailly-Comte, V., 2007. Seasonal variations of CO_2 and ^{222}Rn in a Mediterranean sinkhole-spring (Causse d'Aumelas, SE France). International Journal of Speleology 36, 51-56.

Bourges, F., Mangin, A. and D'Hulst, D., 2001. Carbon dioxide in karst cavity atmosphere dynamics: the example of the Aven d'Orgnac. Earth and Planetary Sciences 333, 685–692.

Bourges, F., Genthon, P., Mangin, A. and D'Hulst, D., 2006. Microclimates of L'Aven D'Orgnac and other French limestone caves (Chauvet, Esparros, Marsoulas). International Journal of Climatology 26, 1651-1670.

Buecher, R.H., 1999. Microclimate study of Kartchner Caverns, Arizona. Journal of Cave and Karst Studies 61, 108-120.

Cooke, M.J., Stern, L.A., Banner, J.L. and Mack, L.E. 2007. Evidence for the silicate source of relict soils on the Edwards Plateau, central Texas. Quaternary Research 67, 275-285.

Cowan, B.D., Osborne, M.C. and Banner, J.L., 2009. Temporal variability of cave-air CO_2 in central Texas. Proceedings of the 15th International Congress of Speleology, 1018.

Crossey, L., Springer, A., Kalstrom, K., Newell, D., Atudorei, V., Fischer, T. and Hilton, D., 2006. CO_2 degassing in high volume springs in the Southern Colorado Plateau region-Understanding deep inputs and geochemical mixing in regional groundwater. Geological Sociery of America, Rocky Mountain Section-58th Annual Meeting, Abstracts with Programs 38, 5.

Daly, E., Oishi, A.C., Porporato, A. and Katul, G.G., 2008. A stochastic model for daily subsurface CO_2 concentration and related soil respiration. Advances in Water Resources 31, 987-994.

Denis, A., Lastennet, R., Huneau, F. and Malaurent, P., 2005. Identification of functional relationships between atmospheric pressure and CO_2 in the cave of Lascaux using the concept of entropy of curves. Geophysical Research Letters 32, 1.

Dueñas, C., Fernández, M., and Cañete, S., 2005. ^{222}Rn concentrations and the radiation exposure levels in the Nerja Cave. Radiation Measurements 40, 630-632.

Ek, C. and Gewalt, M., 1985. Carbon dioxide in cave atmospheres: New results in Belgium and comparison with some other countries. Earth Surface Processes and Landforms 10, 173-187.

Faimon,J., Stelcl, J. and Sas, D., 2006. Anthropogenic CO_2-flux into cave atmosphere and its environmental impact: A case study in the Cisarska Cave (Morivian Karst, Czech Republic). Science of the Total Environment 369, 231-245.

Fairchild, I.J., Smith, C.L., Baker, A., Fuler, L., Spotl, C., Mattey, D., and McDermott, F., 2006. Modification and preservation of environmental signals in speleothems. Earth-Science Reviews 75, 105-52.

Fairchild, I.J., Frisia, S., Borsato, A. and Tooth, A.F., 2007. Speleothems, in: Nash, D.L. and McLaren, S.J. (Eds.) Geochemical Sediments and landscapes. Blackwell Publishing Ltd., Malden, MA, 201-245.

Fernandez, P.L., Gutierrez, I., Quindos, L.S., Soto, J. and Villar, E., 1986. Natural ventilation of the Paintings Room in Altamira Cave. Nature 321, 586-588.

Fernandez-Cortes, A., Sanchez-Moral, S., Cuezva, S., Carols, J., Cañaveras, J.C., and Abella, R., 2009. Annual and transient signatures of gas exchange and transport in the Castañar de Ibor cave (Spain). International Journal of Speleology, 38, 153-162.

Fleitmann, D., Burns, S., Neff, U., Mudelsee, M., Mangini, A., and Matter, A., 2004. Palaeoclimatic interpretation of high-resolution oxygen isotope profiles derived from annually laminated speleothems from Southern Oman. Quaternary Science Reviews 23, 925-935.

Frappier, A.B., Sahagian, D., Carpenter, S.J., Gonzalez, L.A. and Frappier, B.R., 2007. Stalagmite stable isotope record of recent tropical cyclone events. Geology 35, 111-114.

Frisia, S., Borsato, A., Fairchild, I.J., and McDermott, F., 2000. Calcite fabrics, growth mechanisms, and environment of formation in speleothems from the Italian Alps and southwestern Ireland. Journal of Sedimentary Research 70, 1183–1196.

Genty, D., and Quinif, Y., 1996. Annually laminated sequences in the internal structure of some Belgian stalagmites—importance for paleoclimatology. Journal of Sedimentary Research 66, 275–288.

Hanson, P.J., Edwards N.T., Garten, C.T. and Andrews, J.A., 2000. Separating root and soil microbial contributions to soil respiration: A review of methods and observations. Biogeochemistry 48, 115-146.

Hauwert, N.M., 2009. Groundwater flow and recharge within the Barton Springs Segment of the Edwards Aquifer, Southern Travis and Northern Hays Counties, PhD Thesis University of Texas at Austin.

Hendy, C.H., 1971. The isotopic composition of speleothems: 1. The calculation of the effects of different modes of formation on the isotopic composition of speleothems and their applicability as paleoclimatic indicators. Geochimica et Cosmochimica Acta 35, 801-824.

Henninger, S., 2008. Analysis of near surface CO_2 variability within the urban area of Essen, Germany. Meterologische Zeitschift 17, 19-27.

Holland, H.D., Kirsipu, T.V., Huebner, J.S. and Oxburgh ,U.M., 1964. On some aspects of the evolution of cave water. Journal of Geology 72, 36-67

Hoyos, M., Soler, V., Canaveras, C., Sanchez-Moral, S. and Sanz-Rubio, E., 1998. Microclimate characterization of a karstic cave: human impact on microenvironmental parameters of a prehistoric rock art cave (Candamo Cave northern Spain). Environmental Geology 33, 231-242.

James, E.W. and Banner, J.L., 2008. Preservation bias in speleothem proxy records due to seasonal ventilation of caves. Geological Society of America, Abstracts with Programs, 583.

Kowalczk, A.J. and Froelich, P.N., 2010. Cave ventilation and CO_2 outgassing by radon-222 modeling: how fast do caves breathe? Earth and Planetary Science Letters 289, 209-219.

Linan, C., Vadillo, I. and Carrasco, F., 2008. Carbon dioxide concentration in air within the Nerja Cave (Malaga, Andalusia, Spain). International Journal of Speleology, 37, 99-106.

Lloyd, J. and Taylor, J.A., 1994. On the temperature dependence of soil respiration. Functional Ecology 8, 315-323.

Maclay, R.W. and Small, T.A., 1976. Progress report on geology of the Edwards Aquifer, San Antonio area, Texas, and preliminary interpretation of borehole geophysical and laboratory data on carbonate rocks. U.S. Geological Survey Open-File Report 76–627, 65 p.

Mattey, D.P., Fairchild, I.J., Atkinson, T.C., Latin, J., Ainsworth, M., Durell, R., 2009. Seasonal microclimate control of calcite fabrics, stable isotopes and trace elements in modern speleothem from St. Michaels Cave, Gibraltar. in: Tufas and Speleothems: Unravelling the Microbial and Physical Controls, Geological Society of London Special Volume Number 336.

P.J. Melcior, 1993. The Tides of Planet Earth (2nd ed.) Pergamon Press: New York, NY.

Mickler, P.J., Banner, J.L., Stern, L., Asmerom, Y., Edwards, R.L. and Ito, E., 2004. Stable isotope variations in modern tropical speleothems: Evaluating equilibrium vs. kinetic isotope effects. Geochimica et Cosmochimica Acta 68, 4381-4393.

Micker, P. J., Stern, L.A. and Banner, J.L., 2006. Large kinetic isotope effects in modern speleothems. Geollogical Society of America Bulletin 118, 65-81.

Moore, G.W. and Sullivan, N., 1997. Speleology: Caves and the cave environment (3rd ed.). Cave Books, St. Louis, MO.

Musgrove, M., Banner, J.L., Mack, L.E., Combs, D.M., James, E.W., Cheng, H. and Edwards, R.L., 2001. Geochronology of late Pleistocene to Holocene speleothems from central Texas: Implications for regional paleoclimate. Bulletin of the Geological Society of America 113, 1532.

Perrier, F. and Richon, P., 2010. Spatiotemporal variation of radon and carbon dioxide concentrations in an underground quarry: coupled processes of natural ventilation, barometric pumping and internal mixing. Journal of Environmental Radioactivity in press, 1-18.

Polyak, V., and Asmerom, Y., 2001. Late Holocene Climate and Cultural Changes in the Southwestern United States. Science 294, 148-151.

Qin, X., Tan, M., Liu, T., Wang, X., Li, T., and Lu, J., 1999. Spectral analysis of a 1000-year stalagmite lamina-thickness record from Shihua Cavern, Beijing, China, and its climatic significance. The Holocene 9, 689–694.

Raich, J.W. and Schlesinger, W.H., 1992. The global carbon dioxide flux in soil respiration and its relationship to vegetation and climate. Tellus 44B, 81-99.

Railsback, L.B., Brook, G.A., Chen, J., Kalin, R., and Fleisher, C.J., 1994. Environmental controls on the petrology of a late Holocene speleothem from Botswana with annual layers of aragonite and calcite. Journal of Sedimentary Research 64, 147–155.

Richon, P., Perrier, F., Pili, E., Boudon, G., Villemant, B. and J. Sabroux, 2007. Detectability and significance of the 12h barometric tide in the radon-222 signal, dripwater flow rate, carbon dioxide concentration and air temperature of an underground laboratory. American Geophysical Union, Fall Meeting, Abstract H11B-0487.

Rose, P.R., 1972. Edwards Group, surface and subsurface, central Texas: Austin. University of Texas Bureau of Economic Geology Report of Investigations 74, 198.

Russell, W.H., 2007. Stratigraphic distribution of cave volume in the Edwards Limestone, Southern Travis County, Texas. Austin Geological Society Bulletin 3, 37-42.

Slaughter, B.H., 1966. Platygonus compressus and associated fauna from the Laubach Cave of Texas. American Midland Naturalist, 75, 475.

Small, T.A., Hanson, J.A. and Hauwert, N.M., 1996. Geologic framework and hydrogeologic characteristics of the Edwards Aquifer outcrop (Barton Springs Segment), Northeastern Hayes and Southwestern Travis Counties, Texas. U.S. Geological Survey Water-Resources Investigation Report 96-4306, 21p.

Sondag, F., Ruymbeke, M., Soubies, F., Santos, R., Somerhausen, A., Seidel, A. and P. Boggiani, 2003. Monitoring present day climatic conditions in tropical caves using an Environmental Data Acquisition System (EDAS). Journal of Hydrology 273, 103-118.

Spotl, C., Fairchild, I.J. and Tooth, A.F., 2005. Cave air control on drip water geochemistry, Obir Caves (Austria): Implications for speleothem deposition in dynamically ventilated caves. Geochimica et Cosmochimica Acta 69, 2451-2468.

Taucer, P. and C. Munster, 2005. Development of Smoke Tracer Instrumentation for Groundwater Recharge Investigations in the Edwards Aquifer Region. U.S. Geologic Survey Water Resources Research Grant Completion Report.

Tooth, A.F. and Fairchild, I.J., 2003. Soil and karst aquifer hydrological controls on the geochemical evolution of speleothem-forming drip waters, Crag Cave, southwest Ireland. Journal of Hydrology, 273, 51-68.

Troester, J.W. and White, W.B., 1984. Seasonal fluctuations in the carbon dioxide partial pressure in a cave atmosphere. Water Resources Research 20, 153-156.

USDA Soil Survey Staff. 1974. Soil Survey of Travis County, Texas. U.S. Department of Agriculture.

USDA Soil Survey Staff. 1983. Soil Survey of Williamson County, Texas. U.S. Department of Agriculture.

USDA Soil Survey Staff. 1984. Soil Survey of Comal and Hays Counties, Texas. U.S. Department of Agriculture.

Villar, E., Fernandez, P.L., Quindos, L.S. and Soto, J., 1985. Natural temporal evolution of the CO_2 content in the air of the "Paintings Chamber" at Altamira Cave. National Speleological Society Bulletin 13, 12-16.

Wallace, J.M. and P.V. Hobbs, 2006. Atmospheric Science an Introductory Survey (2nd ed.) Elsevier Academic Press: Burlington, MA.

Wang, Y., Cheng, H., Edwards, R.L., Kong, X., Shao, X., Chen, S., Wu, J., Jiang, X., Wang, X., and An, Z., 2008. Millennial and orbital-scale changes in the East Asian monsoon over the past 224,000 years. Nature, 451, 1090-1093.

Wong, C., 2008. Geochemical evolution of karst vadose water and brush clearing impacts on recharge in central Texas. Masters Thesis University of Texas at Austin.

Vita

Brian Davis Cowan was born in Atlanta, GA in 1980 to parents Jim and Shara Cowan. Brian has always felt the "call of the wild" and has been privileged to travel through (and beneath) many rugged, natural areas by foot, bike, boat and dogsled. Brian entered the University of West Georgia and declared Psychology as his major; but after four years of staring out the window and nearly completing his degree in psychology, Brian found that his true calling in life was geology…outdoors, "playing in the dirt" where he was happiest. Brian graduated from the University of West Georgia with a B.S. in Geology and quite a bit of research experience, in large part thanks to his undergraduate adviser Dr. Jim Mayer. This research experience inspired Brian to continue his education in hydrogeology at the University of Texas at Austin.

Permanent email: BC1774@gmail.com

This thesis was typed by the author, Brian Davis Cowan.